COMPARISON OF TWO SEGMENT MAXIMUM LIKELIHOOD (TSML) FREQUENCY WAVENUMBER SPECTRA WITH THE FAST BEAMED FREQUENCY WAVENUMBER SPECTRA (FKPLOT)

J. W. Lambert, et al

Teledyne Geotech

Prepared for:

Defense Advanced Research Projects Agency
Air Force Technical Applications Center

9 May 1974

Unclassified

SECURITY CLASSIFICATION OF THIS PAGE (When Data Entered)

REPORT DOCUMENTATION PAGE		READ INSTRUCTIONS BEFORE COMPLETING FORM
1 REPORT NUMBER SDAC-TR-74-6	2 GOVT ACCESSION NO	3 RECIPIENT'S CATALOG NUMBER AD/A-003481
4 TITLE (and Subtitle) COMPARISON OF TWO SEGMENT MAXIMUM LIKELIHOOD (TSML) FREQUENCY WAVENUMBER SPECTRA WITH THE FAST BEAMED FREQUENCY WAVENUMBER SPECTRA (FKPLOT)		5 TYPE OF REPORT & PERIOD COVERED Technical 6 PERFORMING ORG. REPORT NUMBER
7 AUTHOR(s) Lambert, J. W. and Der, Z. A.		8 CONTRACT OR GRANT NUMBER(s) F08606-74-C-0006
9 PERFORMING ORGANIZATION NAME AND ADDRESS Teledyne Geotech 314 Montgomery Street Alexandria, Virginia 22314		10 PROGRAM ELEMENT, PROJECT, TASK AREA & WORK UNIT NUMBERS
11 CONTROLLING OFFICE NAME AND ADDRESS Defense Advanced Research Projects Agency Nuclear Monitoring Research Office 1400 Wilson Blvd. Arlington, Va. 22209		12 REPORT DATE 9 May 1974 13 NUMBER OF PAGES 113
14 MONITORING AGENCY NAME & ADDRESS (if different from Controlling Office) VELA Seismological Center 312 Montgomery Street Alexandria, Virginia 22314		15 SECURITY CLASS (of this report) Unclassified 15a DECLASSIFICATION DOWNGRADING SCHEDULE

16 DISTRIBUTION STATEMENT (of this Report)

APPROVED FOR PUBLIC RELEASE: DISTRIBUTION UNLIMITED.

17 DISTRIBUTION STATEMENT (of the abstract entered in Block 20, if different from Report)

18 SUPPLEMENTARY NOTES

19 KEY WORDS (Continue on reverse side if necessary and identify by block number)

Frequency Wavenumber Spectra
Multiple Signals
Surface Waves

20 ABSTRACT (Continue on reverse side if necessary and identify by block number)

Empirical comparison of the two segment maximum likelihood f-k spectra with the fast frequency domain beam f-k spectra (FKCOMB FKPLOT) shows that the latter is more suitable for the separation of multiple signals if the amplitudes of the signals differ considerably. This advantage of the beaming process is attributed primarily to the stripping procedure, which has not been developed for the maximum likelihood spectra. The maximum likelihood f-k

DD FORM 1 JAN 73 1473 EDITION OF 1 NOV 65 IS OBSOLETE

Unclassified

SECURITY CLASSIFICATION OF THIS PAGE (When Data Entered)

spectra, on the other hand, are less sensitive to the array response and easier to interpret, especially if the array used contains only a few elements, since the sidelobes of the array response are more confusing on the FKCOMB output of this case. Both processes require a good signal to noise ratio (~2) for successful application.

Composited recordings of long period Rayleigh waves recorded at LASA were utilized for the comparison using various subarray configurations and signal and noise levels.

COMPARISON OF TWO SEGMENT MAXIMUM LIKELIHOOD (TSML) FREQUENCY WAVENUMBER SPECTRA WITH THE FAST BEAMED FREQUENCY WAVENUMBER SPECTRA (FKPLOT)

SEISMIC DATA ANALYSIS CENTER REPORT NO.: SDAC-TR-74-6

AFTAC Project No.: VELA VT/4709

Project Title: Seismic Data Analysis Center

ARPA Order No.: 1620

ARPA Program Code No.: 3F10

Name of Contractor: TELEDYNE GEOTECH

Contract No.: F08606-74-C-0006

Date of Contract: 01 July 1973

Amount of Contract: $2,152,172

Contract Expiration Date: 30 June 1974

Project Manager: Royal A. Hartenberger
(703) 836-3882

P. O. Box 334, Alexandria, Virginia 22314

ABSTRACT

Empirical comparison of the two segment maximum likelihood f-k spectra with the fast frequency domain beam f-k spectra (FKCOMB, FKPLOT) shows that the latter is more suitable for the separation of multiple signals if the amplitudes of the signals differ considerably. This advantage of the beaming process is attributed primarily to the stripping procedure, which has not been developed for the maximum likelihood spectra. The maximum likelihood f-k spectra, on the other hand, are less sensitive to the array response and easier to interpret, especially if the array used contains only a few elements, since the sidelobes of the array response are more confusing on the FKCOMB output of this case. Both processes require a good signal to noise ratio (~2) for successful application.

Composited recordings of long period Rayleigh waves recorded at LASA were utilized for the comparison using various subarray configurations and signal and noise levels.

TABLE OF CONTENTS

LIST OF FIGURES

LIST OF FIGURES (Continued)

LIST OF FIGURES (Continued)

LIST OF FIGURES (Continued)

LIST OF FIGURES (Continued)

LIST OF TABLES

ACKNOWLEDGEMENT

The authors wish to thank Mr. Terence W. Harley of Texas Instruments, Inc. for making the TSML programs available and Mr. Philip R. Laun of Texas Instruments for his invaluable assistance in running the programs. We also thank Captain J. W. Woods for many useful suggestions and discussions, which is initiated during the course of this project.

INTRODUCTION

The purpose of this report is to compare the performance of two ways of estimating the frequency wavenumber structure. The first method is a fast frequency domain beamforming program which was developed at the Seismic Array Analysis Center by E. Smart. Of the various programmed versions of this method, we used FKPLOT, which forms the frequency wavenumber spectra at a selected frequency. A later version (FKCOMB) searches for the frequency with the highest signal-to-noise ratio and automatically determines the azimuths and velocities of the prominent peaks in the f-k plane. Detailed descriptions of these programs and the method can be found in SAAC Report No. 9; and in papers by Smart and Flinn (1971) and Mack and Smart (1971). An important feature of this method is a procedure called "stripping" which subtracts the most prominent spectral peaks and the associated side lobes from the f-k spectra to reveal any hidden weak signals. Blandford, Cohen, and Woods (1973) have shown that stripping is the first iteration of an approximation to a two-signal maximum likelihood processor.

The second method used is the maximum likelihood f-k analysis described by Capon (1969), Lintz (1968) and McCowan and Lintz (1968). The output obtained by this method is the power passed by a set of maximum likelihood filters which were designed to pass a plane

wave corresponding to a particular point in the f-k plane and reject the rest of the waves present. The computation of the maximum likelihood spectra uses an estimate of the power spectral matrix of all the sensors. In the method originally proposed by Capon et al. (1967), this power spectral matrix was estimated by the Fourier transformation of many time segments of data, forming all the auto- and cross-products for each segment, and finally averaging over many time segments. This procedure gives the necessary statistical stability to the estimates. The procedure described can be used for long noise samples, but difficulties arise when dealing with earthquake signals. The duration of these signals is relatively short and the stability of the spectral estimates has to be sacrificed. For the computations given in this report only two segments of 128 seconds duration were used; we call the output the "two segment maximum likelihood f-k spectra" (TSML f-k spectrum).

In comparing the two methods we examined the following features:

1. Ability of the two processes to separate two events close to azimuth of arrival and nearly equal in amplitude, with high S/N ratio.

2. Ability to separate two events close in azimuth and unequal amplitude, with high S/N ratio.

3. Sensitivity of the two processes to noise.

4. Effect of reducing the array size and the number of sensors.

Theoretical analyses of the two methods have been made for idealized cases which show that the maximum likelihood method is in many ways superior to the fast beamed f-k spectra. The resolution should be considerably better, the TSML spectra in the noiseless case should be independent of the array response, and two uncorrelated signals at different azimuth should be completely separable (Lintz and Woods, 1972). It is not clear, however, how these processors would perform in the presence of noise, and what effect accidental correlations of the two signals within the short time windows would have. In the following we will define these events to be "separated" if two peaks appear in the TSML output which correspond to azimuths and directions of the known signals and if these peaks are at least 2-3 dB above the general background. The same definition is used for the FKPLOT (original and stripped) outputs. An additional criterion requiring that the peaks in the f-k plane should correspond to realistic Rayleigh wave velocities will also be used occasionally. The velocity 3.6 km/sec corresponding to average phase velocity of Rayleigh waves around 30 sec period is marked by a circle on all f-k plots. Infinite velocity is marked by a cross at the center of the plot.

The contouring used in the presentation conforms to that of the FKPLOT output, that is, the first contour is at 1 dB below the peak, the second 3 dB below peak, and the following ones are separated by 3 dB.

The TSML outputs are similarly contoured, although the program gives the output at 1 dB intervals. The reproductions of the printer plot shows all these subintervals and they are occasionally indicated by dashed contours. Velocities, azimuths, S/N ratios and F-statistics computed by FKPLOT are shown in Table II.

In testing the two processes we did not compare their computational efficiency, since while the production-oriented FKPLOT was considerably optimized with respect to running time, the research programs made available to us by Texas Instruments for computing the TSML spectra were not. Therefore, it would have been unfair to compare the running times of the two processes, although the simplicity of the FKPLOT beaming process makes it likely that even with the inclusion of stripping it would be faster than computing the maximum likelihood spectra.

DATA

Throughout this report, long-period vertical component data for LASA have been used. Because of data quality problems, some sensors had to be omitted. For parallel runs of the two processors the number of sensors used was kept the same to make the comparisons valid. The elements C_1 and C_2 were omitted at all times because of gain and data quality problems, and element D_2 was also omitted when Event 5 was present. To test the processors six events were selected. The epicentral data for these events are shown in Table I. Three of the events occurred in the western Pacific region with Rayleigh waves arriving at LASA from the WNW direction. The three other events are roughly south of LASA. The Rayleigh wave train for the Baja event (Event 4) is short and fits entirely within the 256 second window used in the calculations. In order to make the results mutually comparable, the f-k spectra were computed for a common frequency f_o=.04688 cps. (T=21.3). In order to eliminate undesirable leakage of energy due to short time windows, the windows were selected by visually estimating the dominant frequency along the wavetrain and placing the window at the portion of the wavetrain where the chosen reference frequency f_o was dominant. Subsequent exact Fourier analysis showed that the dominant frequency was sufficiently close to f_o to rule out excessive leakage from other frequencies which would result in false velocities (Smart, 1971). The length of time windows

used in FKPLOT was 256 seconds. The TSML method used the same length of record divided into two time segments. Figures 1 to 6 show plots of all traces of the events used with the time windows marked. All western Pacific events show considerable variation in the surface wave forms across the array, which indicates multipathing. This is somewhat less pronounced in the New Britain event (Event 2). The Baja California event (Event 4) has a short surface wavetrain. The Argentine event (Event 5) and the Guatemala event (Event 6) show considerable multipathing, as evidenced by beats on the wavetrain. All events chosen were of a sufficiently high magnitude for the signal to be considerably above the background noise level. Statistical measures of S/N ratio computed during the FKPLOT runs are measures of the deviation of the input from a single plane wave rather than that of ratios of signal level to background noise.

Figure 7 shows the power spectra of the events within the signal windows chosen, averaged over all sensors and the two time segments used for TSML analysis. The chosen reference frequency f_o is at or very near to the spectral peak for all events. Small differences should not affect the results presented.

F-K ANALYSES OF DATA USING THE FULL ARRAY

General

In the following, the analyses of various signals and signal and noise combinations is given, using all the available vertical elements of the LASA long period array. The results are representative of the capabilities of a large array, which is not likely to be duplicated in the near future. In the latter part of the report only parts of LASA will be used, reducing the resolution but at the same time giving results more indicative of the performance of smaller arrays presently being contemplated.

Analyses of individual signals and noise samples

Figure 8 shows the f-k spectra obtained for Event 1, the FKPLOT output with the stripped region in the center, the TSML f-k spectrum on the right. The TSML output shows a peak at azimuth 347, with velocity $\sim$ 3.6 km/sec. The FKPLOT output shows a secondary peak at a slightly different azimuth on the stripped f-k plot, which is probably due to a multipath arrival. In general the stripped peaks will be rejected for false events because they will have low values for the "F" statistic.

Figure 9 shows f-k spectra for Event 2. The TSML output shows a well-defined peak showing no more multipathing than Event 1. The FKPLOT output shows a much broader peak at roughly the same azimuth, with high

S/N ratio, evidently modified by the array response. The stripped output shows a spurious peak at a low S/N ratio, which is probably meaningless.

Event 3 is more spread out in azimuth than Event 2, as evidenced by the TSML output (Figure 10). The difference is not evident on the FKPLOT output, since this technique has a lower resolution. The stripped version again shows spurious peaks at low S/N ratio.

Event 4 shows a single peak on the TSML f-k plot on Figure 11; the FKPLOT output again shows a broad peak on the original f-k plot and two spurious peaks at moderate S/N ratio on the stripped version. If these peaks are multipath arrivals it is not evident on the TSML output.

Event 5 has broader peaks on both kinds of f-k spectra indicating multipathing or scattering of surface waves (Figure 12). This is again quite plausible considering the travel path of these waves across the Andes Mountains and Central America. The stripped version shows a peak at low S/N ratio, possibly due to a multipath arrival. Similar conclusions can be reached for Event 6 shown in Figure 13.

The above events are thought to be fairly representative of real earthquake signals with respect to the azimuthal spread of Rayleigh waves. Real earthquake signals are not plane waves and theoretical evaluation of the performance of processors using plane wave models can be misleading. It is important to test the processors using real signals.

Figure 14 shows the f-k plots of a noise sample used for superposition on the various inputs to be analyzed to simulate noisy signals. Although it shows some directionality, it is thought to be fairly representative of noise in general. Visually the noise seems to be uncorrelated between sensors. The noise f-k spectra are included here for comparison with the f-k analyses of the noisy signals.

ANALYSIS OF COMBINED EVENTS

In order to simulate two signals which arrive simultaneously at the array the signals of two events are added within the windows previously used. By combining the events at various relative amplitude levels and adding noise one can test the sensitivity of the two processes to different signal amplitudes and to varying noise levels. The signal levels were scaled to maximum amplitudes occurring within the selected windows at the center array element for each event. This rough scaling is sufficient for our purposes, although scaling the spectral amplitudes at the preselected reference frequency f_o would be more appropriate. Various cases were tested and the results are given below.

It should be noted that the additional signal will cause the statistics which are indicators of the S/N ratio (F statistics and S/N ratio given by FKPLOT) to decrease. Therefore, these indicators will lose their original meanings. Low values of these parameters do not indicate the presence of high ambient noise. If one event is removed by stripping, these indicators can increase in value since the energy seems to come from fewer directions. This phenomenon is discussed by Blandford (1972).

Case 1

The two signals are equal in amplitude; no noise is added.

The f-k spectra for the combination of events 1 and 2 are shown in Figure 15. The FKPLOT output shows that without stripping there are only faint indications of the presence of Event 1, but stripping removes Event 2 effectively and Event 1 then becomes visible. The S/N ratio for both cases is fair. The TSML output records both signals, with Event 1 about 5 dB below Event 2. Thus both processes resolved the signals successfully.

The combination of Events 1 and 3 are well resolved on both the TSML and the unstripped FKPLOT outputs. On the TSML output Event is 4 dB above Event 3 while the FKPLOT peaks are on the same level. Stripping leaves Event 3, the weaker signal. Again both processes performed equally well (Figure 16).

Figure 17 shows that Events 4 and 5 are not well separated on the TSML output, the second event is indicated by a bulge in the -2 dB contour. Only this secondary dashed contour separates the two events. The FKPLOT output shows only a large maximum including both events. After stripping Event 5 dominates. The indicated S/N ratio is small due to the large azimuthal spread. Both processes performed equally well, resulting in a doubtful separation if no other information is available.

Events 4 and 6, however, are well separated (Figure 18) by both processes. Stripping leaves Event 6 after Event 4 is removed. The TSML output shows two well-defined maxima at about the correct azimuths. S/N indicators are moderately low for the original FKPLOT output, somewhat higher on the stripped output. The reasons for this have been previously stated in the discussion above.

Summarizing the above results it seems that both processes perform equally well if the two events have roughly the same amplitude within the window and the S/N ratio is high.

Case 2

One signal is scaled to be three times the amplitude of the other; no noise was added.

Because the scaling was done using maximum amplitudes and not spectra, the actual amplitude ratio is somewhat different from 3:1.

The combination of Events 2 and 1 with the amplitude ratio 3:1 could not be resolved by the TSML processor but can be well resolved by FKPLOT if stripping is used. The actual amplitude ratio at the reference frequency f_o is higher than 3:1 as shown in the previous section (Figure 19), the discrepancy resulted from the rough scaling procedure used.

For the combination of Events 3 and 1 (Figure 20) with 3:1 amplitude ratio, (which is actually somewhat less at f_o) both processes separate the two events quite well if stripping is used for FKPLOT.

The superposition of Events 4 and 5 (Figure 21) shows Event 4 with high S/N on the unstripped FKPLOT output and Event 5 with moderate S/N on the stripped output. TSML fails to separate the two events with certainty, only a bulge in the -9 dB contour indicating the presence of a second signal. FKPLOT in this case performed considerably better.

The combination of Events 4 and 6 (Figure 22) shows separation of events for both processes. The Event 6 peak on the TSML output is about 6 dB down from the Event 4 peak, barely detectable and at not exactly the right azimuth but separated more from Event 4 than the original azimuth. After stripping, FKPLOT yields the Event 6 peak with a reasonable certainty but somewhat farther from the Event 4 azimuth than the original. In this example we feel that TSML performed somewhat better, since the azimuth of Event 6 is better on the TSML output although it is not much above the background level. However, the peak on the stripped FKPLOT is about 4 dB higher than the general background, but the azimuth is wrong.

Overall, if two signals are not on the same amplitude level, FKPLOT with stripping may out-perform the two segment maximum likelihood method.

Case 3

Events combined with equal maximum amplitudes, noise added. S/N ratio 2.

For this case the noise sample selected was added to the combined events.

The combination of Events 2 and 1 with noise added (Figure 23) does not separate well on the TSML frequency wavenumber spectra where a peak in the ENE direction is only slightly below the level of the very weak peak corresponding to Event 1. The separation is better on FKPLOT including the stripped version.

Both processes fail for the combination of Events 3 and 1 (Figure 24).

Comparing the outputs for the superposed Events 4 and 5 (Figure 25) it seems that both processes fail to separate the two events with certainty. The FKPLOT output has a broad peak containing both events, after stripping one obtains a peak coinciding with the direction of Event 4, but within 1 dB of many other similar peaks. The TSML output shows a complicated picture, the main peak is in a direction considerably off the direction of Event 4, possibly influenced by the noise added.

Events 4 and 6 seem to separate well on both FKPLOT and TSML outputs (Figure 26), but the azimuth corresponding to Event 4 is considerably off on the TSML output. This can be caused by a noise peak.

Case 4

Events combined with equal maximum amplitudes, noise added, S/N ratio 1.

The results of this test are shown in Figures 27 through 30. In general it can be said that both FKPLOT and the TSML process break down, showing many peaks at the wrong azimuths and velocities, which have apparently no relationship to the actual signals present, while also revealing occasional signal peaks which cannot be distinguished from false peaks. Thus both f-k processes require a signal to noise ratio of about 2 to perform adequately.

F-K ANALYSES WITH THE LASA F RING OMITTED

General

The omission of the F ring reduces the array diameter from 200 to 125 km (Figure 72) with a corresponding reduction of resolving power. All runs were repeated with the reduced array, including the individual event and noise samples, to give a basis of reference for comparison of various signal and noise combination f-k plots using this array configuration.

Individual signals and noise

The f-k plots of individual signals are shown in Figures 31 through 36. There are no basic differences between the plots shown and those computed using the full array except for the reduction in the resolution for both processes, although the resolution should not reduce as much in the case of TSML according to theory. The sidelobe pattern is naturally different for this array configuration, but otherwise the removal of F ring did not make much difference. Event 5 (Figure 35) shows a peculiar double arrival pattern, not seen before. The noise sample analysis are shown in Figure 37.

ANALYSIS OF COMBINED EVENTS

Except for the array configuration, all cases are identical to those mentioned previously.

Case 1

Events are equal in amplitude; no noise added.

As in the case of the full array, the combination of Events 1 and 2 is resolved by both processes (Figure 38); the combination of Events 1 and 3 is resolved well by TSML but not well by FKPLOT (Figure 39) because it stripped on the wrong peaks at the right side of the figure. The combination of Events 4 and 5 fails again as in the previous case as can be expected with reduced resolution (Figure 40). The separation is successful for the combination of Events 4 and 6 (Figure 41).

Case 2

One signal is scaled to be three times the amplitude of the other; no noise is added.

As in the full array, the combination of Events 2 and 1 (Figure 42) could not be resolved well by TSML, although there are indications of the second signal (dashed contours). FKPLOT, on the other hand, resolves both signals with a little ambiguity, a southwesterly peak at 3 dB below the first peak. The combination of Events 3 and 1 (Figure 43) is resolved by both processes. The combination of Events 4 and 5

(Figure 44) is resolved by FKPLOT but not by the TSML process. The combination of Events 4 and 6 (Figure 45) is resolved by both.

Case 3

Events combined with equal maximum amplitudes, noise added. S/N ratio 2.

A brief summary of these runs is as follows: combinations of Events 1 and 2 (Figure 46) and Events 4 and 6 (Figure 49) are poorly resolved by TSML, fairly well resolved by FKPLOT. The other combinations (Figures 47 and 48) are not resolved by either process.

Case 4

Events combined with equal maximum amplitudes, noise added. S/N ratio 1.

None of these cases (Figures 50-53) is resolved, except the combination of Events 1 and 2 (Figure 50) by FKPLOT.

F-K ANALYSES USING THE D RING AND CENTER ELEMENT ONLY

General

This configuration has a very small array diameter (∿50 Km) and contains only five array elements (see Figure 72). This diameter is comparable to that of the seven-element hexagonal array exemplified by the inner part of ALPA, which was proposed as a standard for long-period arrays. Although our array has only five elements, it is fairly characteristic of small arrays consisting of only a few elements such as the seven-element hexagonal array. Because of a bad D2 trace, Event 5 and combinations involving it were omitted from this array analysis.

Individual signals and noise

Figures 54 through 58 show the f-k plots of the individual events and Figure 59 that of the noise. The f-k spectra of the individual events clearly demonstrate the differences between the appearance of the outputs of both processes. The TSML outputs all show a well localized peak, low or no side lobes, while the spectral peak of the FKPLOT output is considerably broadened, and the side lobes are prominent. Although the peaks of TSML output also broadened with the reduction of the array diameter, this broadening is relatively small compared to that of the FKPLOT output (compare with Figures 8 through 13).

ANALYSIS OF COMBINED EVENTS

Case 1

Events are equal in amplitude; no noise added.

The combination of Events 1 and 2 (Figure 60) is considered to be resolved on both types of outputs, although a special -4 dB contour is needed to show a second peak on the TSML output. However, the bulge of the -6 dB contour is so conspicuous that it inevitably suggests the presence of a second signal. FKPLOT resolves both signals with stripping. The combination of Events 1 and 3 (Figure 61) is also resolved with questionable accuracy. The TSML shows a -9 dB peak at the right place for Event 3. The original FKPLOT shows both peaks, but it strips on the wrong peak leaving a very doubtful signal peak. The combination of Events 4 and 6 (Figure 62) is resolved by FKPLOT but not by the TSML.

Case 2

One signal is scaled to be three times the amplitude of the other, no noise added (Figures 63-65).

This case can be summarized as follows: the combination of Events 2 and 1 (Figure 63) is not clearly resolved by either method. Signal 1 on TSML output is indicated by a bulge in the -12 dB contour. FKPLOT shows Event 2 clearly, but the stripped version is somewhat ambiguous. The combination of Events 3 and 1

(Figure 64) is considered to be resolved by both processes, although an additional -7 dB contour is needed to define a second peak on the TSML. The combination of Events 4 and 6 (Figure 65) is resolved by FKPLOT but not by TSML.

Case 3

Events combined with equal maximum amplitudes, noise added, S/N ratio 2 (Figures 66-68).

None of these combinations is resolved except for Events 1 and 2 (Figure 66) by FKPLOT.

Case 4

Events combined with equal maximum amplitudes, noise added, S/N ratio 1 (Figures 69-71).

None of the combinations is resolved.

SUMMARY AND CONCLUSIONS

Comparison of the two segment maximum likelihood process (TSML) and the fast frequency domain beaming process (FKPLOT, FKCOMB) combined with stripping shows that the two processes are comparable in performance, but the latter process performs somewhat better since more multiple signal separations were achieved by FKPLOT as demonstrated by Table III. The advantage of FKPLOT can be attributed to the stripping process which can uncover weak signals in the presence of strong signals. It is possible, however, to combine the TSML with a procedure which is equivalent to stripping, such as spectral eigenvector-eigenvalue analysis, in which case TSML performs as well or even better than FKPLOT; this is the subject of a report now in preparation. One clear advantage of the TSML process is the small dependence of the F-K spectra on the array response. The inspection of the TSML f-k spectra immediately gives a clear idea about the azimuthal and velocity distribution of energy, while FKPLOT gives a confusing picture full of distracting side lobes which are almost as large as the main lobe, especially if the array has only a few widely spaced elements (see Figure 64, for example). Another disadvantage of the stripping procedure is that it can strip on a false signal consisting of the combined side lobes of two signals or sidelobes combined by noise peaks, resulting in the complete breakdown of the process

(see Figures 38 and 63, for example). The problem can be minimized by stripping on peaks which fall into the expected velocity range of the signal.

Another advantage of FKPLOT is that it seems to be somewhat more stable in the presence of noise. (This is confirmed by theory of Capon and Goodman [1970].) Both processes require a signal to noise amplitude ratio of about 2 to perform adequately.

REFERENCES

Blandford, R., 1972. Qualitative properties of the F detector, Seismic Data Laboratory Report #?91, Teledyne Geotech, Alexandria, Virginia, AD #753-059.

Blandford, R., Cohen, T., and Woods, J., 1973. An iterative approximation to the mixed-signal processor, SDAC Report TR-73-7, Teledyne Geotech, Alexandria, Virginia.

Capon, J., Greenfield, R. J., and Kolker, R. J., 1967. Multidimensional maximum likelihood processing of a large aperture seismic array; Proc. IEEE, 55, 192-211.

Capon, J., 1969. High resolution frequency wavenumber spectrum analysis; Proc. IEEE, 57, 1408-1418.

Capon, J. and Goodman, N. R., 1970. Probability distribution for estimators of the frequency-wavenumber spectrum; Proc. IEEE letters, 58, 1785-1786.

Lintz, P. R., 1968. An analysis of a technique for the generation of high resolution wavenumber spectra. Seismic Data Laboratory Report #218, Teledyne Geotech, Alexandria, Virginia. AD #834-725.

McCowan, D. W. and Lintz, P. R., 1968. High resolution frequency wavenumber spectra, Seismic Data Laboratory Report #206, Teledyne Geotech, Alexandria, Virginia. AD #827-959.

REFERENCES (Continued)

Mack, H. and Smart, E., 1972. Frequency domain processing of digital microbarograph data, J. Geophys. Res., 77, 488-490.

Smart, E., 1971. Erroneous phase velocities from frequency-wavenumber spectral sections, Geophys. J. R. Astr. Soc., 36, 247-254.

Smart, E., 1972. FKCOMB, A fast general-purpose array processor, SAAC Report No. 9, Teledyne Geotech, Alexandria, Virginia.

Smart, E. and Flinn, E., 1971. Fast frequency-wavenumber analysis and Fisher signal detection in real-time infrasonic array data processing, Geophys. J. R. Astr. Soc., 26, 279-284.

Woods, J. W. and Lintz, P. R., 1973. Plane waves at small arrays. Geophysics, v. 38, 1023-1041.

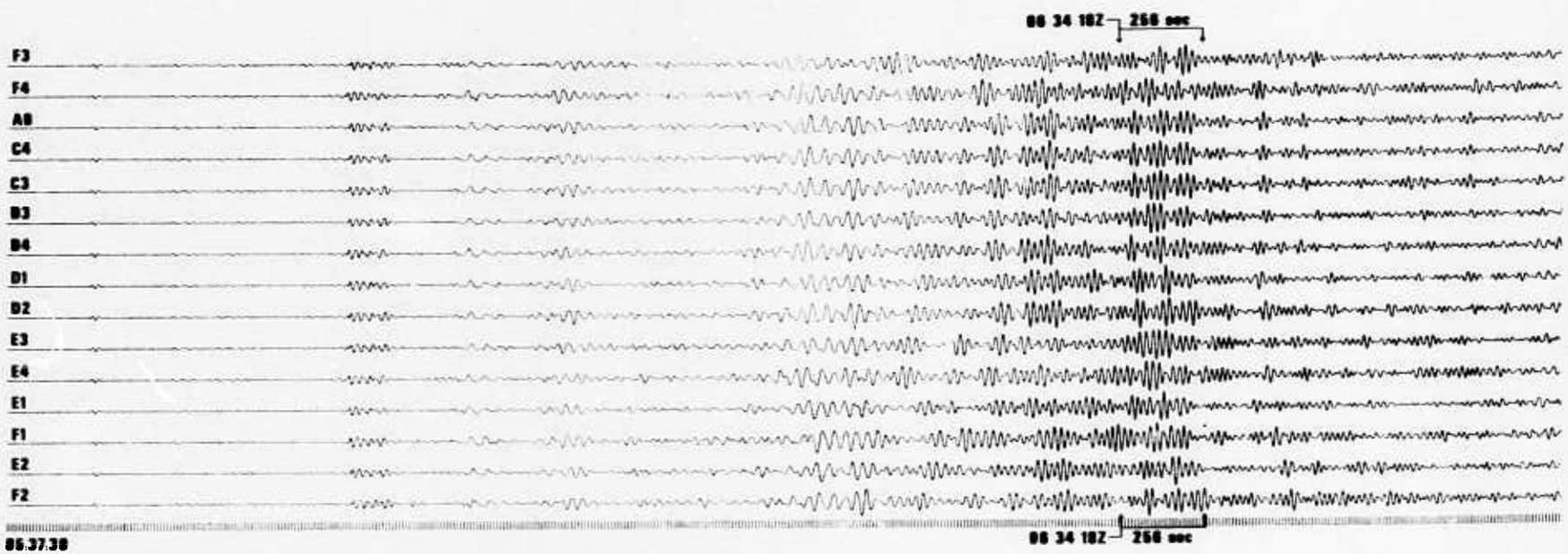

Figure 1. Event 1, Philippine Islands Region, 8 January 1972.

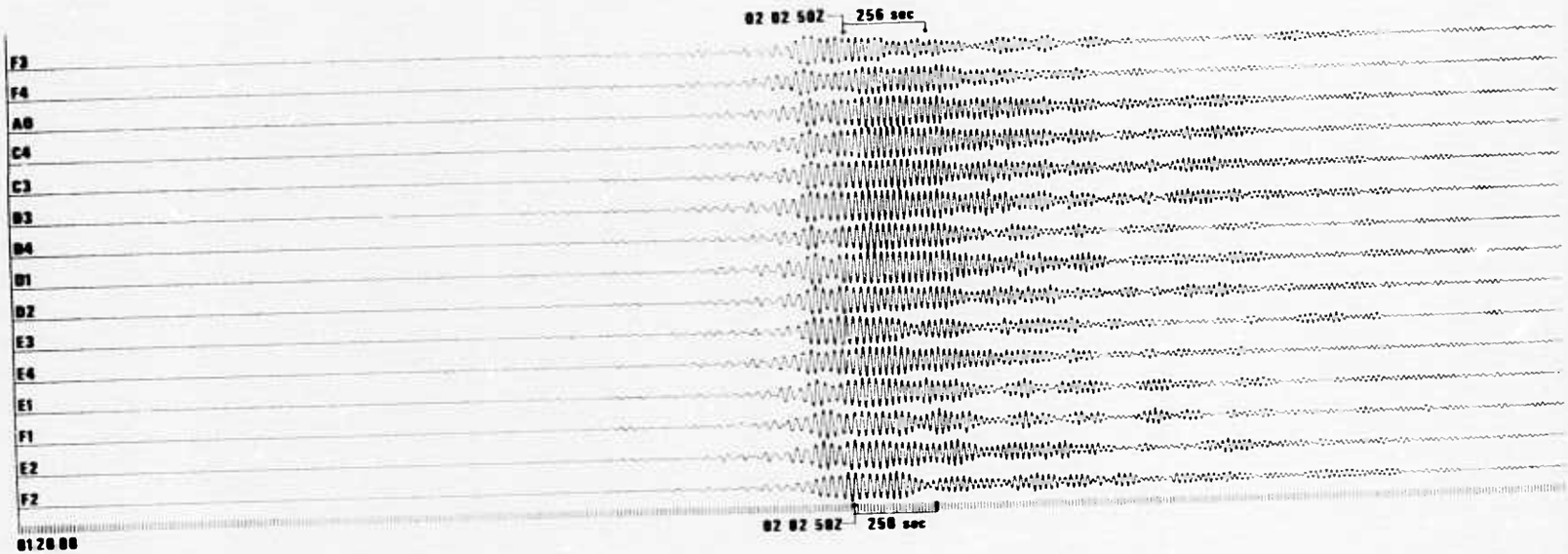

Figure 2. Event 2, New Britain Region, 28 July 1971.

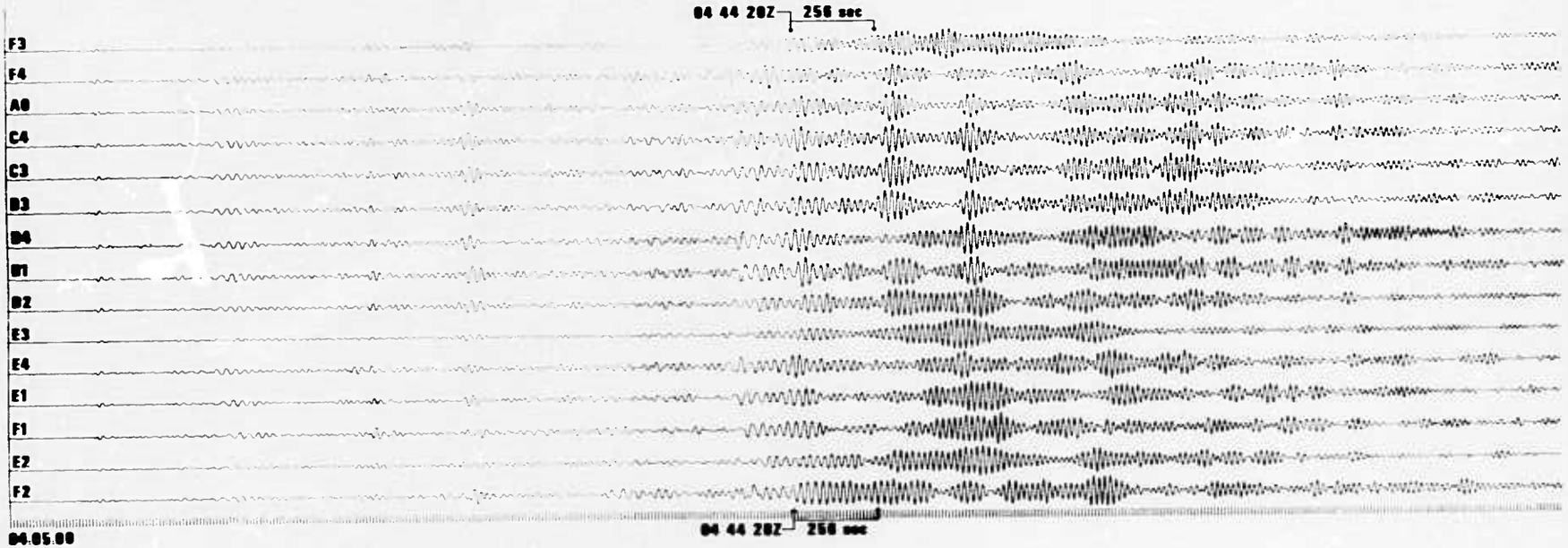

Figure 3. Event 3, New Hebrides Islands, 24 January 1972.

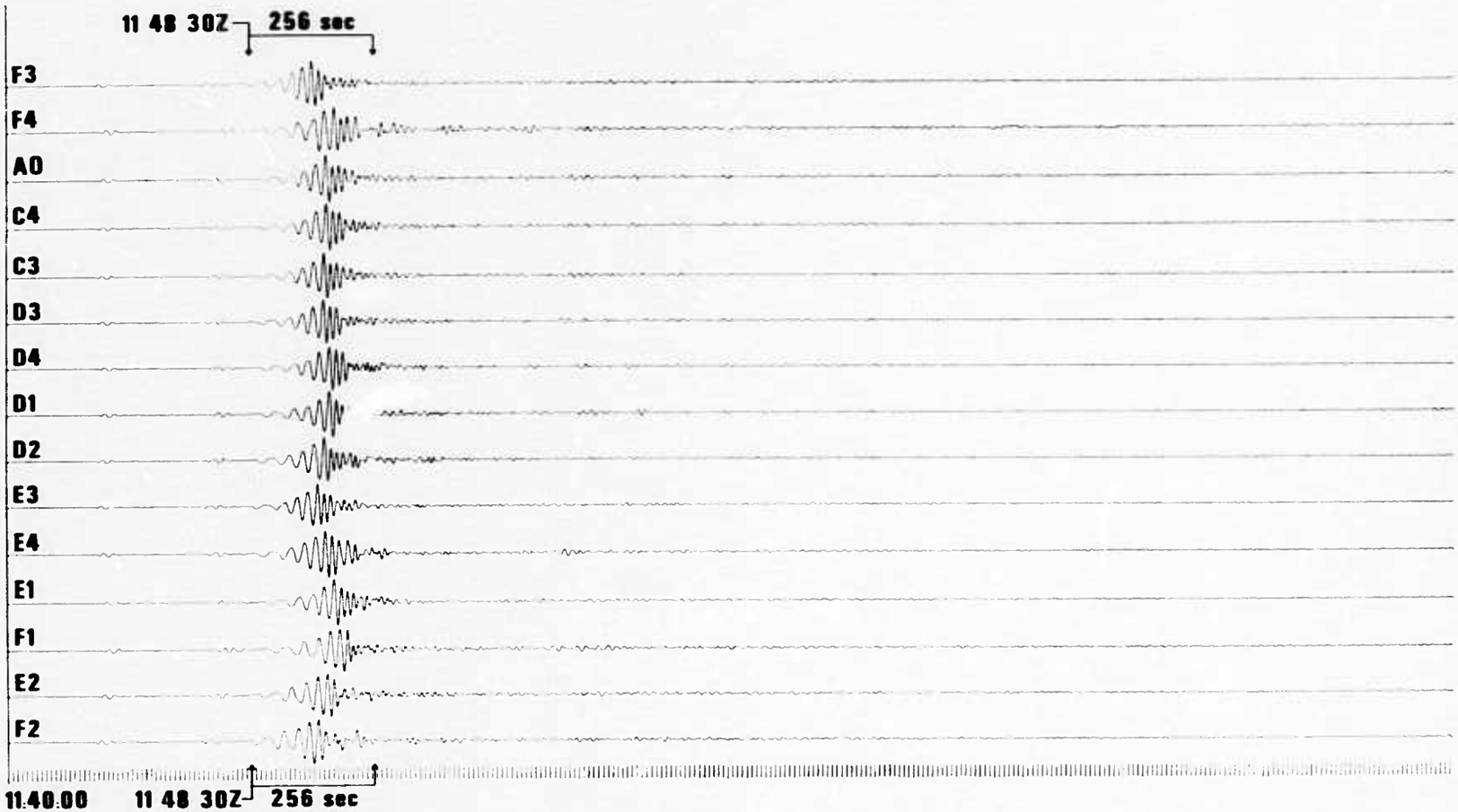

Figure 4. Event 4, Baja California, 14 April 1971.

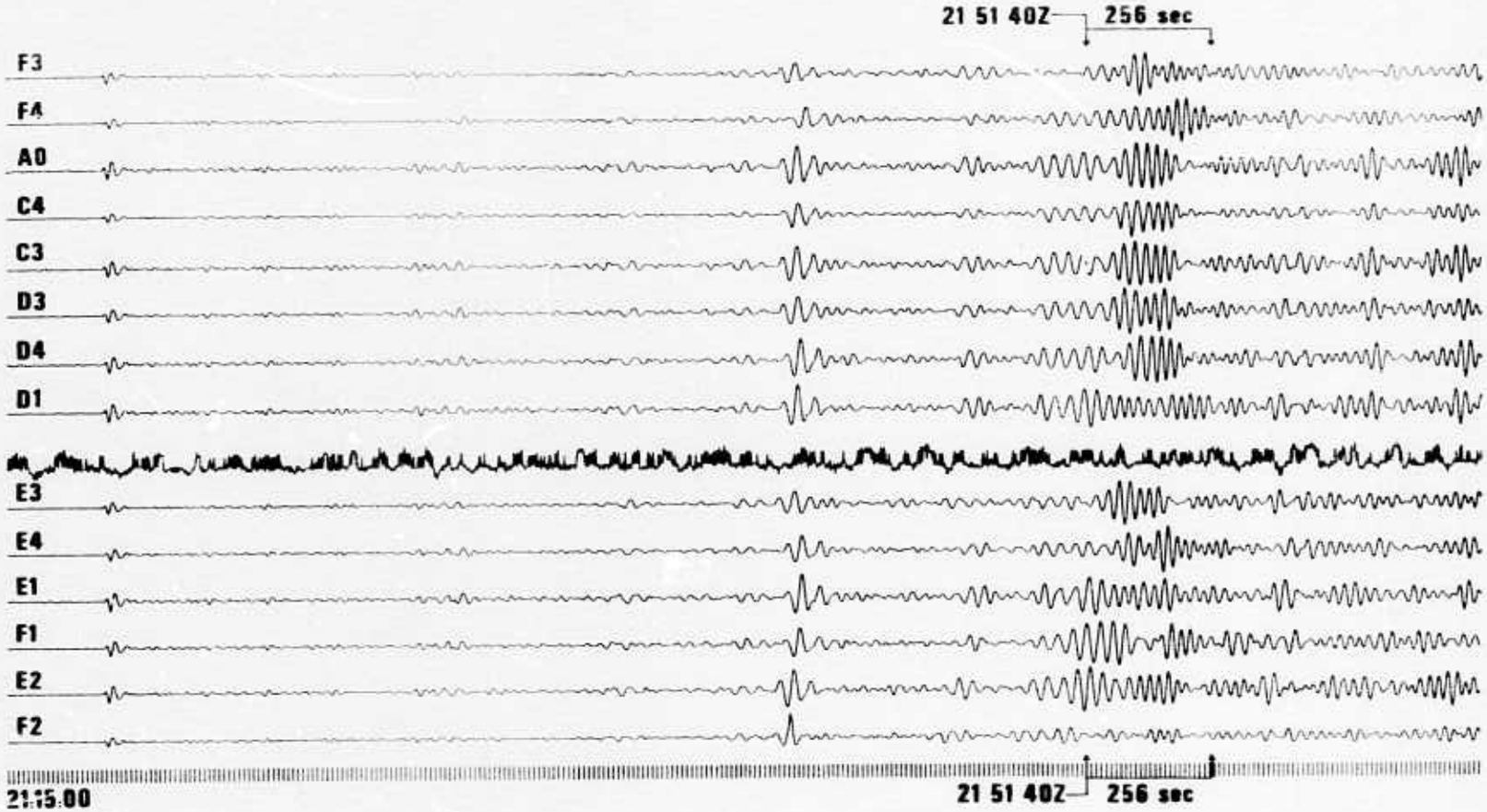

Figure 5. Event 5, San Juan Province, Argentina, 26 September 1972.

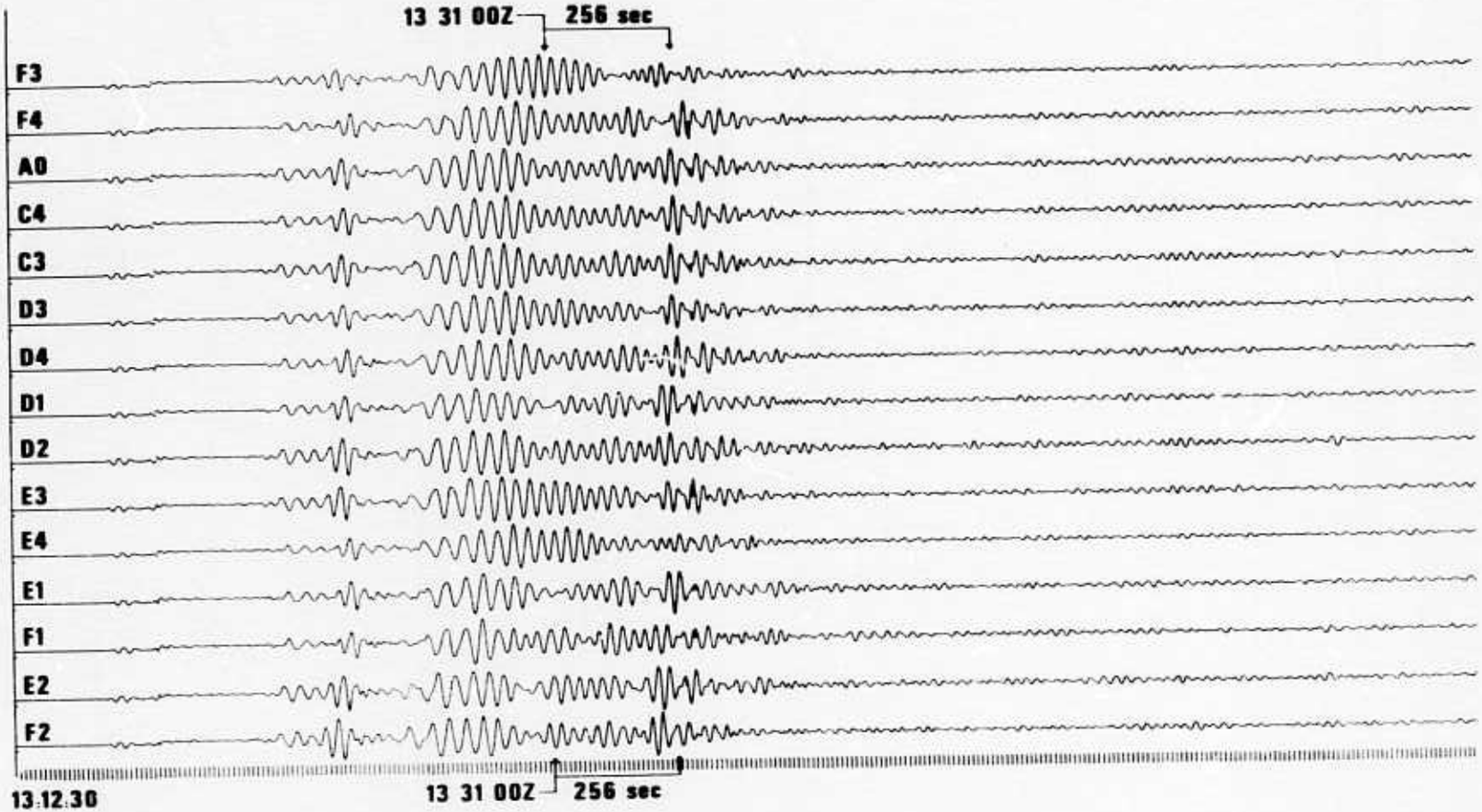

Figure 6. Event 6, Guatemala, 22 January 1972.

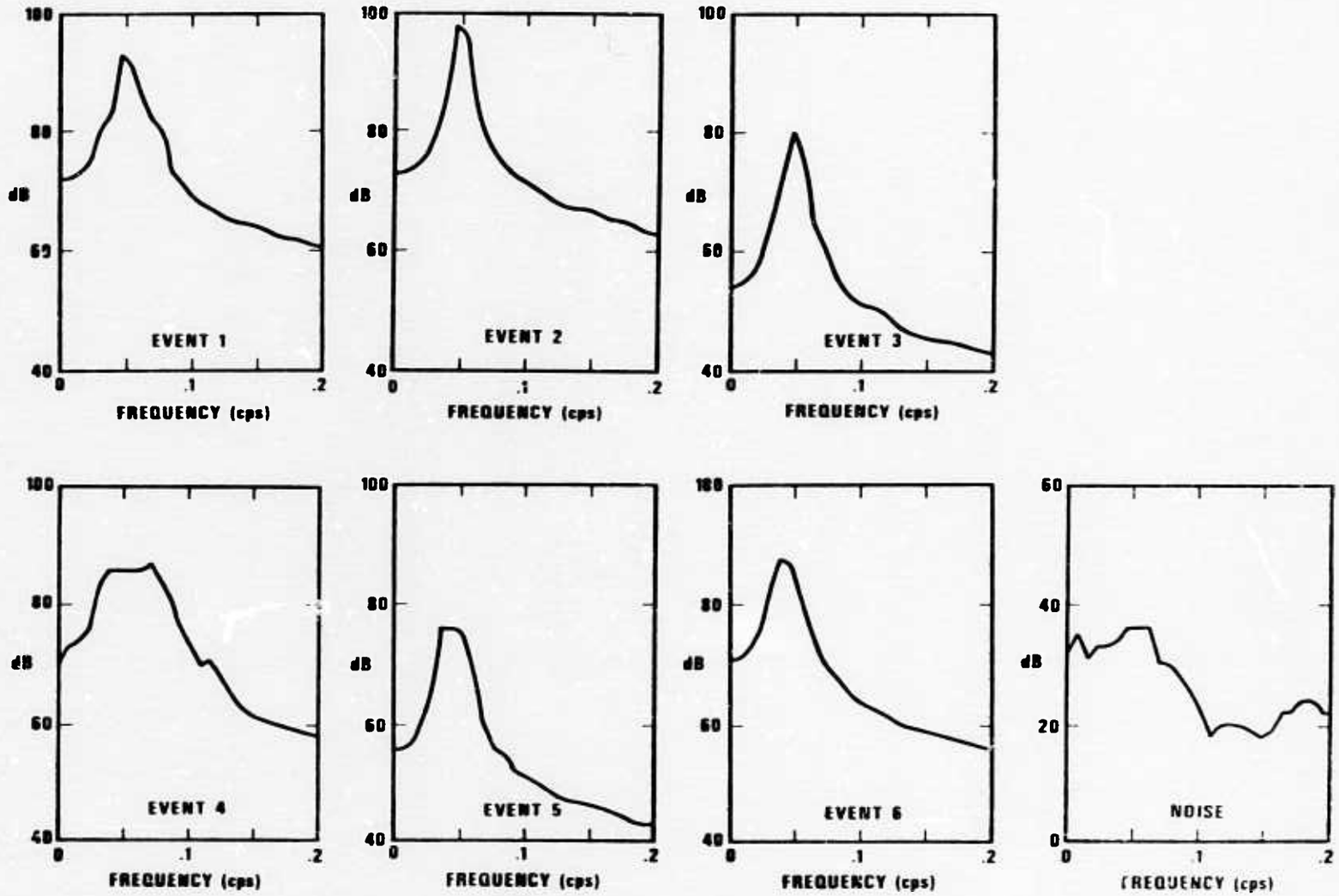

Figure 7. Relative spectral shapes for Events 1 through 6 and the noise sample.

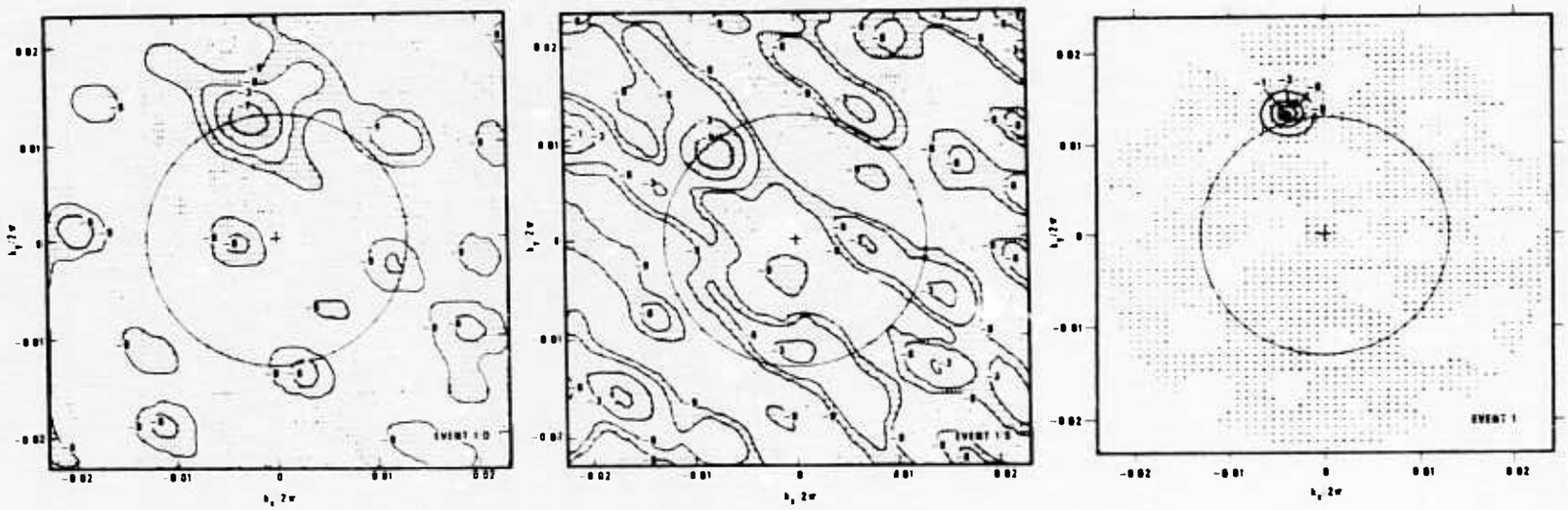

Original FKPLOT

Stripped FKPLOT

TSML

Figure 8. F-K spectra for Event 1.

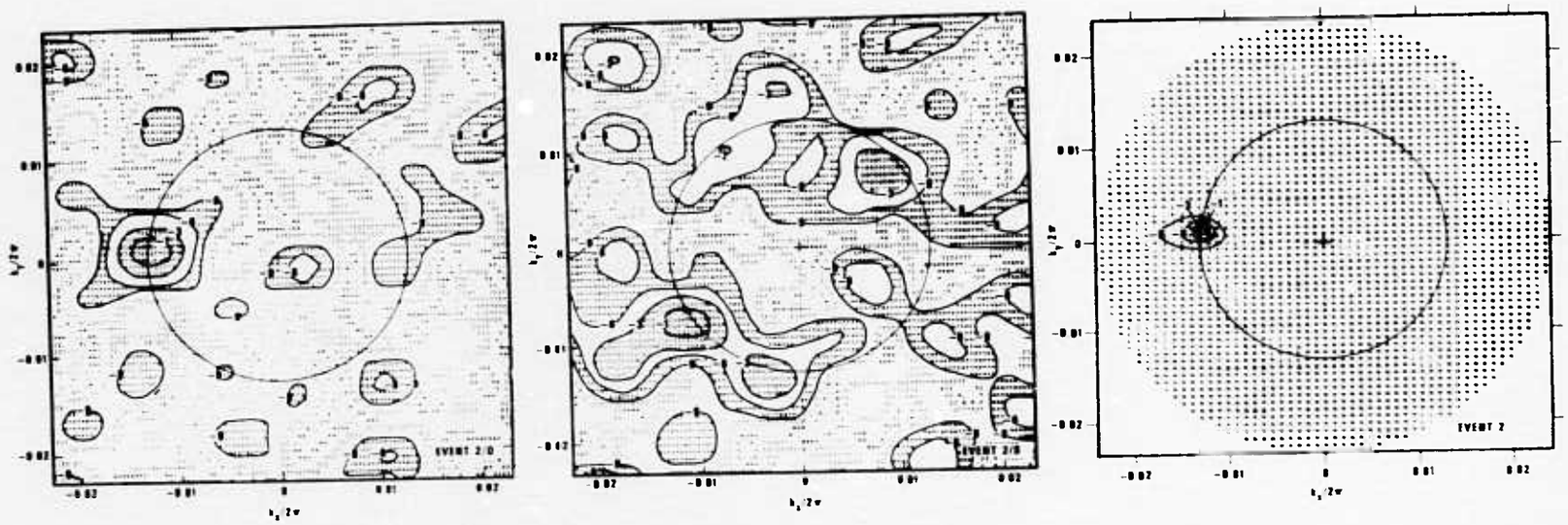

Original FKPLOT

Stripped FKPLOT

TSML

Figure 9. F-K spectra for Event 2.

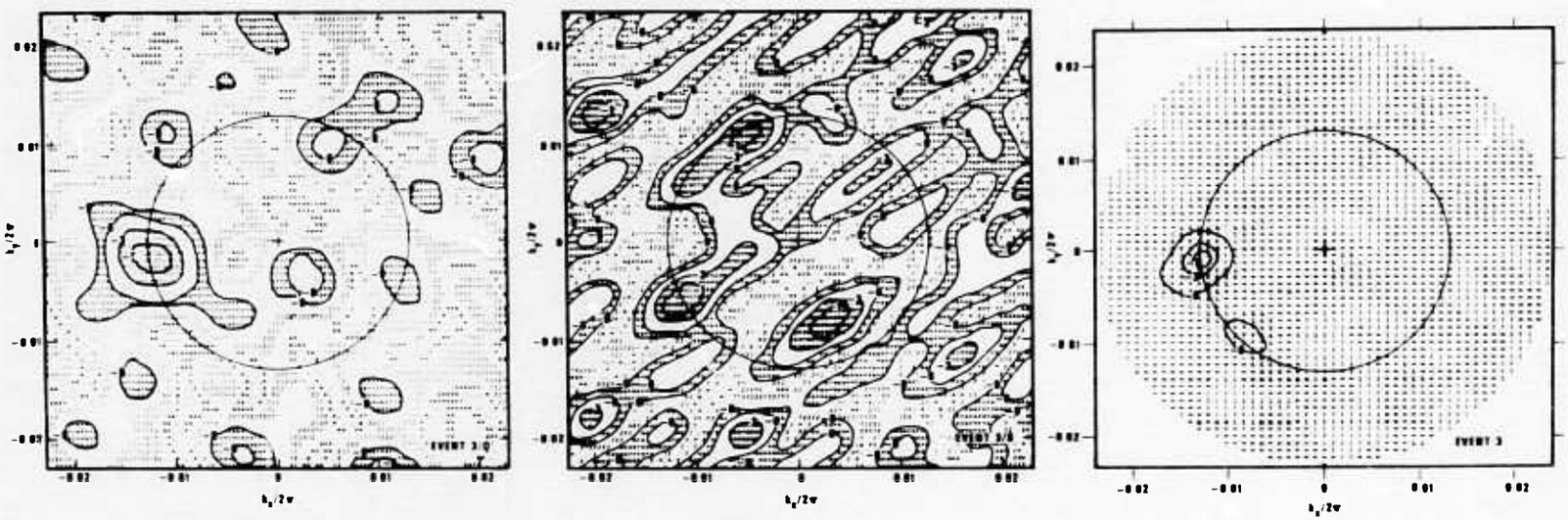

Original FKPLOT

Stripped FKPLOT

TSML

Figure 10. F-K spectra for Event 3.

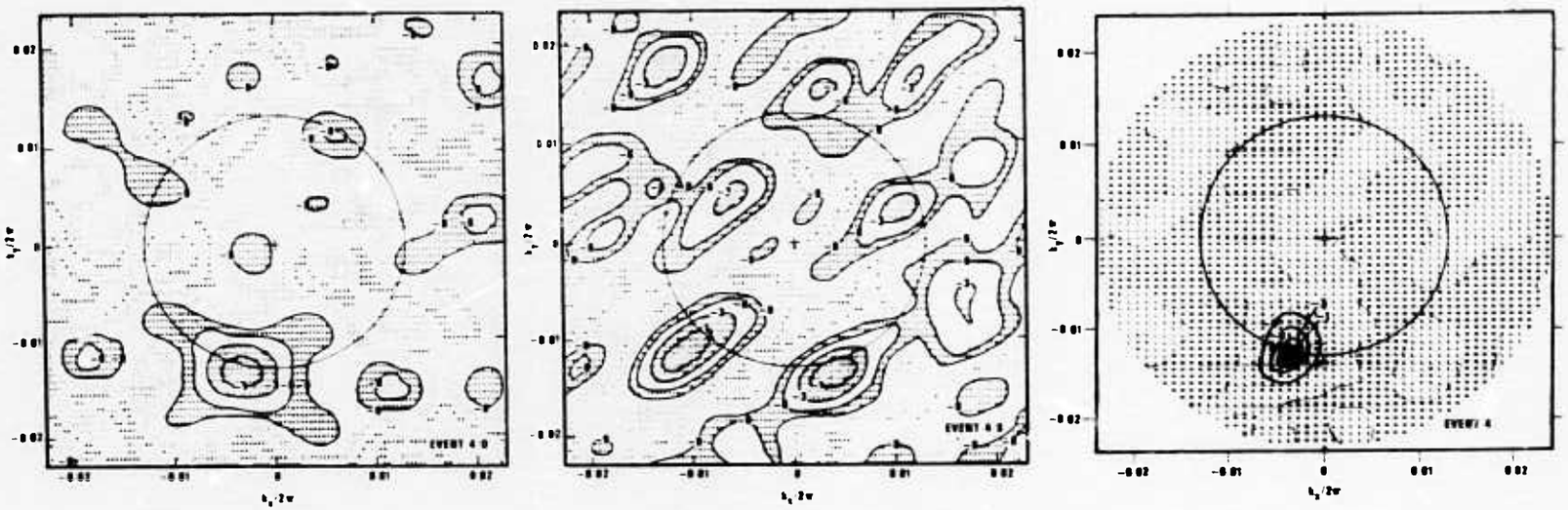

Original FKPLOT

Stripped FKPLOT

TSML

Figure 11. F-K spectra for Event 4.

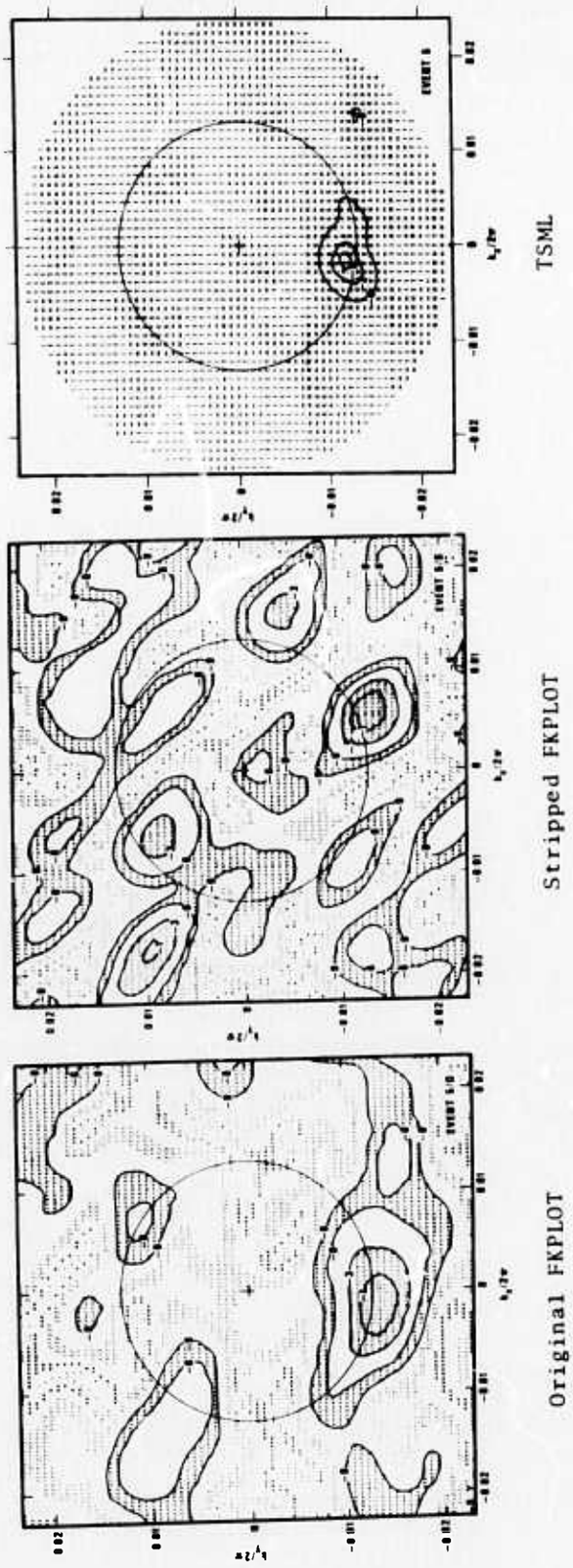

Figure 12. F-K spectra for Event 5.

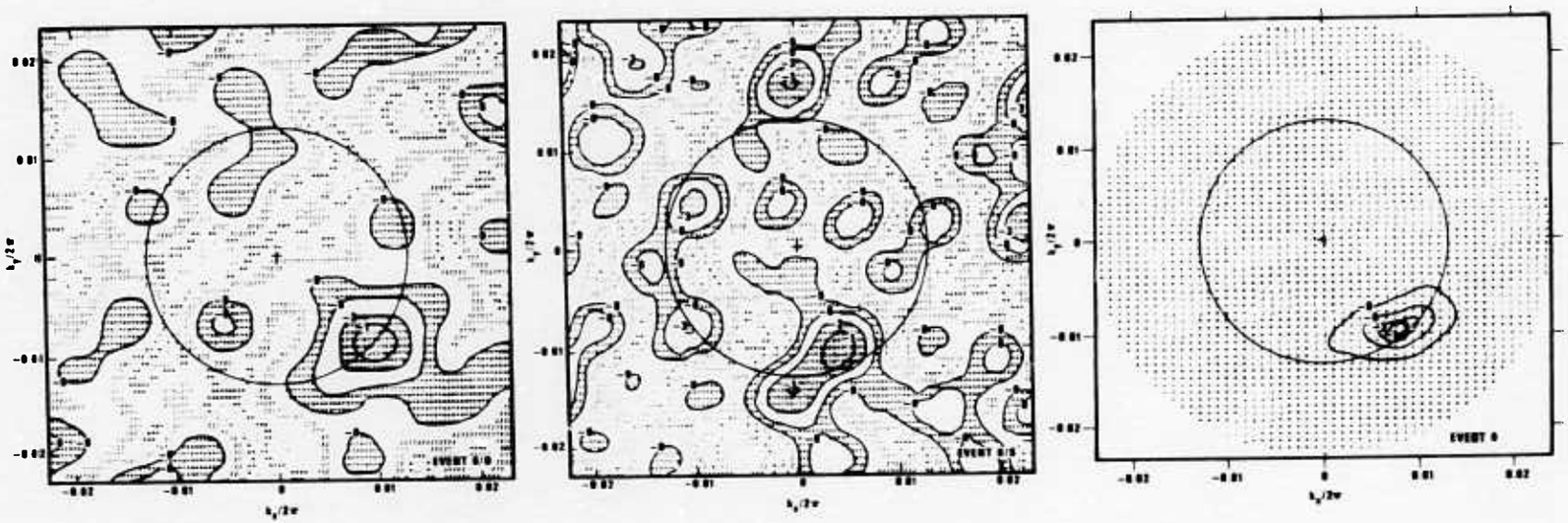

Original FKPLOT

Stripped FKPLOT

TSML

Figure 13. F-K spectra for Event 6.

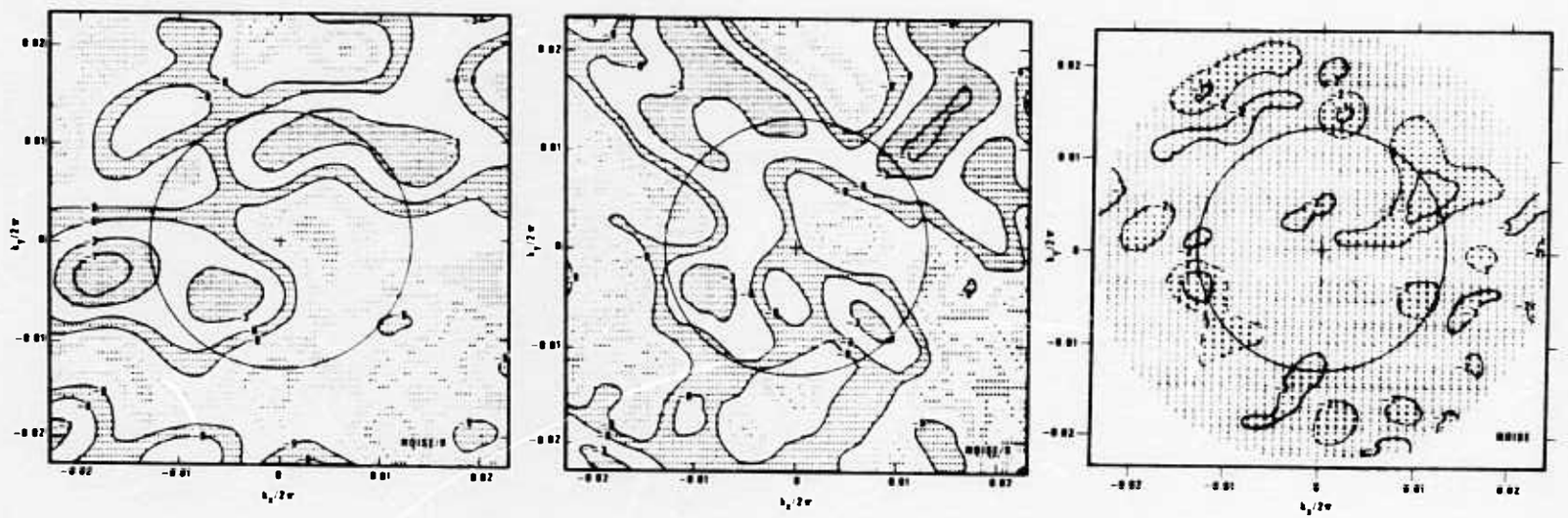

Original FKPLOT

Stripped FKPLOT

TSML

Figure 14. F-K spectra for the noise sample.

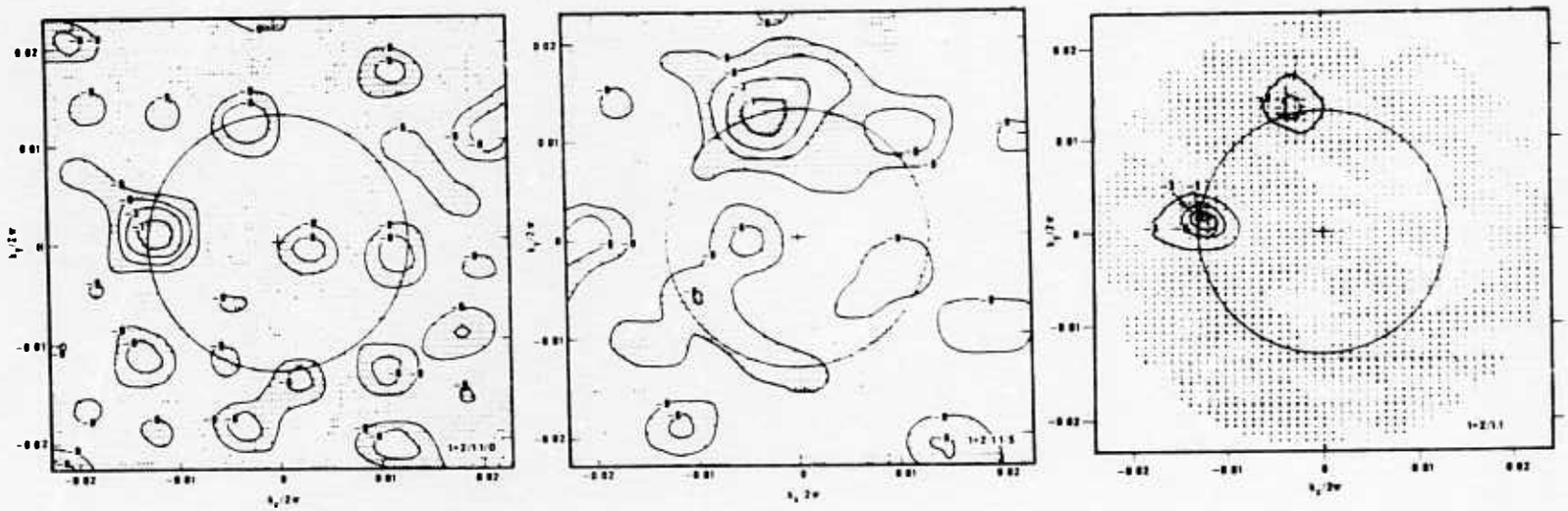

Original FKPLOT Stripped FKPLOT TSML

Figure 15. F-K spectra for Events 1 and 2 combined equally.

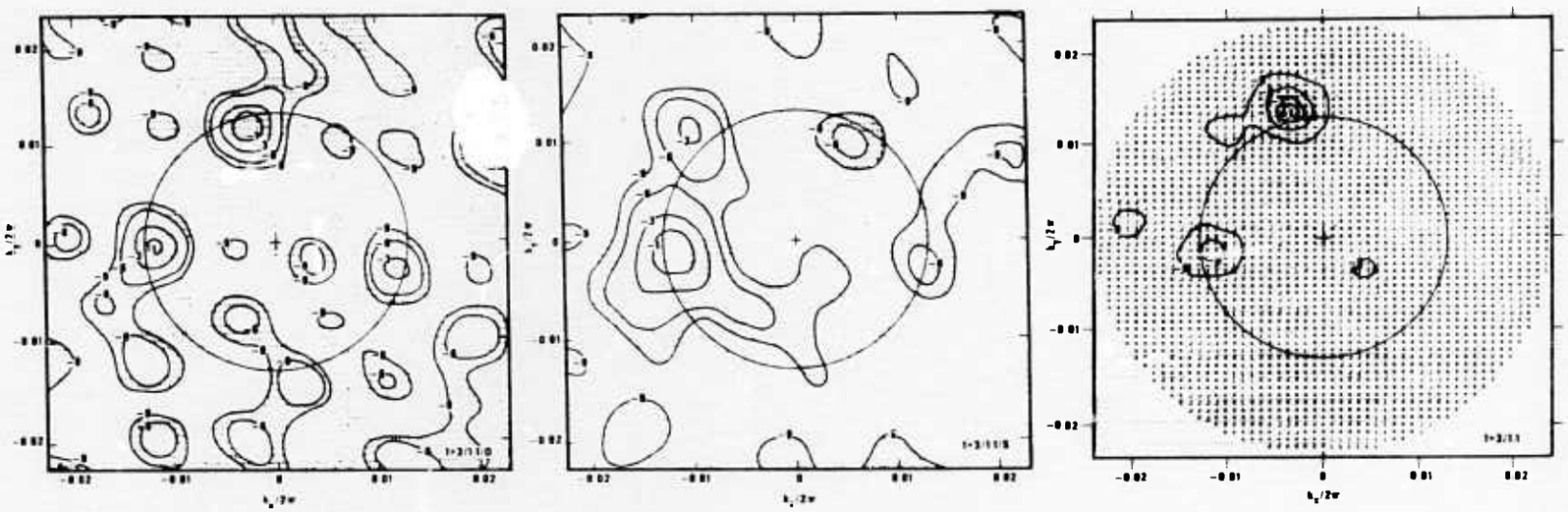

Original FKPLOT Stripped FKPLOT TSML

Figure 16. F-K spectra for Events 1 and 3 combined equally.

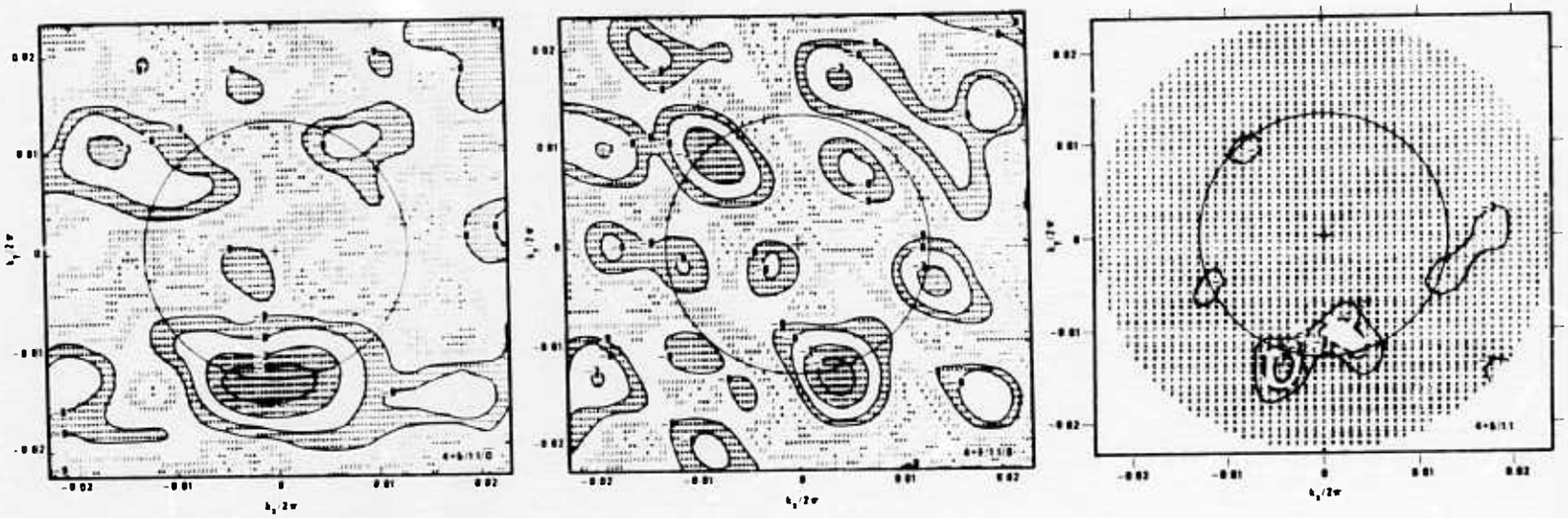

Original FKPLOT

Stripped FKPLOT

TSML

Figure 17. F-K specta for Events 4 and 5 combined equally.

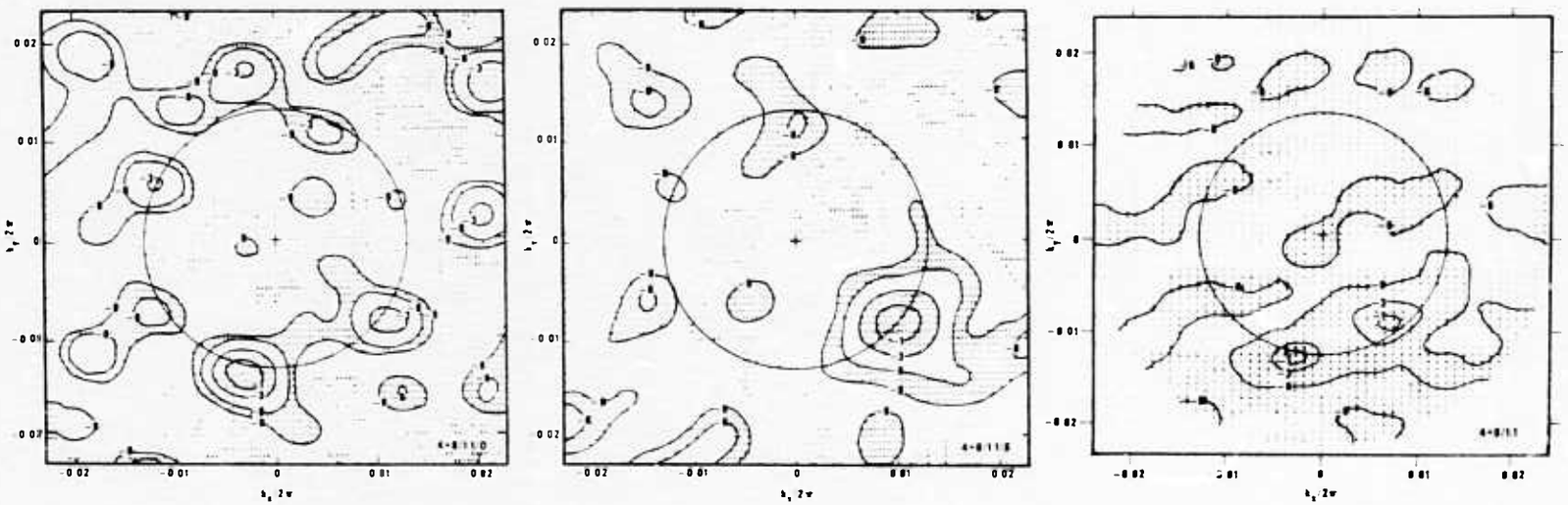

Original FKPLOT Stripped FKPLOT TSML

Figure 18. F-K spectra for Events 4 and 6 combined equally.

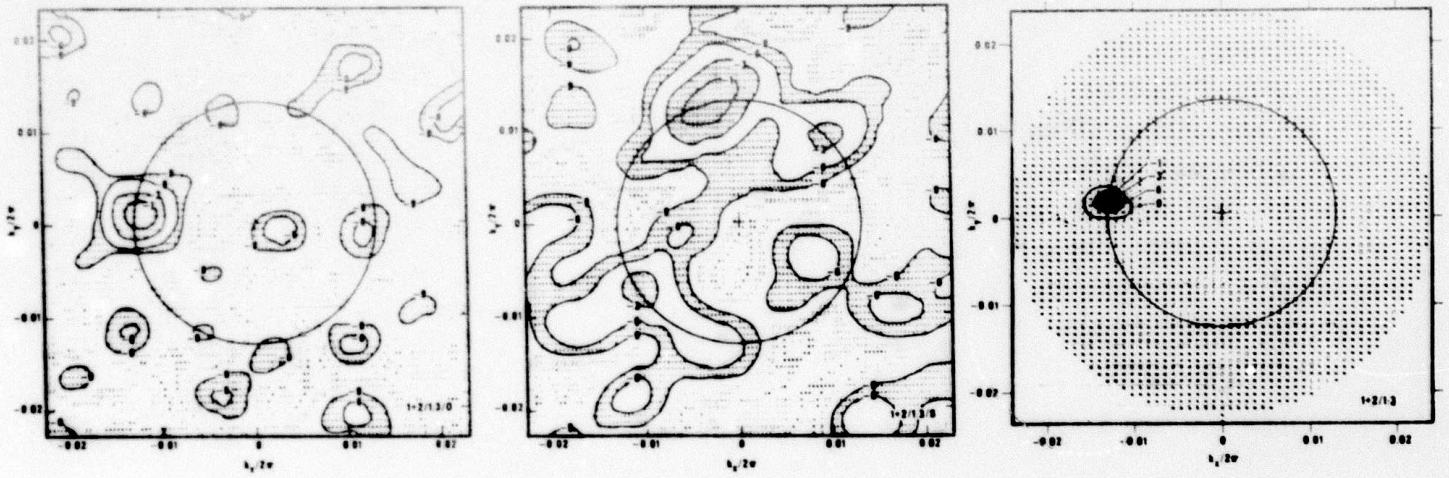

Original FKPLOT Stripped FKPLOT TSML

Figure 19. F-K spectra for Events 2 and 1 combined in a a 3 to 1 ratio.

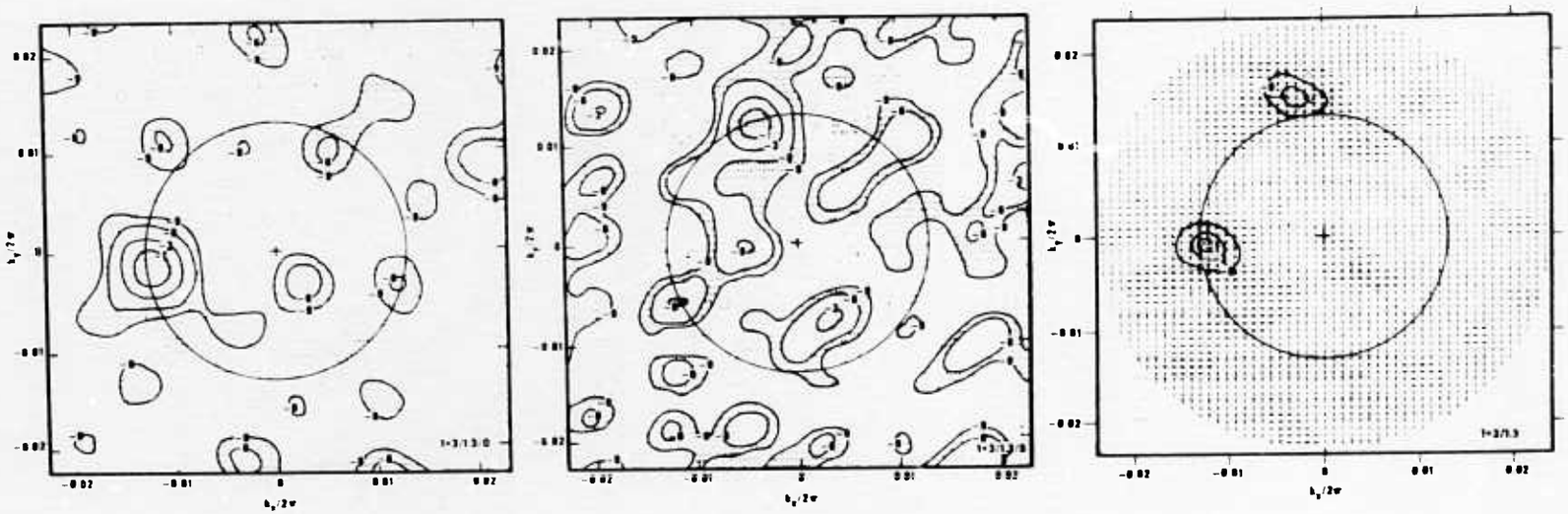

Original FKPLOT

Stripped FKPLOT

TSML

Figure 20. F-K spectra for Events 3 and 1 combined in a 3 to 1 ratio.

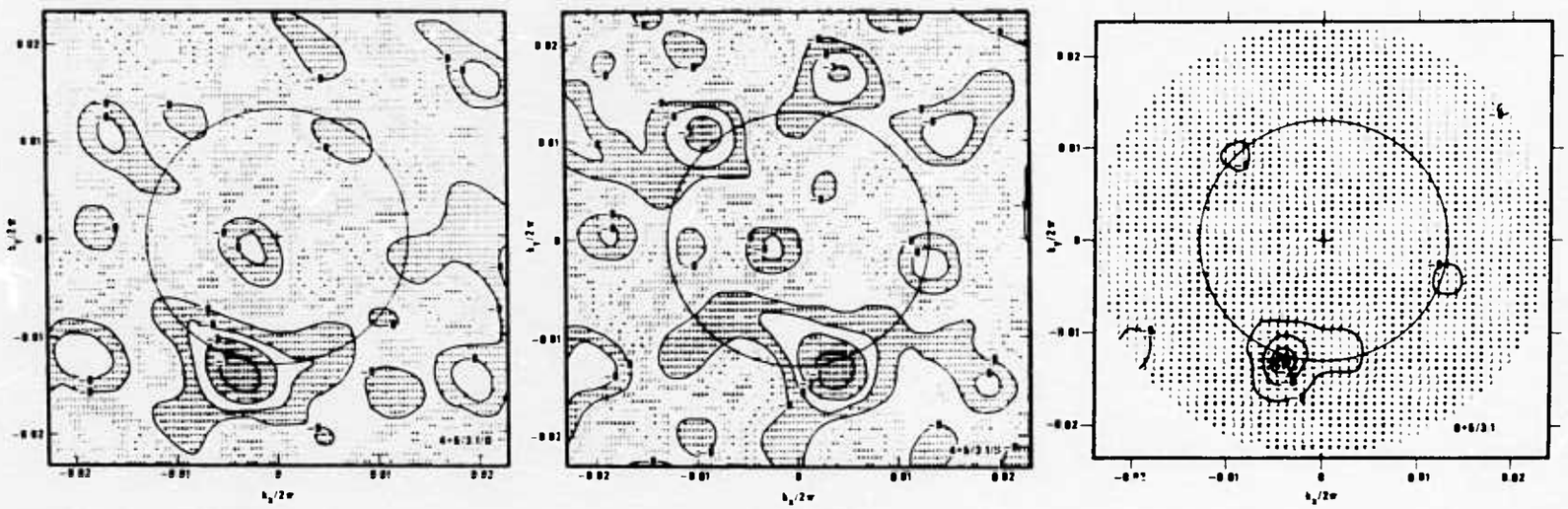

Original FKPLOT

Stripped FKPLOT

TSML

Figure 21. F-K spectra for Events 4 and 5 combined in a 3 to 1 ratio.

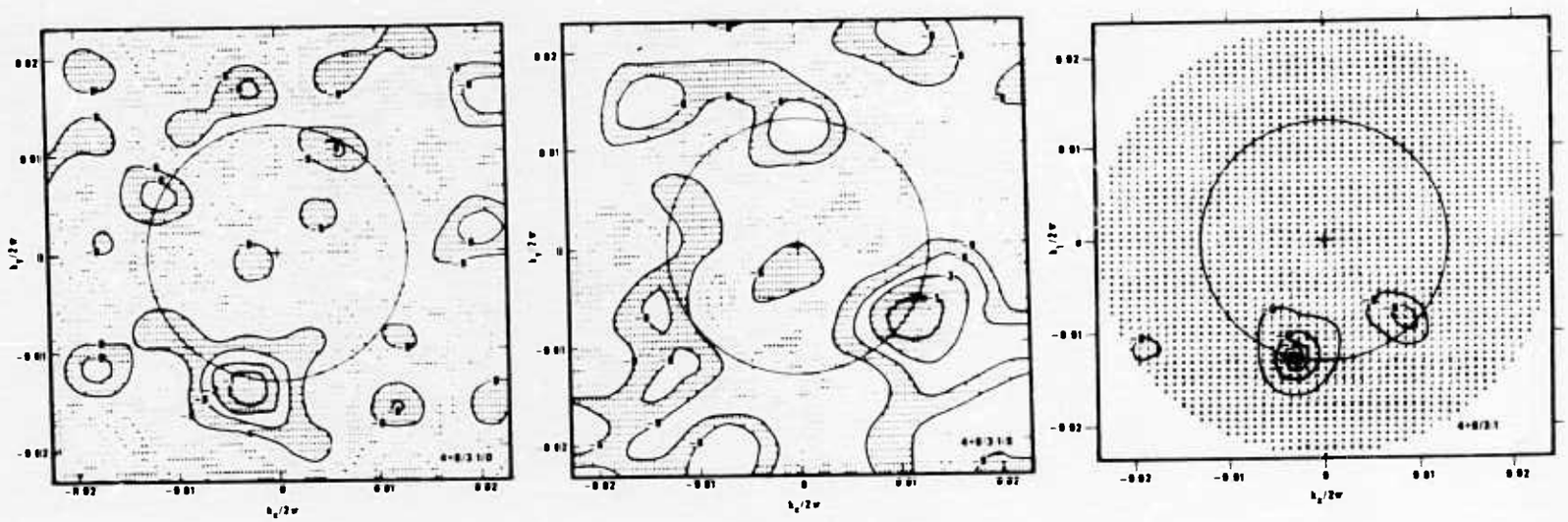

Original FKPLOT

Stri[illegible]ed FKPLOT

TSML

Figure 22. F-K spectra for Events 4 and 6 combined in a 3 to 1 ratio.

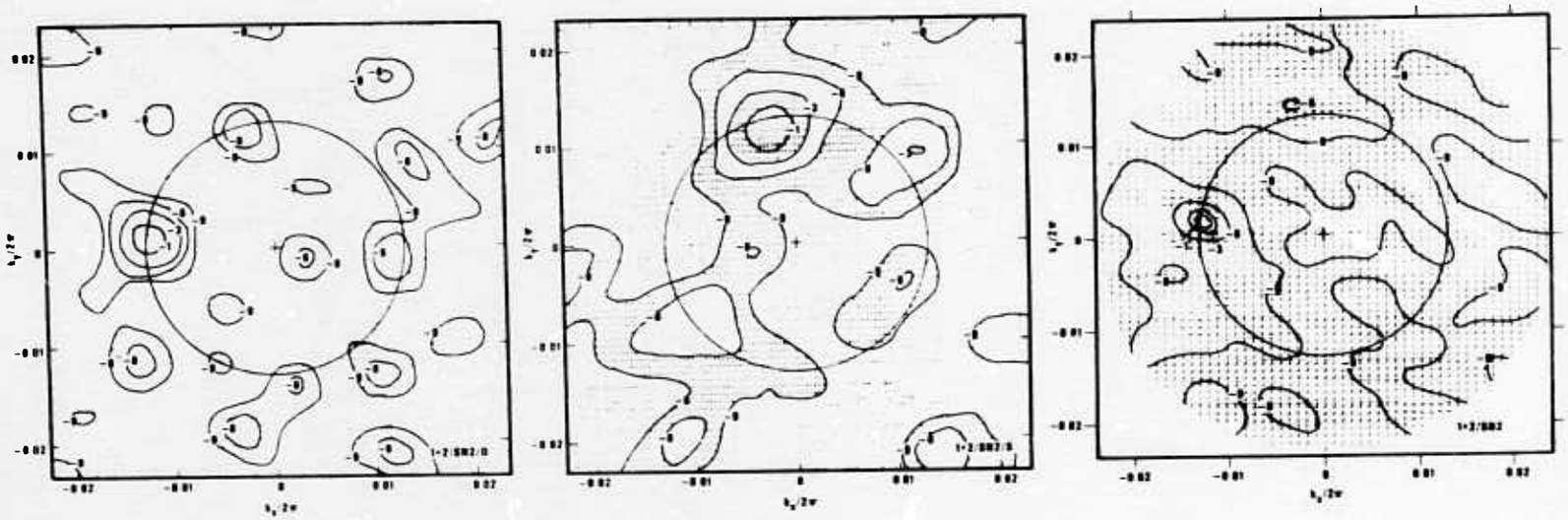

Figure 23. F-K spectra for Events 1 and 2 combined with noise. S/N=2.

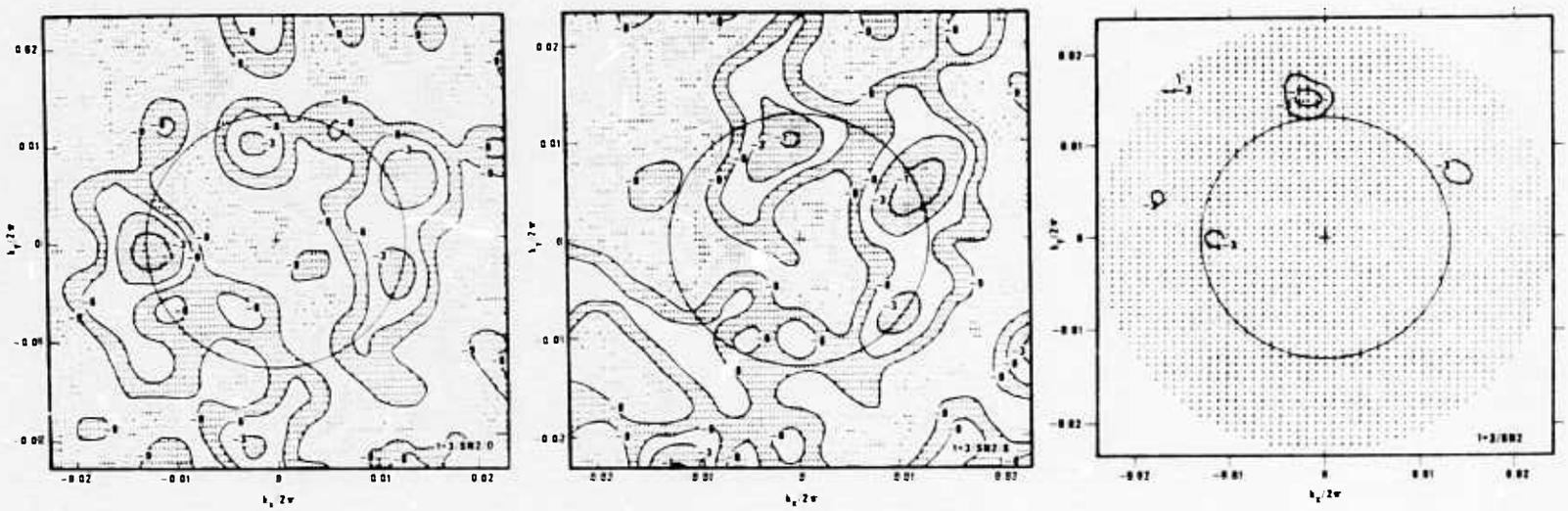

Original FKPLOT Stripped FKPLOT TSML

Figure 24. F-K spectra for Events 1 and 3 combined with noise. S/N=2.

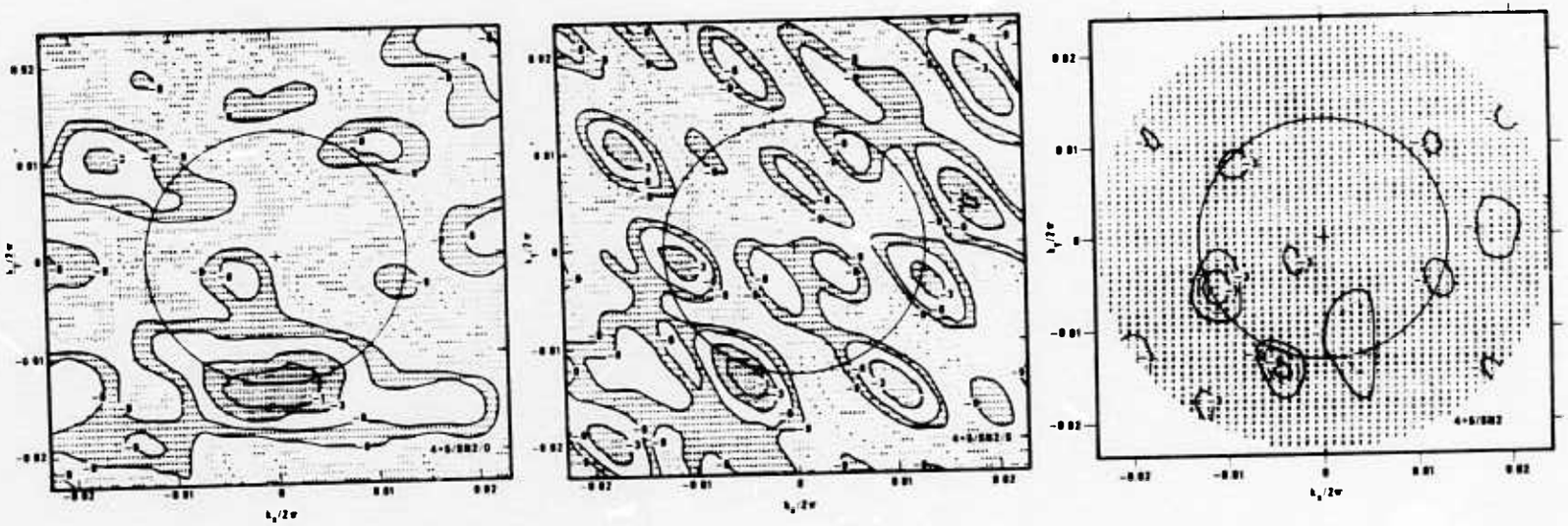

Original FKPLOT

Stripped FKPLOT

TSML

Figure 25. F-K spectra for Events 4 and 5 combined with noise. S/N=2.

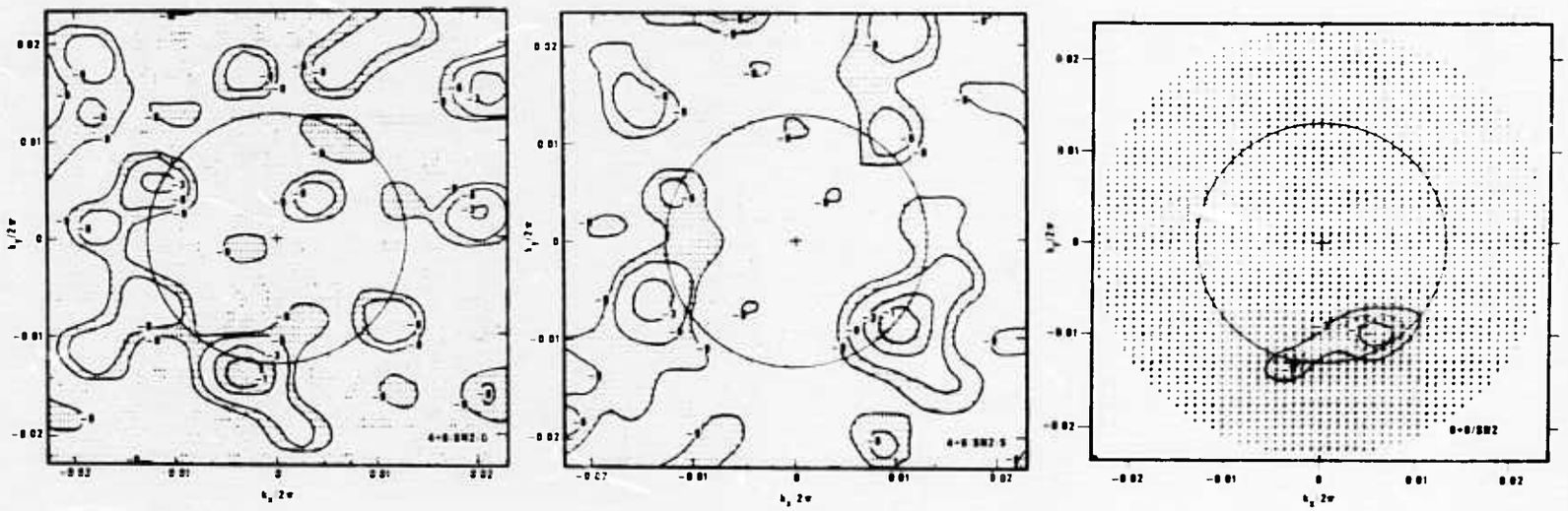

Original FKPLOT

Stripped FKPLOT

TSML

Figure 26. F-K spectra for Events 4 and 6 combined with noise. S/N=2.

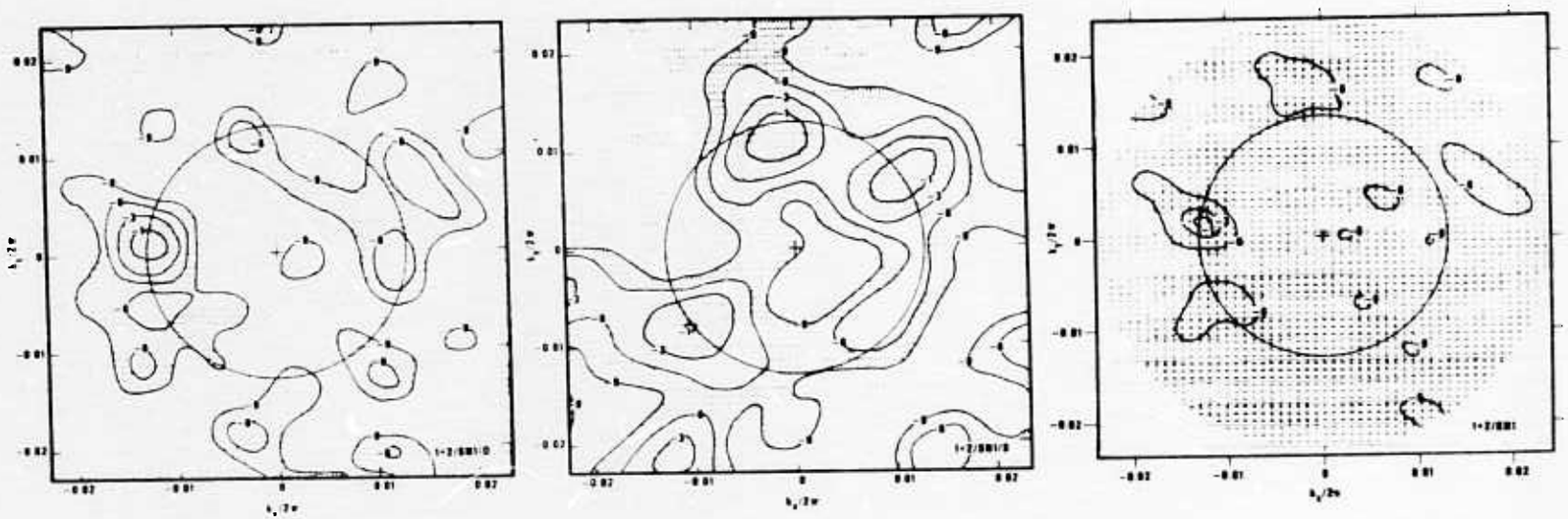

Original FKPLOT

Stripped FKPLOT

TSML

Figure 27. F-K spectra for Events 1 and 2 combined with noise. S/N=1.

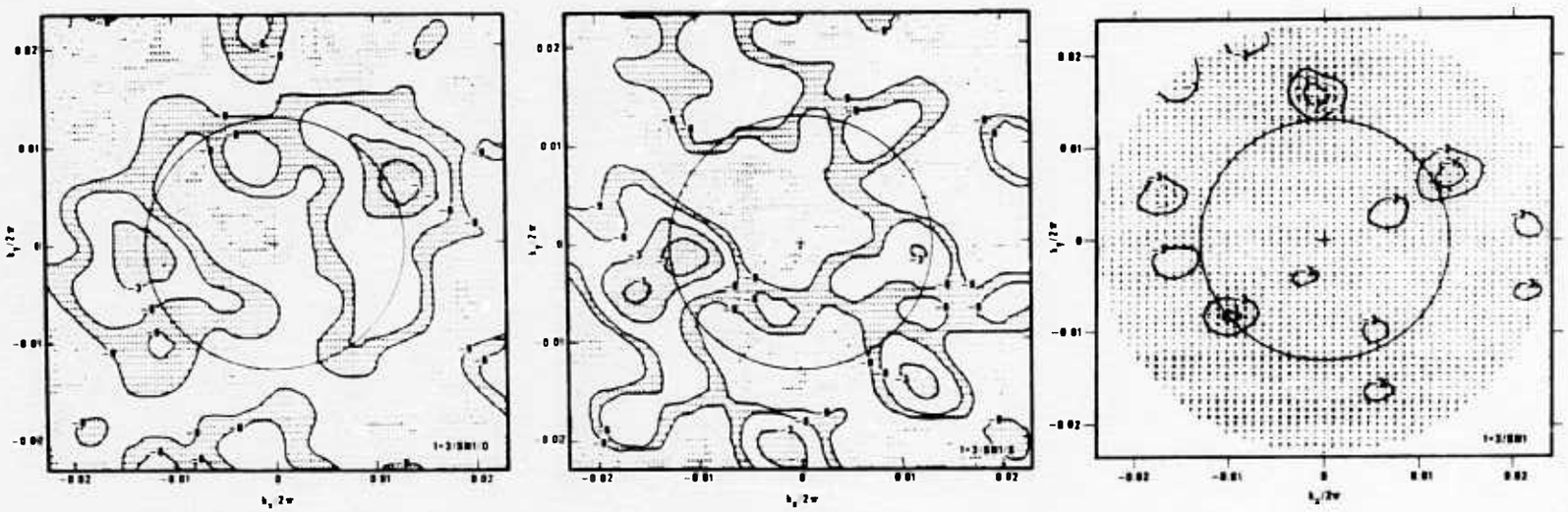

Original FKPLOT | Stripped FKPLOT | TSML

Figure 28. F-K spectra for Events 1 and 3 combined with noise. S/N=1.

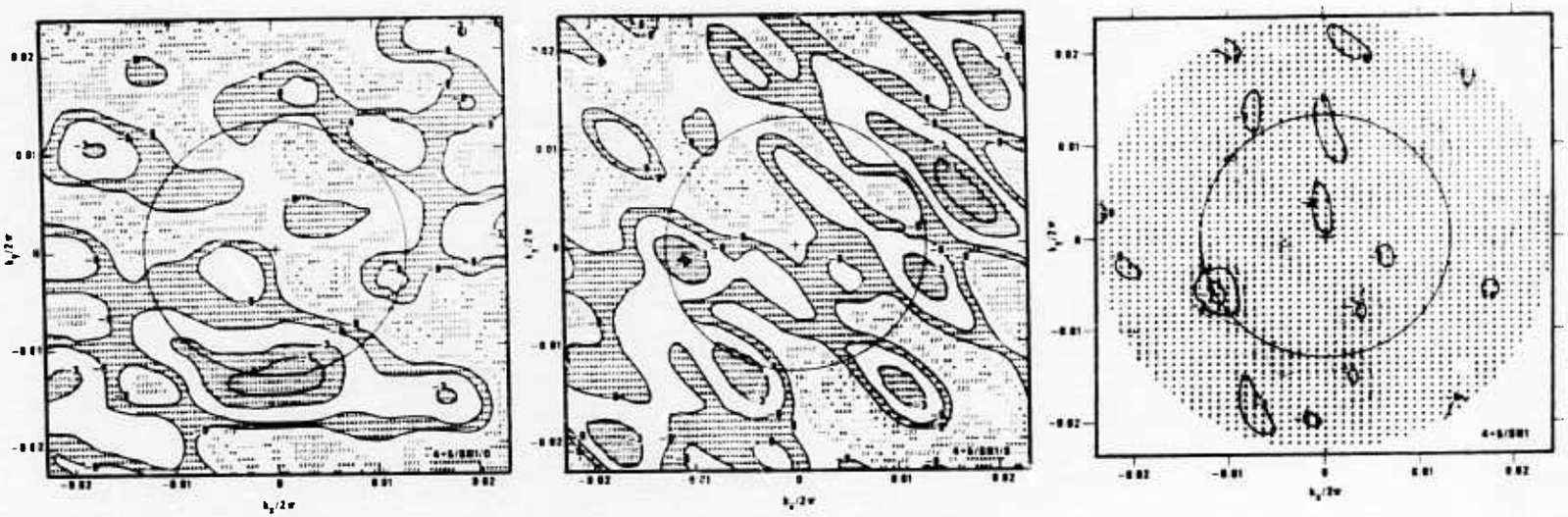

Original FKPLOT

Stripped FKPLOT

TSML

Figure 29. F-K spectra for Events 4 and 5 combined with noise. S/N=1.

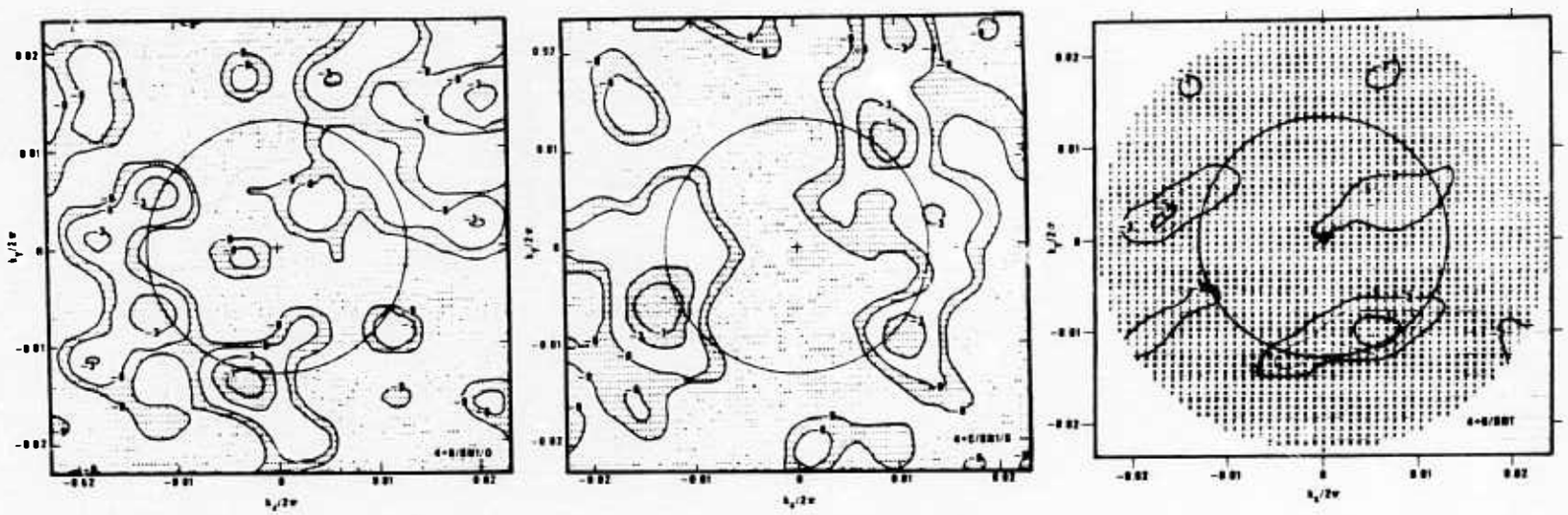

Original FKPLOT

Stripped FKPLOT

TSML

Figure 30. F-K spectra for Events 4 and 6 combined with noise. S/N=1.

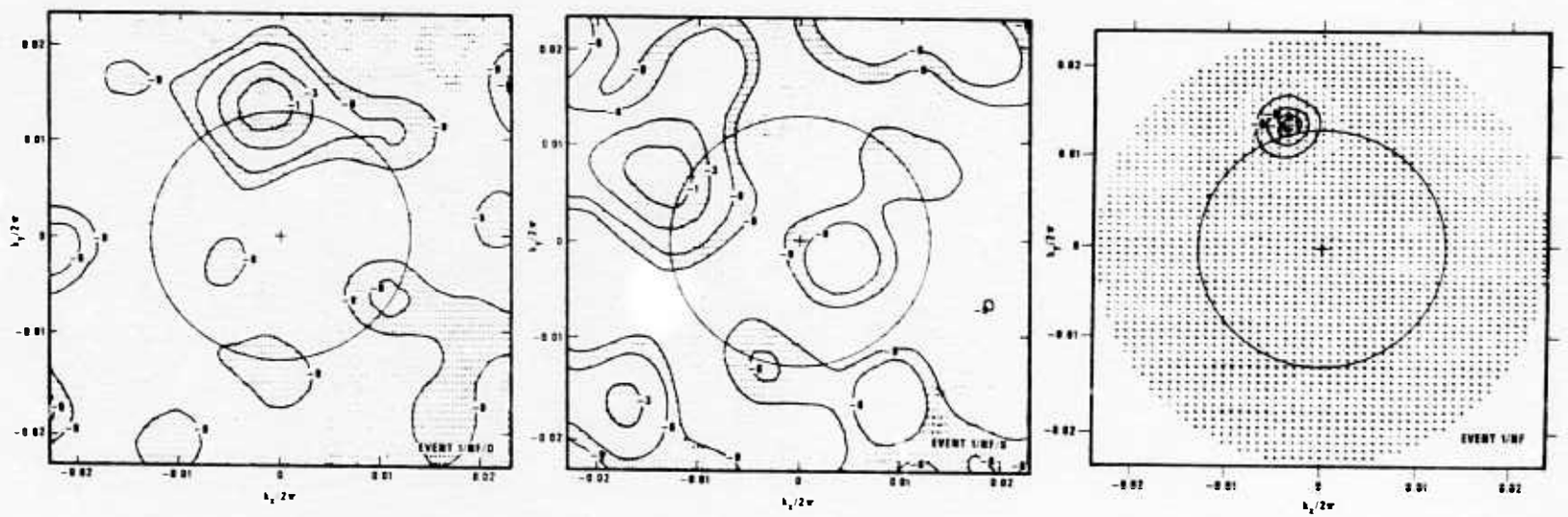

Original FKPLOT

Stripped FKPLOT

TSML

Figure 31. F-K spectra of A0, C, D and E rings for Event 1.

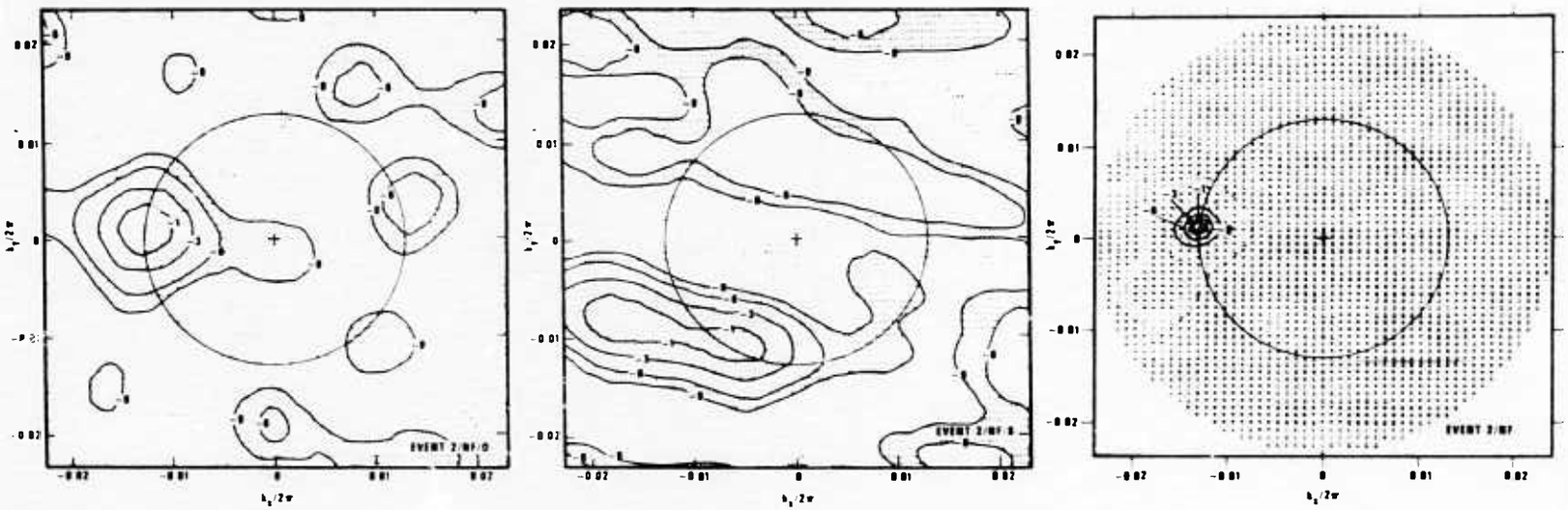

Original FKPLOT | Stripped FKPLOT | TSML

Figure 32. F-K spectra of A0, C, D and E rings for Event 2.

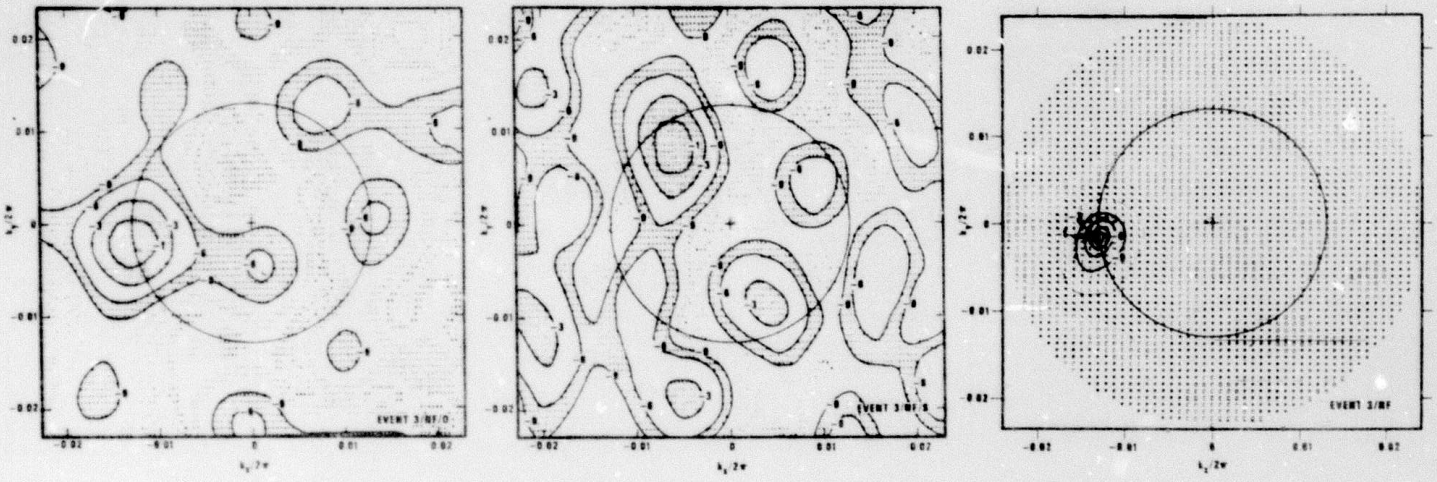

Original FKPLOT | Stripped FKPLOT | TSML

Figure 33. F-K spectra of A0, C, D and E rings for Event 3.

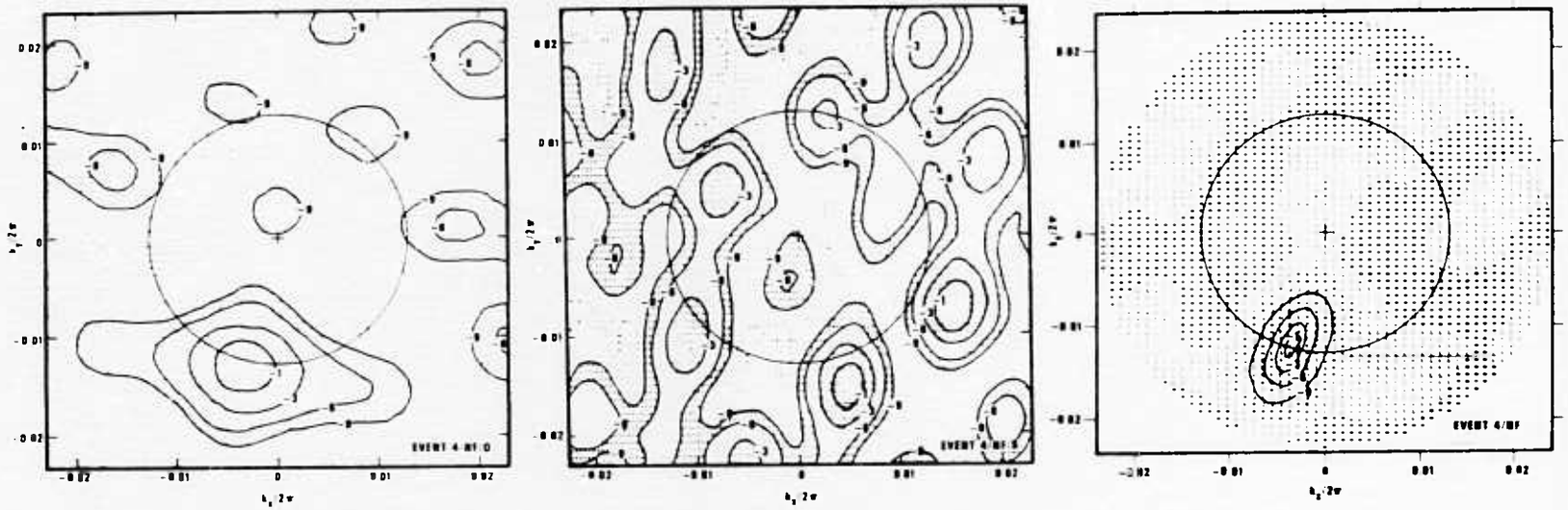

Original FKPLOT Stripped FKPLOT TSML

Figure 34. F-K spectra of A0, C, D and E rings for Event 4.

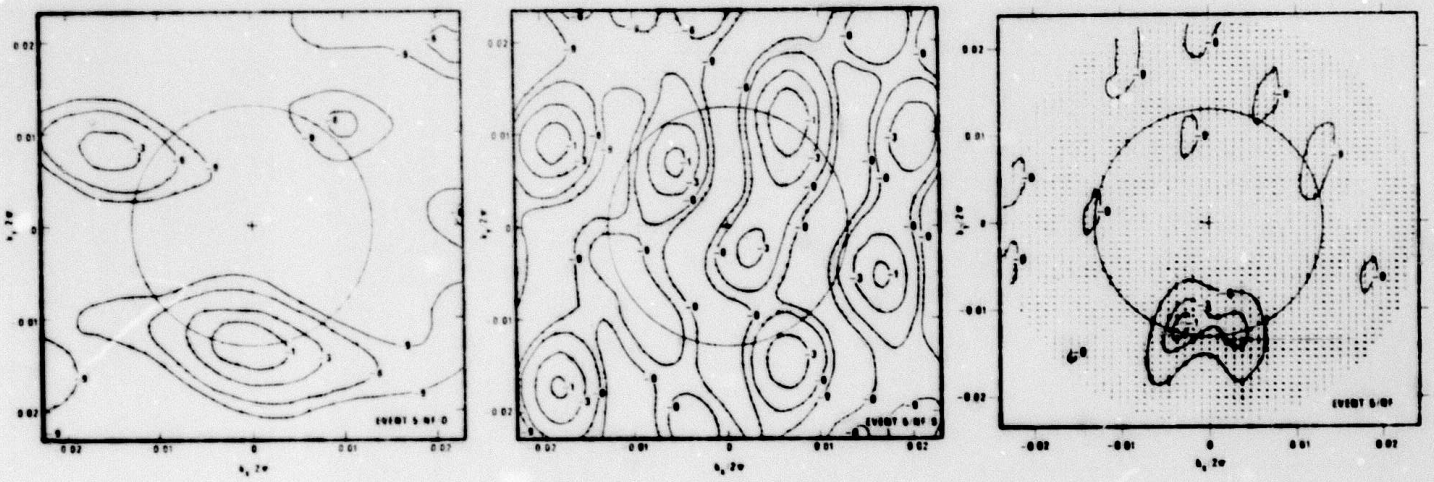

Original FKPLOT | Stripped FKPLOT | TSML

Figure 35. F-k spectra of A0, C, D and E rings for Event 5.

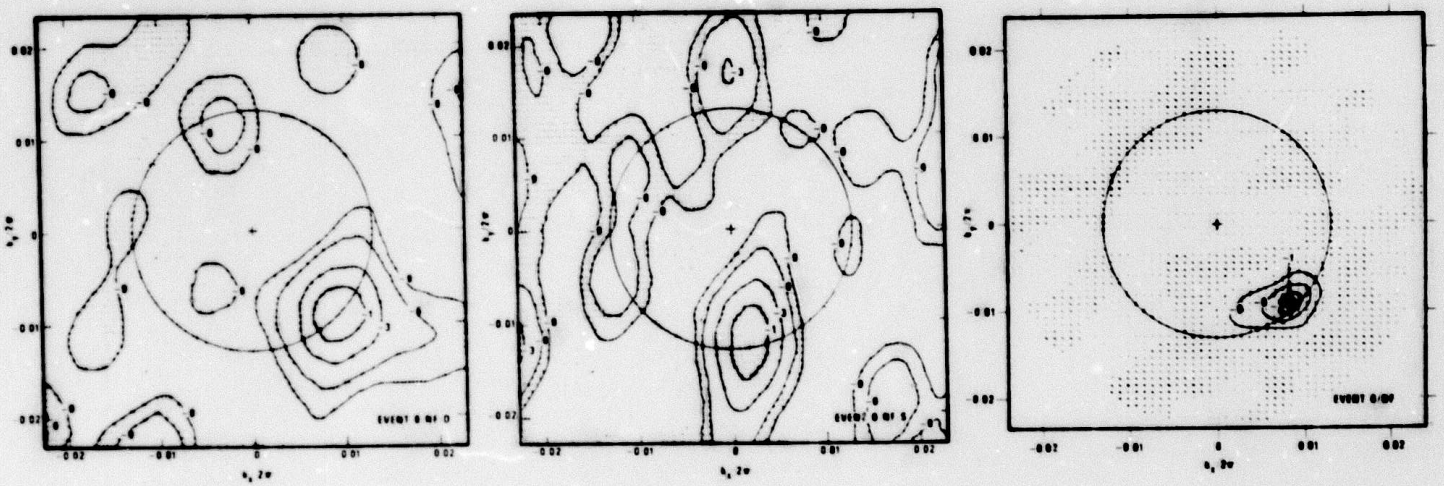

Original EKPLOT Stripped EKPLOT TSML

Figure 36. F-K spectra of A0, C, D and E rings for Event 6.

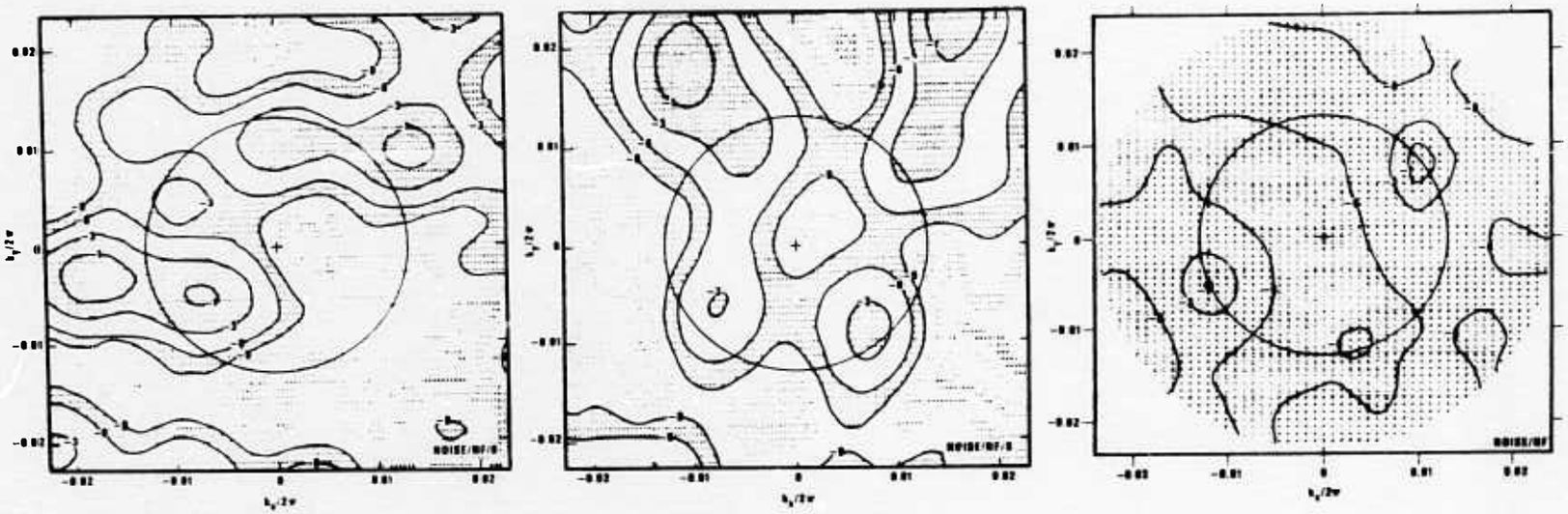

Original FKPLOT | Stripped FKPLOT | TSML

Figure 37. F-K spectra of A0, C, D and E rings for the noise sample.

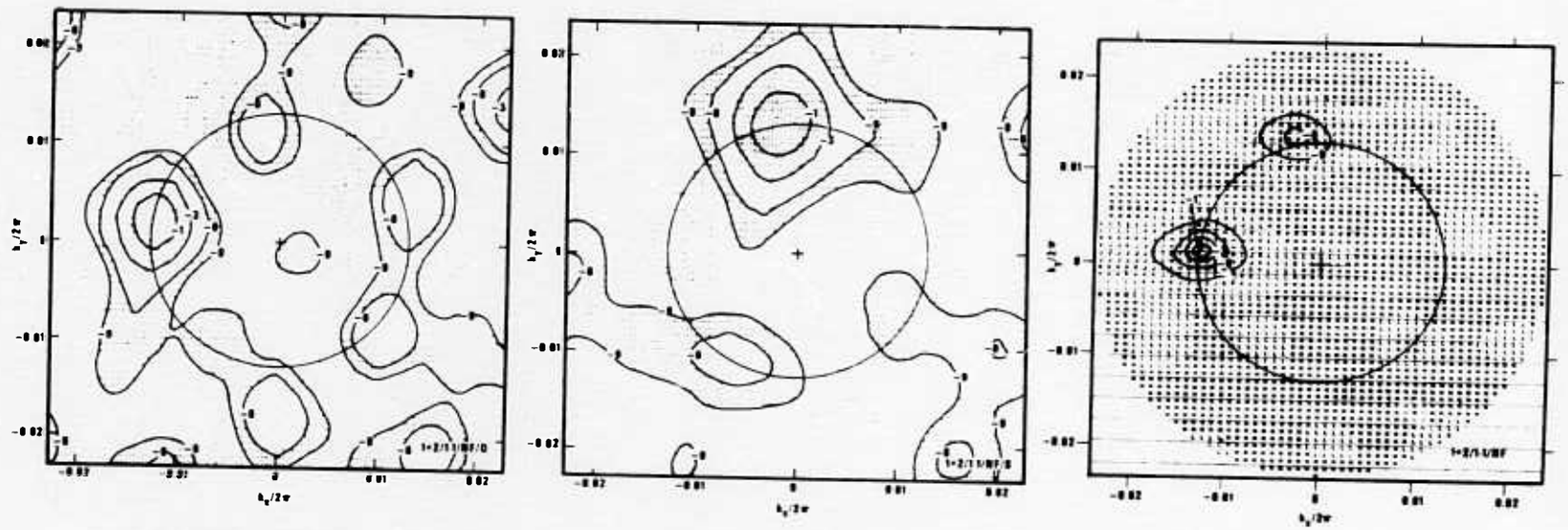

Original FKPLOT

Stripped FKPLOT

TSML

Figure 38. F-K spectra of A0, C, D and E rings for Events 1 and 2 combined equally.

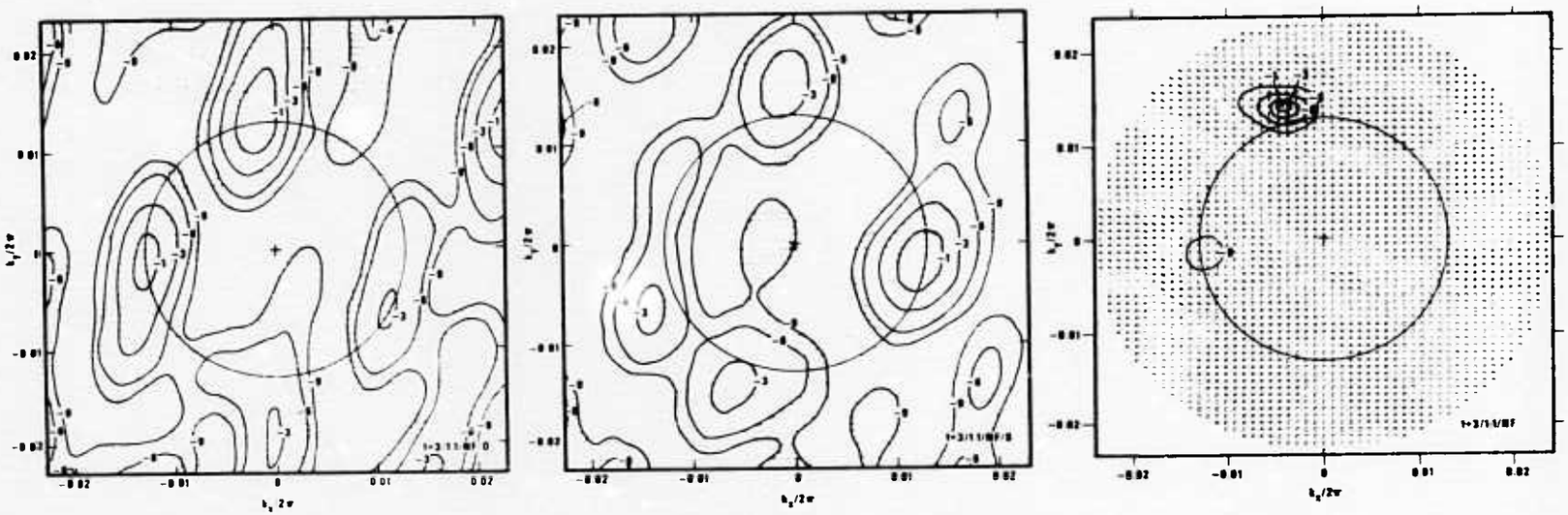

Original FKPLOT

Stripped FKPLOT

TSML

Figure 39. F-K spectra of A0, C, D and E rings for Events 1 and 3 combined equally.

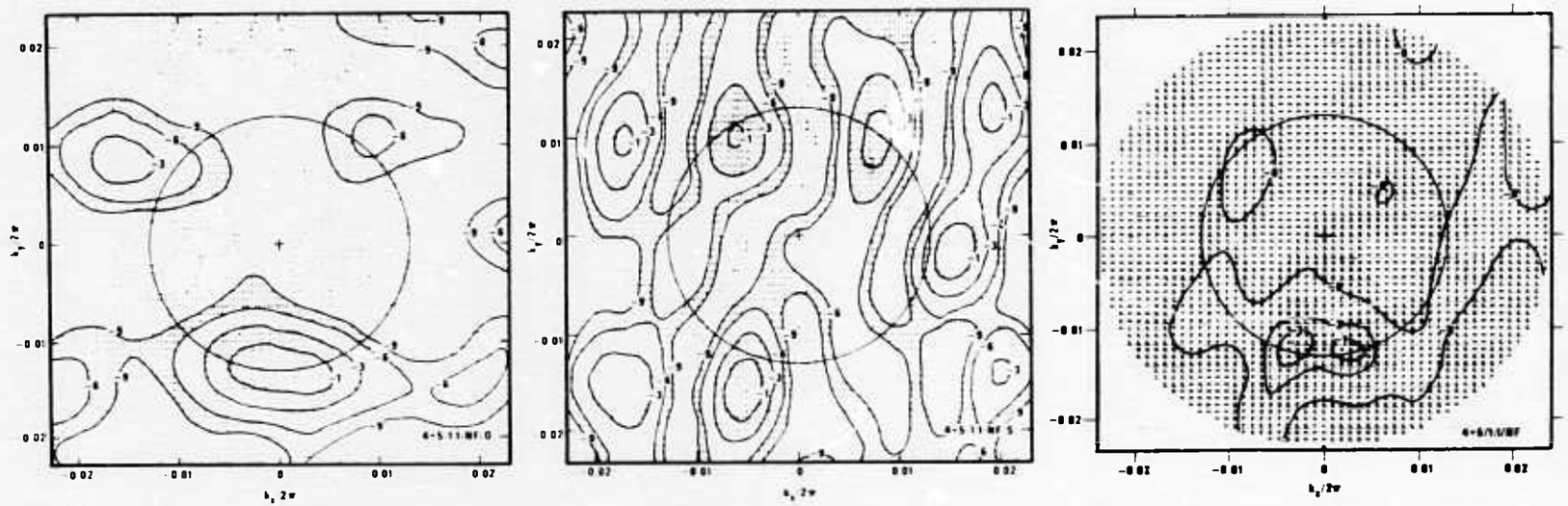

Original FKPLOT

Stripped FKPLOT

TSML

Figure 40. F-K spectra of A0, C, D and E rings for Events 4 and 5 combined equally.

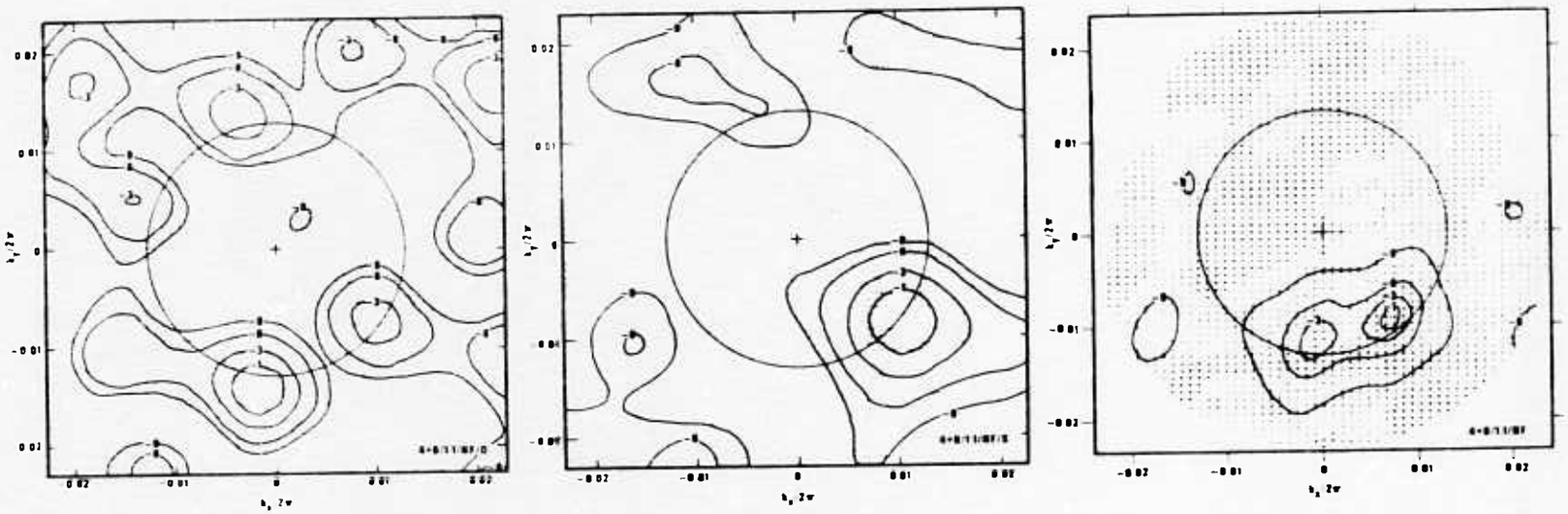

Original FKPLOT

Stripped FKPLOT

TSML

Figure 41. F-K spectra of A0, C, D and E rings for Events 4 and 6 combined equally.

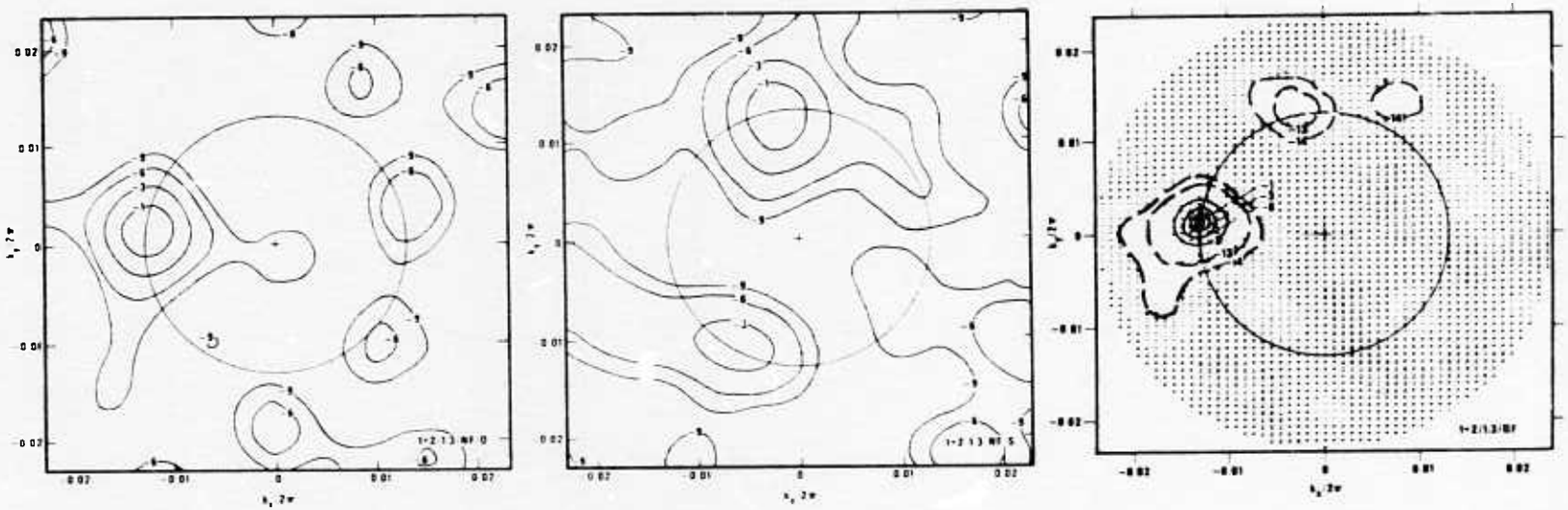

Original FKPLOT

Stripped FKPLOT

TSML

Figure 42. F-K spectra of A0, C, D and E rings for Events 2 and 1 combined in a 3 to 1 ratio.

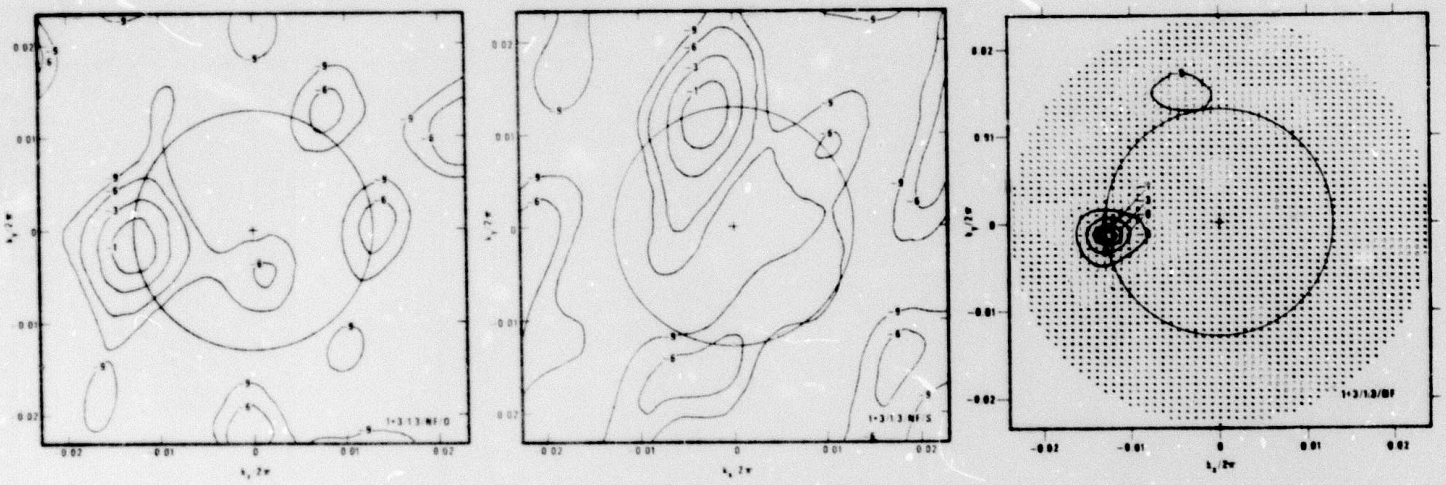

Original FKPLOT | Stripped FKPLOT | TSML

Figure 43. F-K spectra of A0, C, D and E rings for Events 3 and 1 combined in a 3 to 1 ratio.

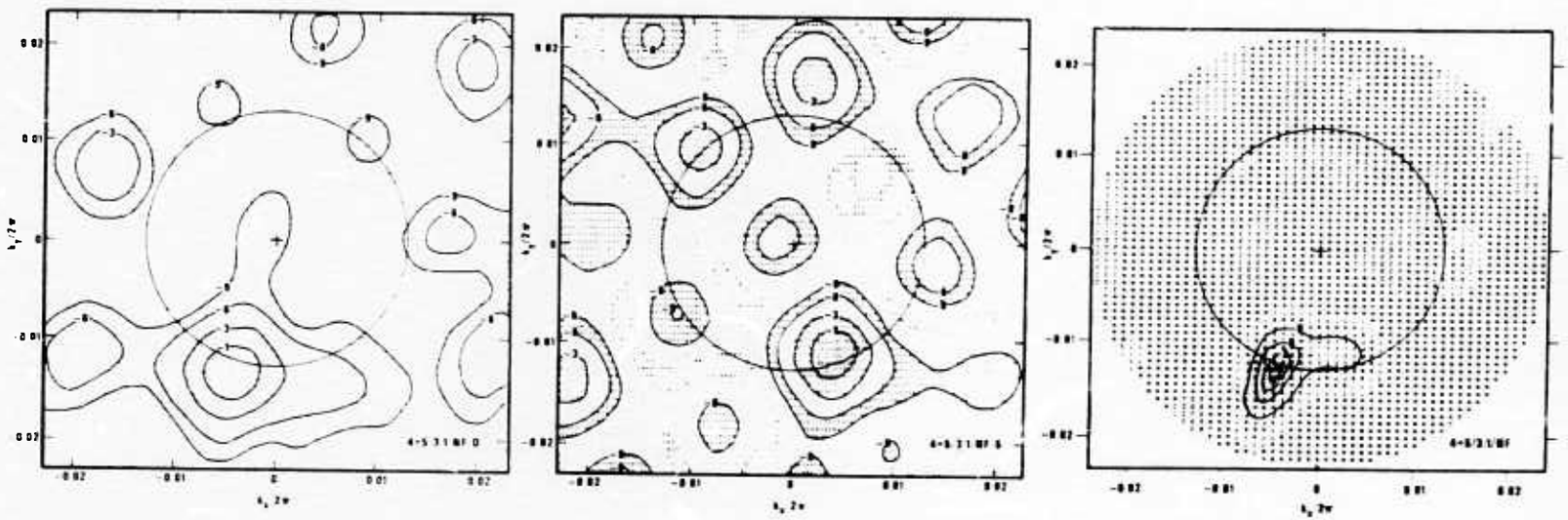

Original FKPLOT

Stripped FKPLOT

TSML

Figure 44. F-K spectra of A0, C, D and E rings for Events 4 and 5 combined in a 3 to 1 ratio.

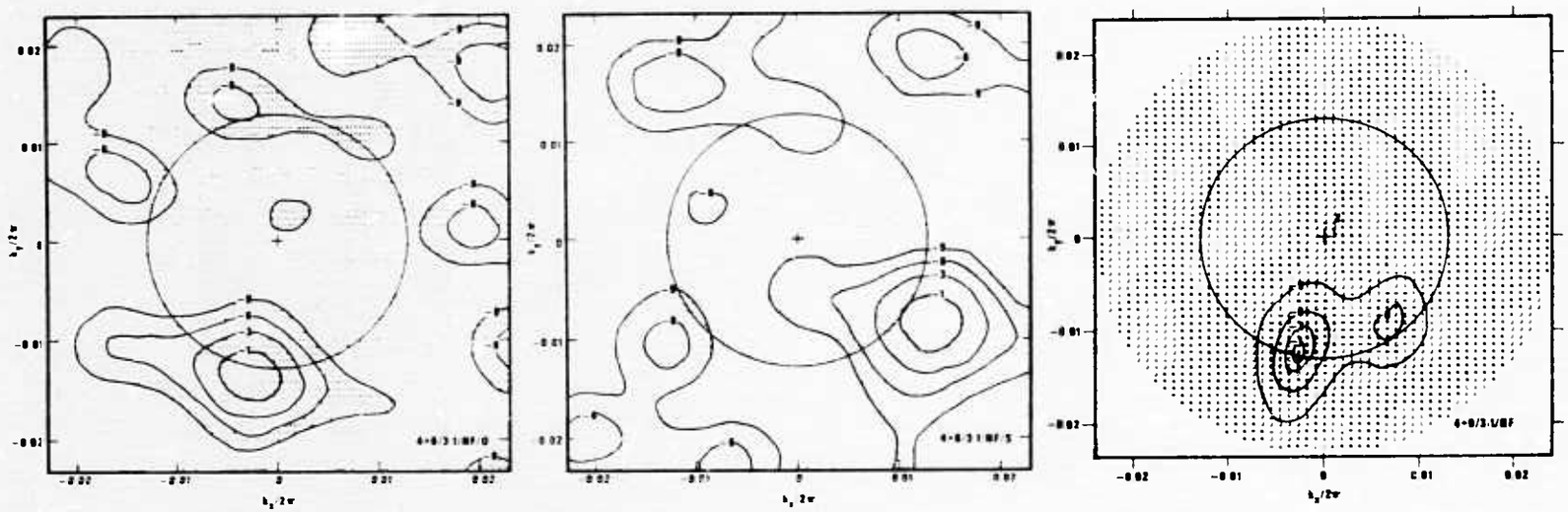

Original FKPLOT Stripped FKPLOT TSML

Figure 45. F-K spectra of A0, C, D and E rings for Events 4 and 6 combined in a 3 to 1 ratio.

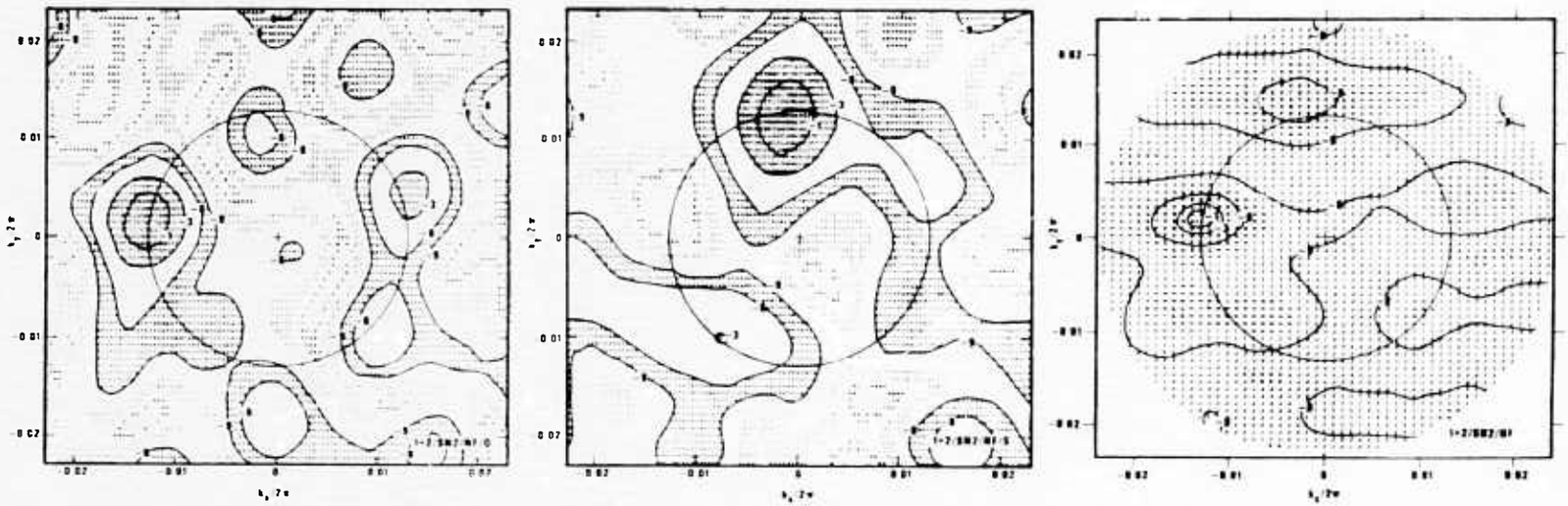

Original FKPLOT Stripped FKPLOT TSML

Figure 46. F-K spectra of A0, C, D and E rings for Events 1 and 2 combined with noise. S/N=2.

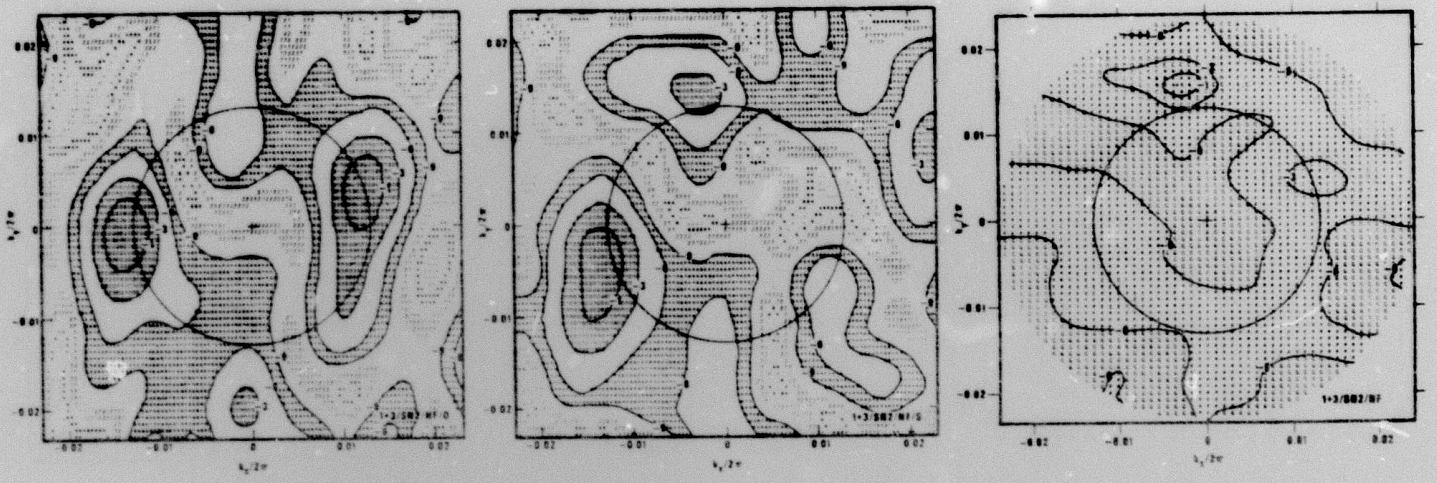

Original FKPLOT Stripped FKPLOT TSML

Figure 47. F-K spectra of A0, C, D and E rings for Events 1 and 3 combined with noise. S/N=2.

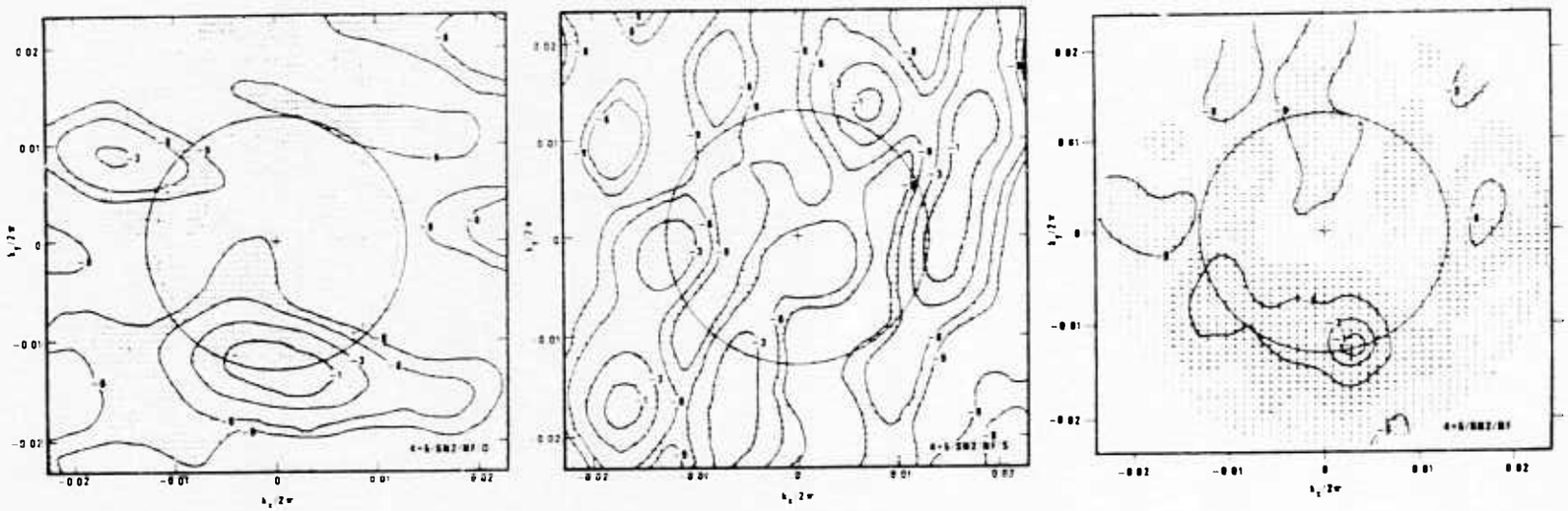

Original FKPLOT | Stripped FKPLOT | TSML

Figure 48. F-K spectra of A0, C, D and E rings for Events 4 and 5 combined with noise. S/N=2.

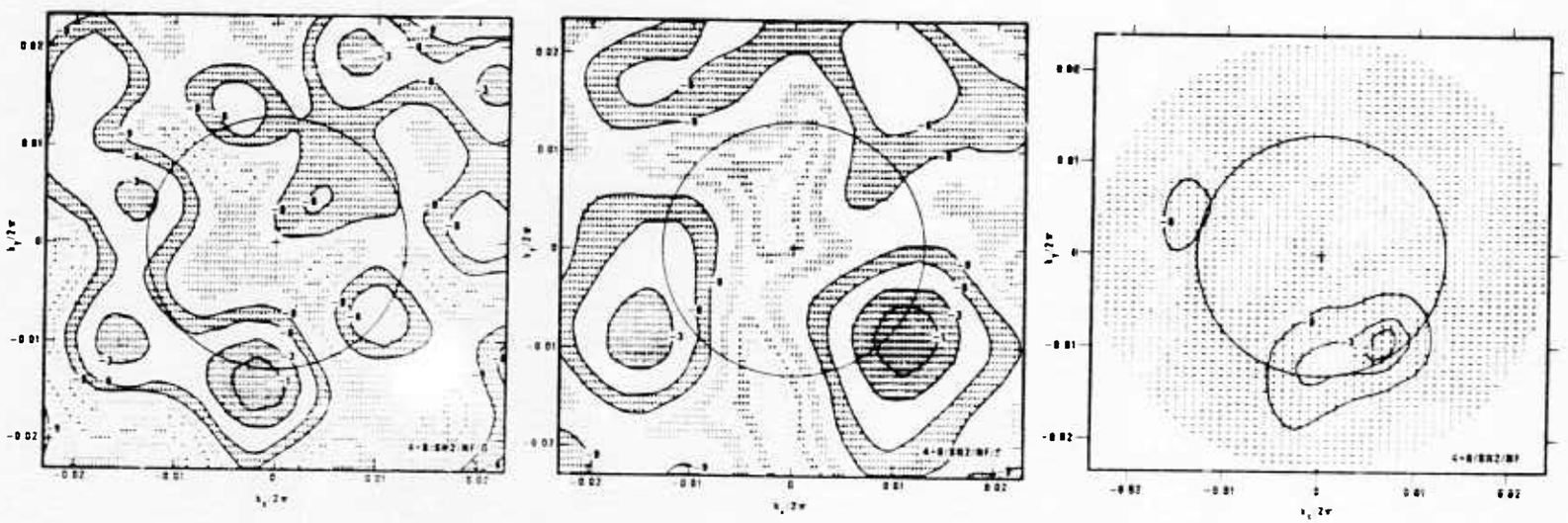

Original FKPLOT

Stripped FKPLOT

TSML

Figure 49. F-K spectra of A0, C, D and E rings for Events 4 and 6 combined with noise. S/N=2.

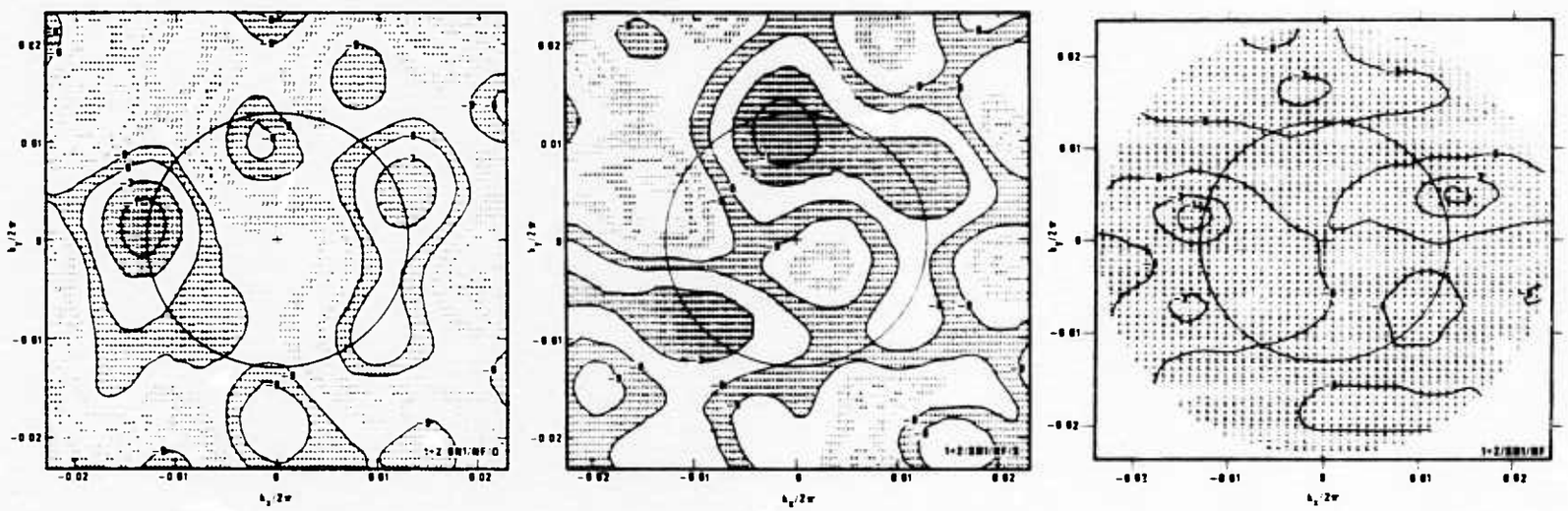

Original FKPLOT Stripped FKPLOT TSML

Figure 50. F-K spectra of A0, C, D and E rings for Events 1 and 2 combined with noise. S/N=1.

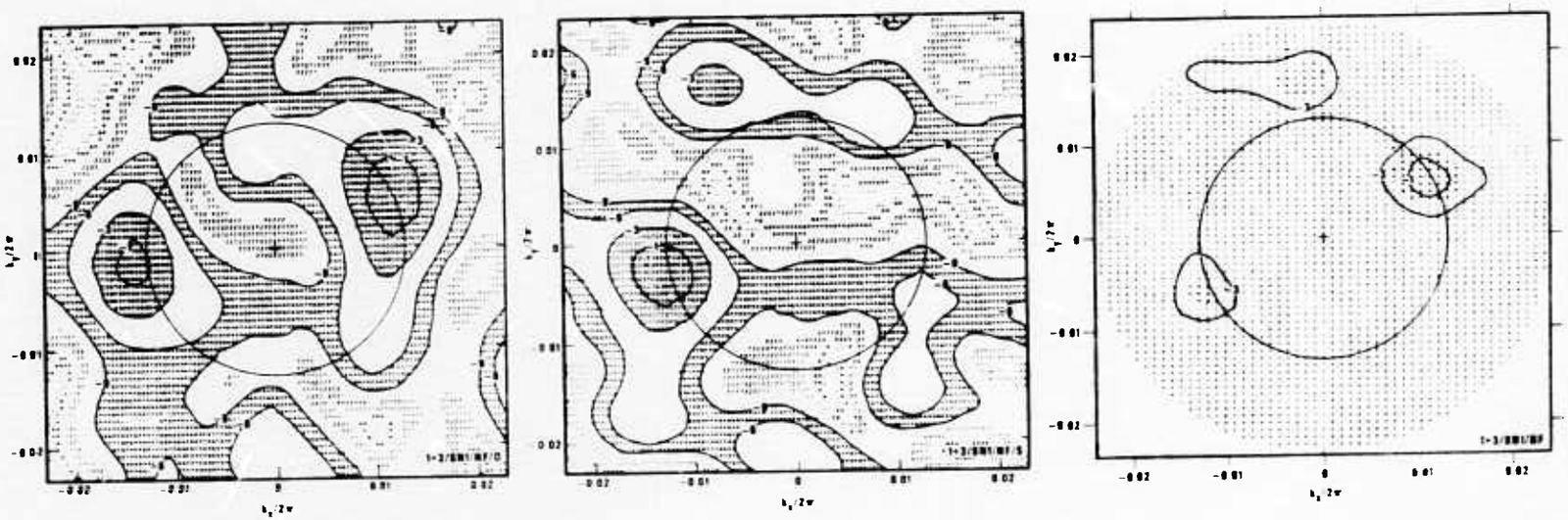

Original FKPLOT

Stripped FKPLOT

TSML

Figure 51. F-K spectra of A0, C, D and E rings for Events 1 and 3 combined with noise. S/N=1.

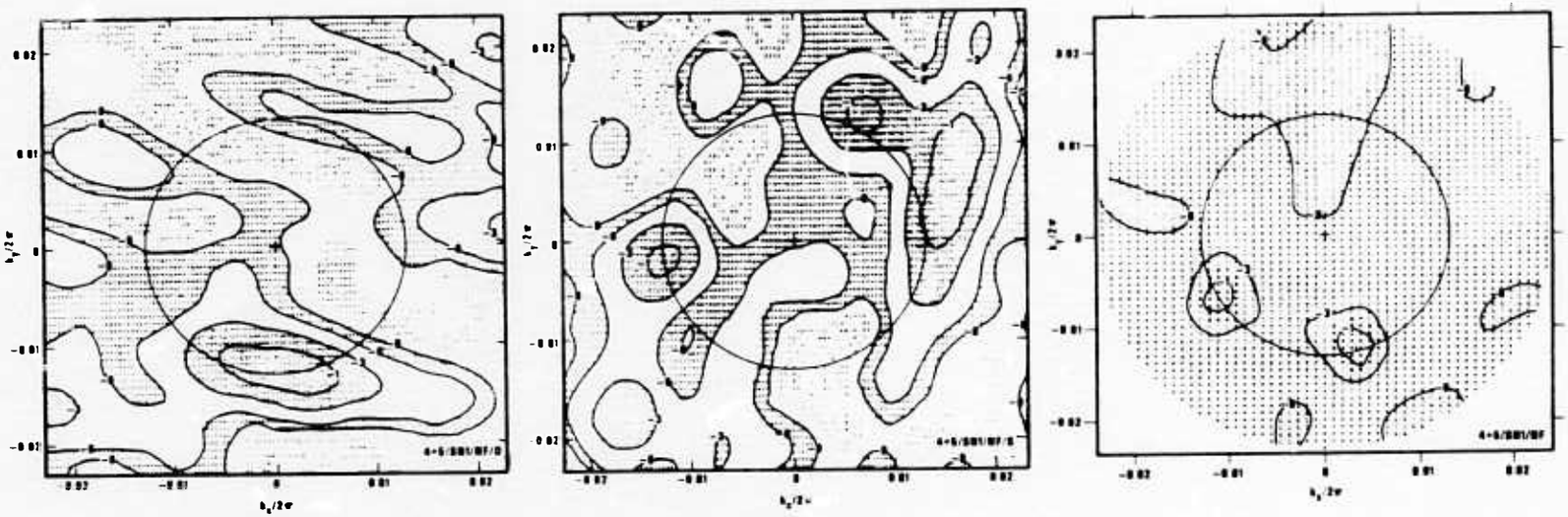

Original FKPLOT | Stripped FKPLOT | TSML

Figure 52. F-K spectra of A0, C, D and E rings for Events 4 and 5 combined with noise. S/N=1.

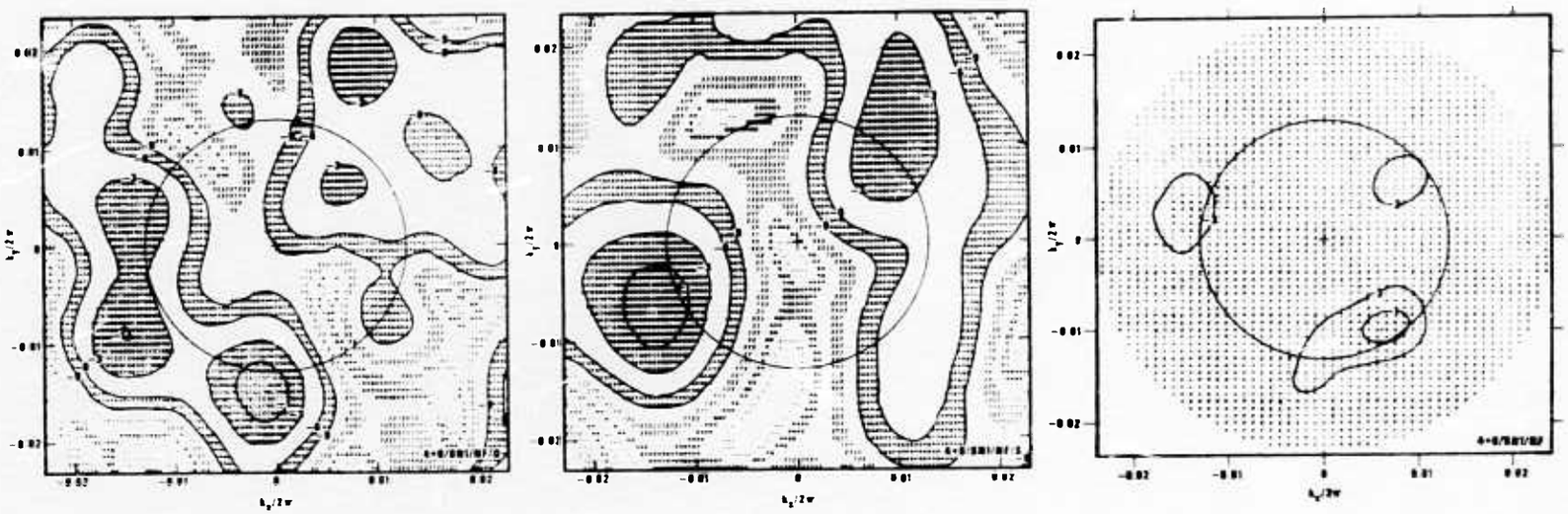

Original FKPLOT | Stripped FKPLOT | TSML

Figure 53. F-K spectra of A0, C, D and E rings for Events 4 and 6 combined with noise. S/N=1.

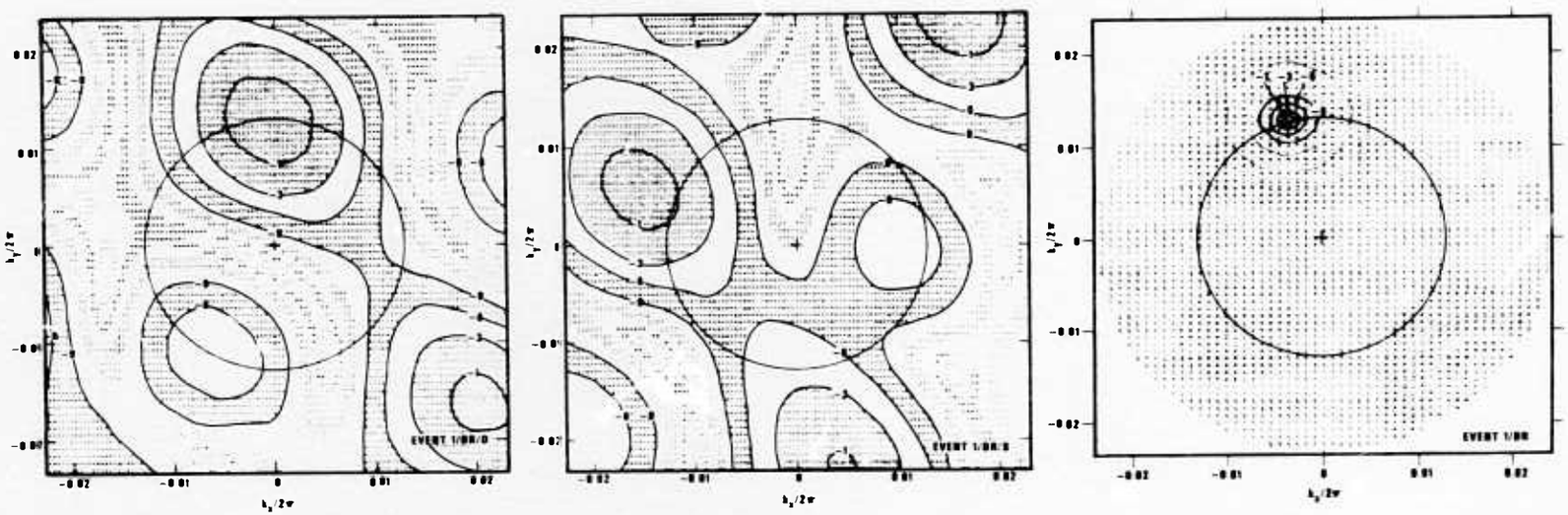

Original FKPLOT

Stripped FKPLOT

TSML

Figure 54. F-K spectra of A0 and the D ring for Event 1.

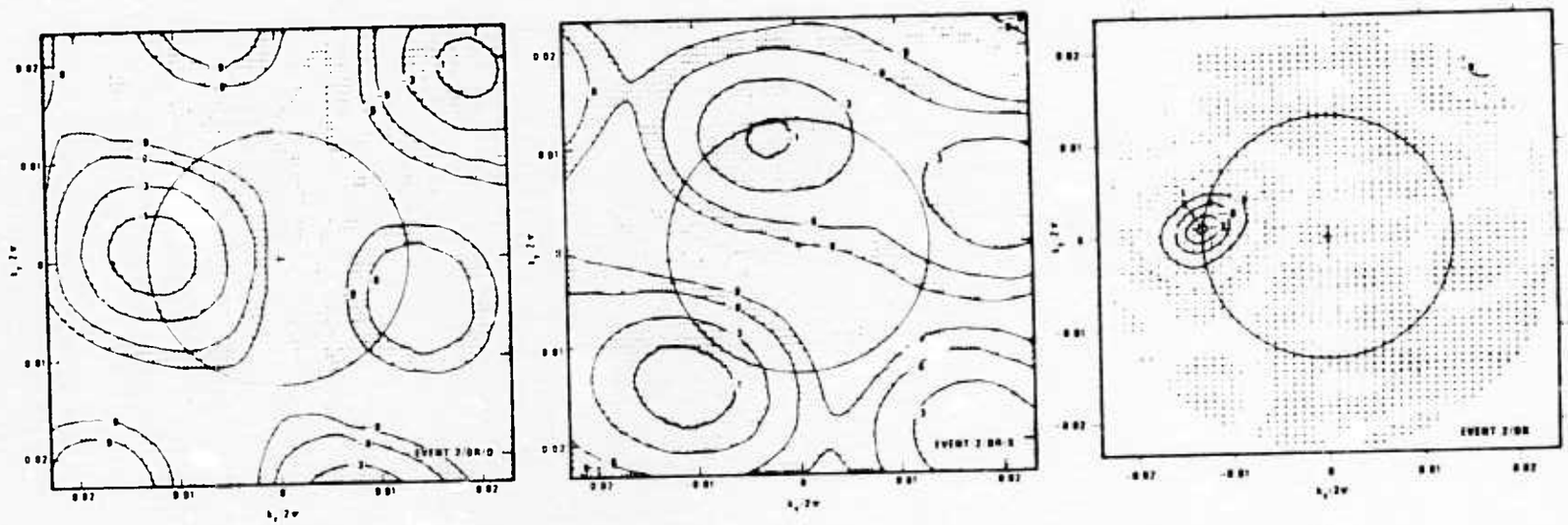

Original FKPLOT

Stripped FKPLOT

TSML

Figure 55. F-K spectra of A0 and the D ring for Event 2.

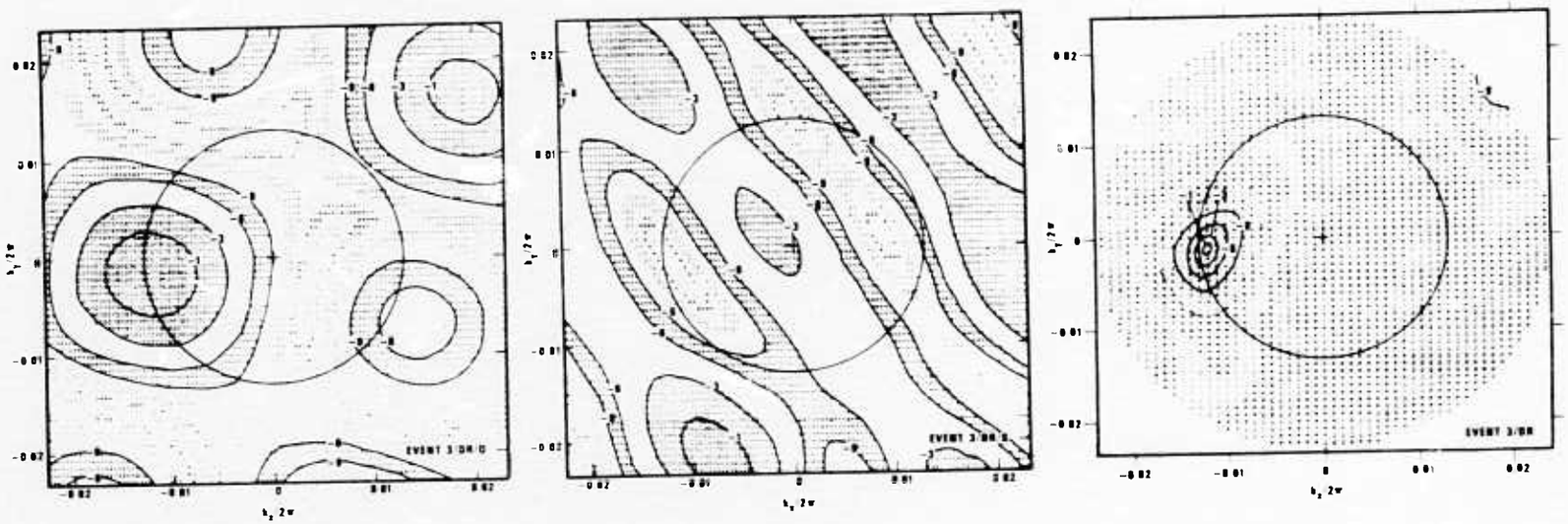

Original FKPLOT

Stripped FKPLOT

TSML

Figure 56. F-K spectra of A0 and the D ring for Event 3.

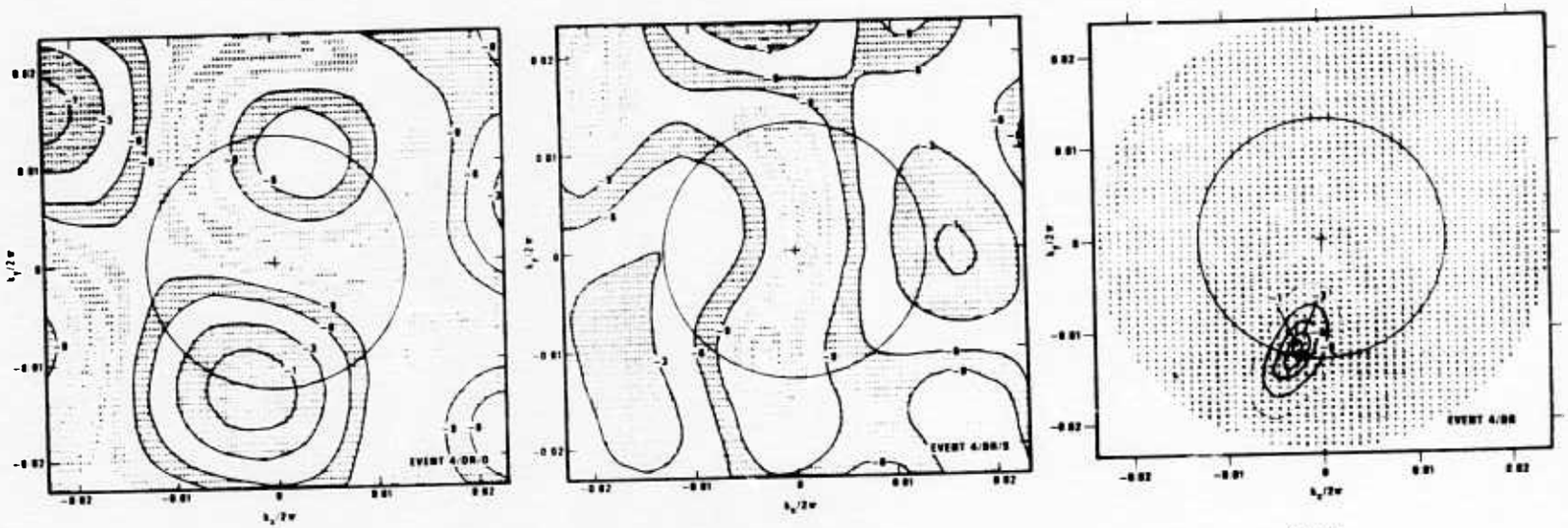

Original FKPLOT

Stripped FKPLOT

TSML

Figure 57. F-K spectra of A0 and the D ring for Event 4.

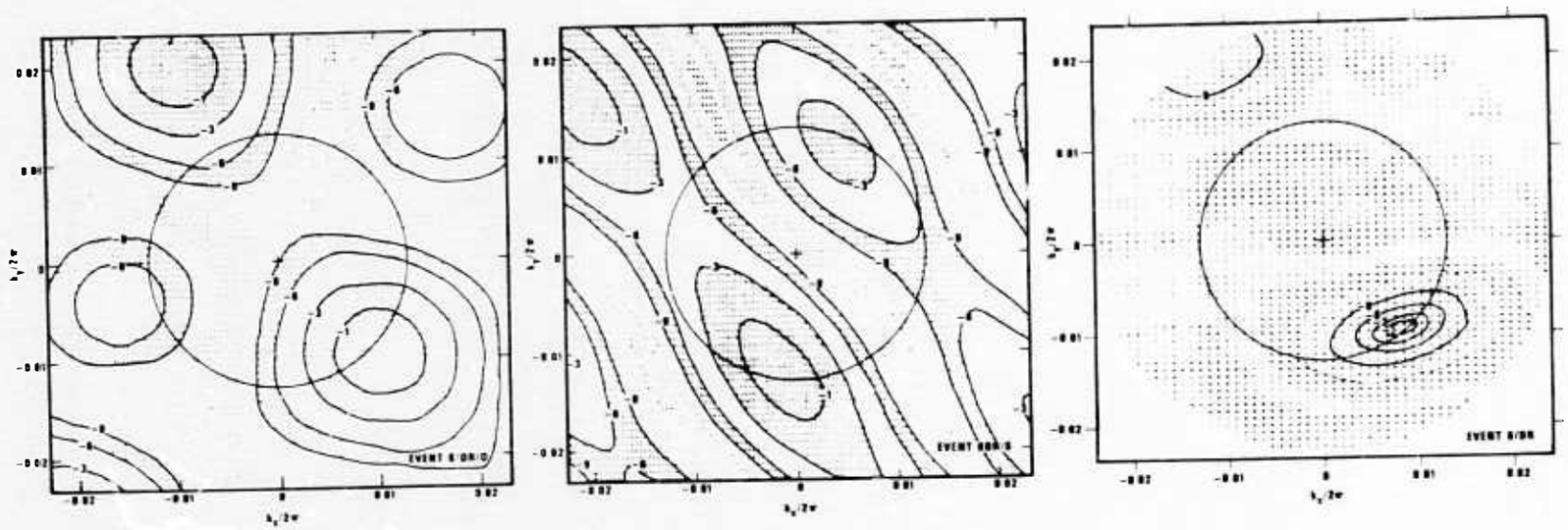

Original FKPLOT

Stripped FKPLOT

TSML

Figure 58. F-K spectra of A0 and the D ring for Event 6.

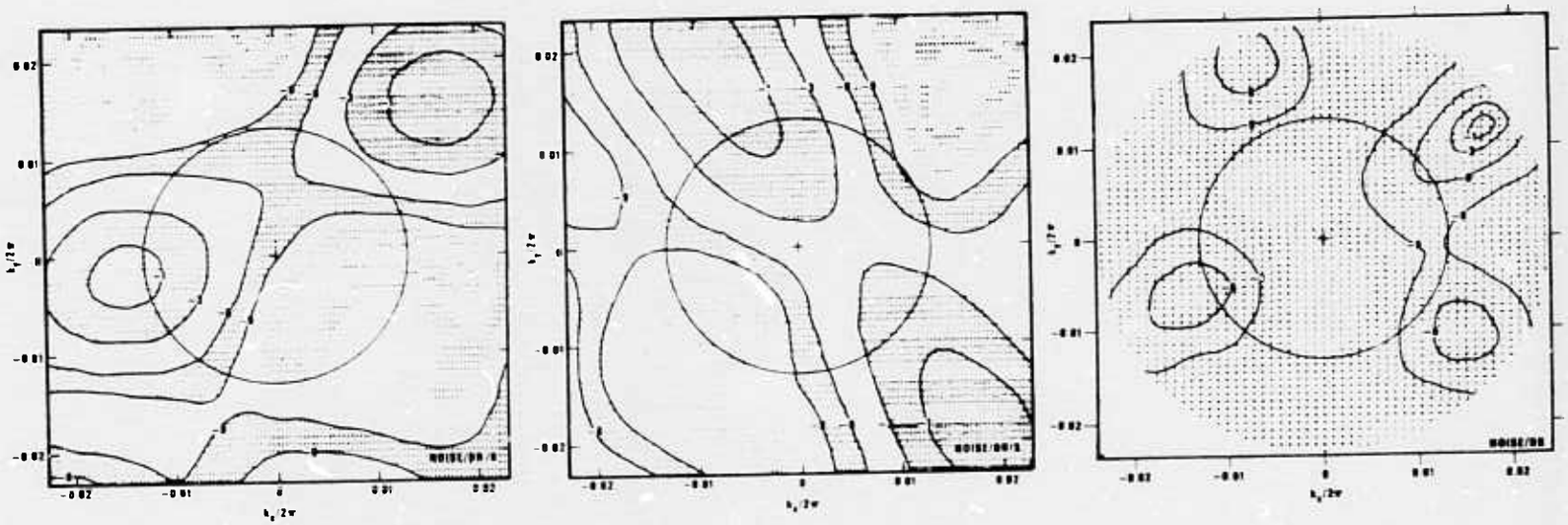

Original FKPLOT

Stripped FKPLOT

TSML

Figure 59. F-K spectra of A0 and the D ring for the noise sample.

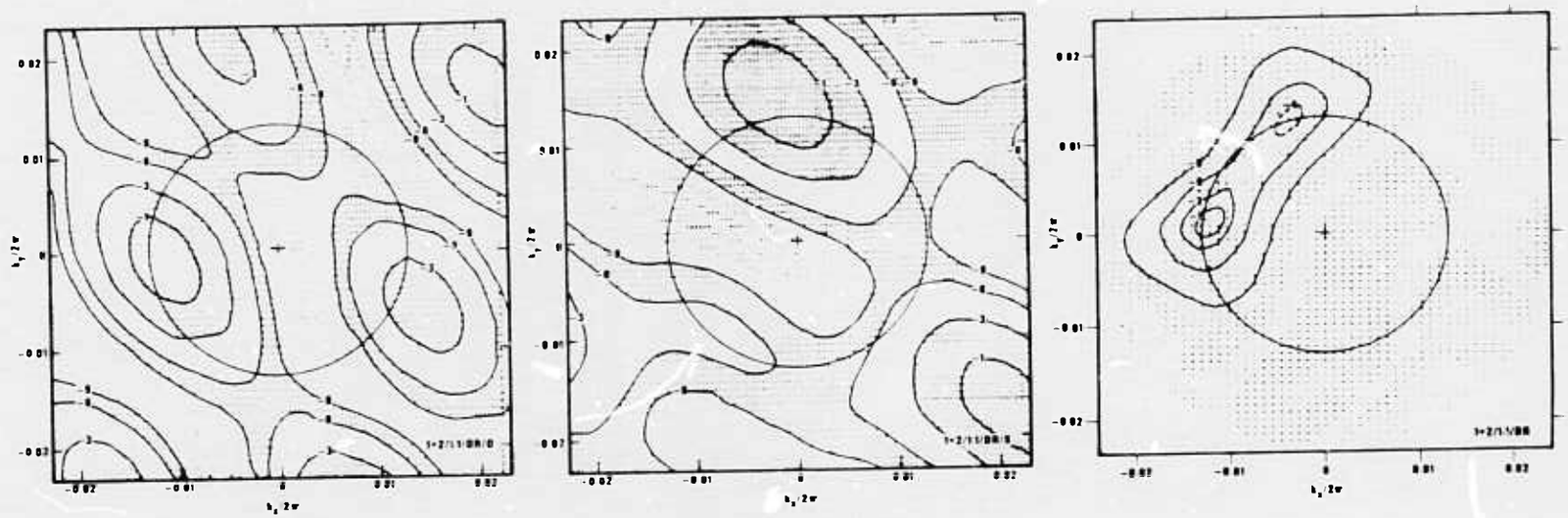

Original FKPLOT

Stripped FKPLOT

TSML

Figure 60. F-K spectra of A0 and the D ring for Events 1 and 2 combined equally.

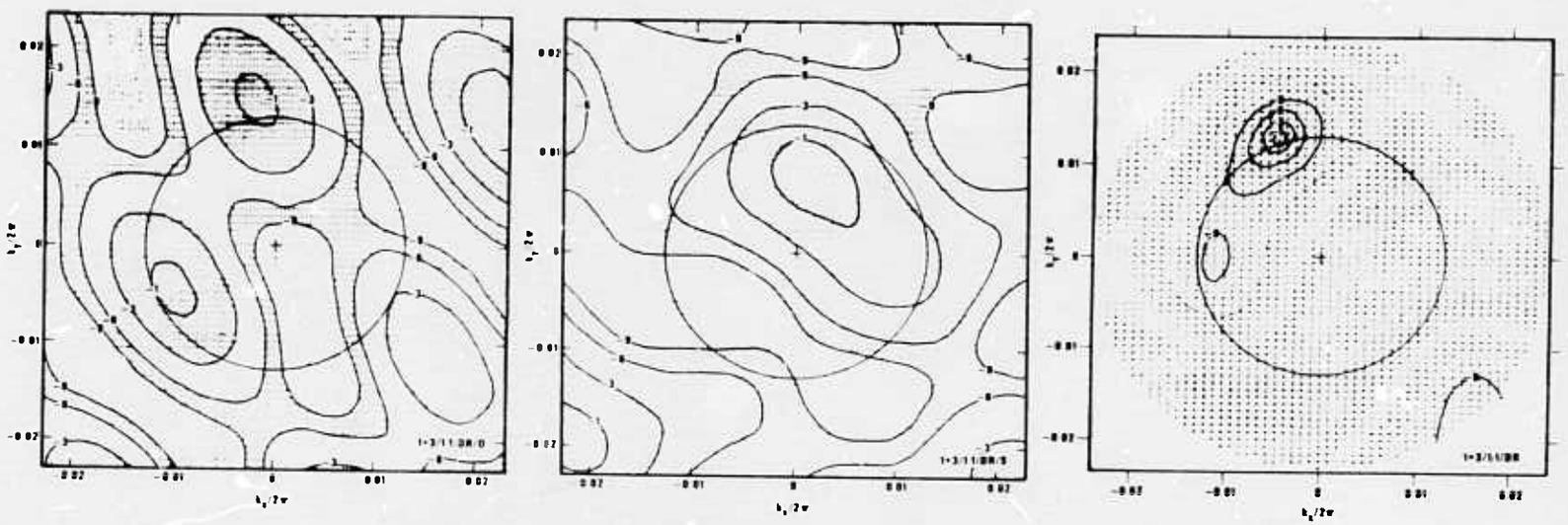

Original FKPLOT

Stripped FKPLOT

TSML

Figure 61. F-K spectra of A0 and the D ring for Events 1 and 3 combined equally.

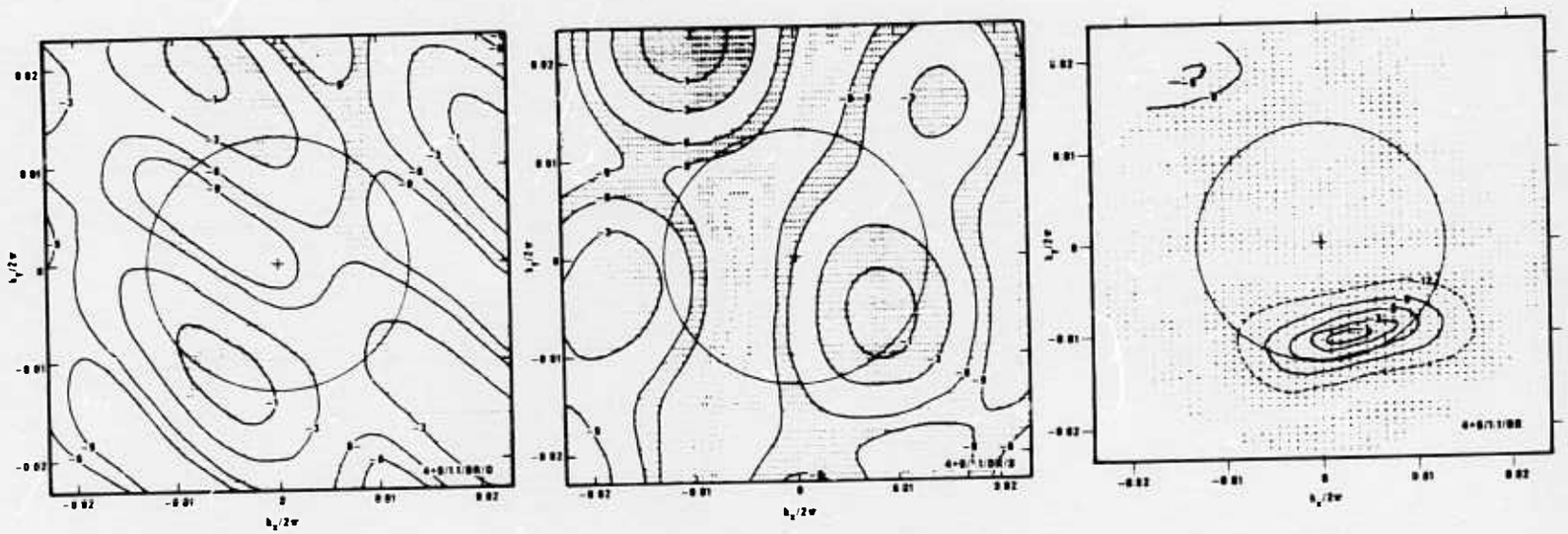

Original FKPLOT

Stripped FKPLOT

TSML

Figure 62. F-K spectra of A0 and the D ring for Events 4 and 6 combined equally.

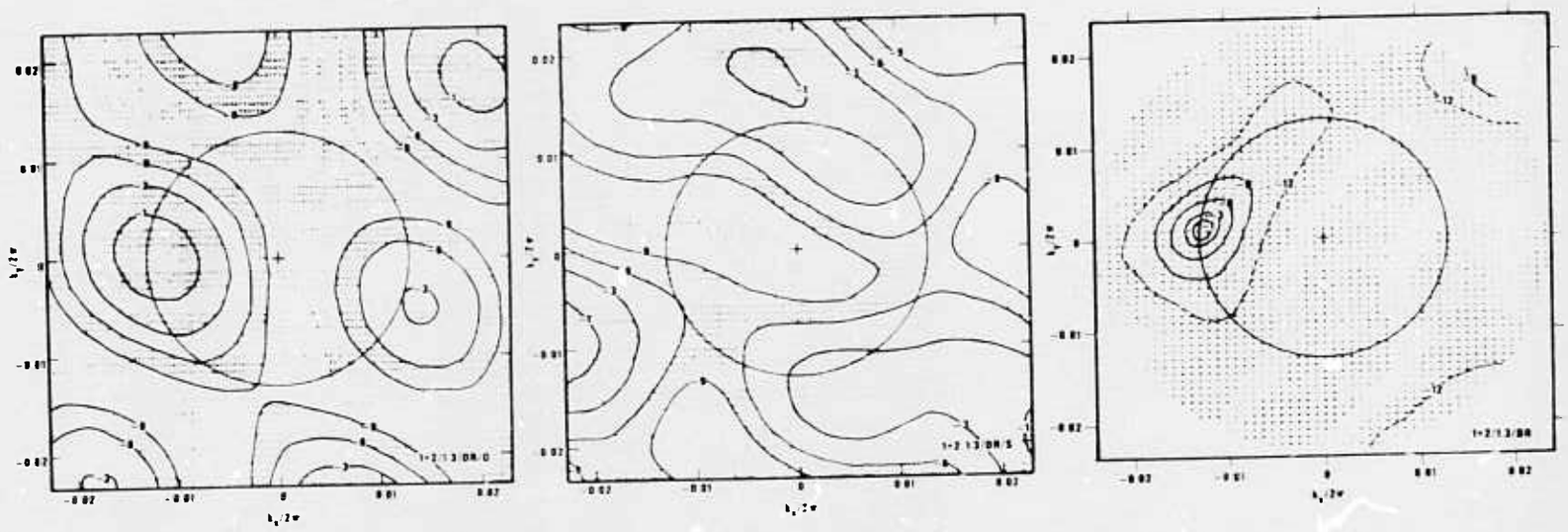

Original FKPLOT

Stripped FKPLOT

TSML

Figure 65. F-K spectra of A0 and the D rings for Events 2 and 1 combined in a 3 to 1 ratio.

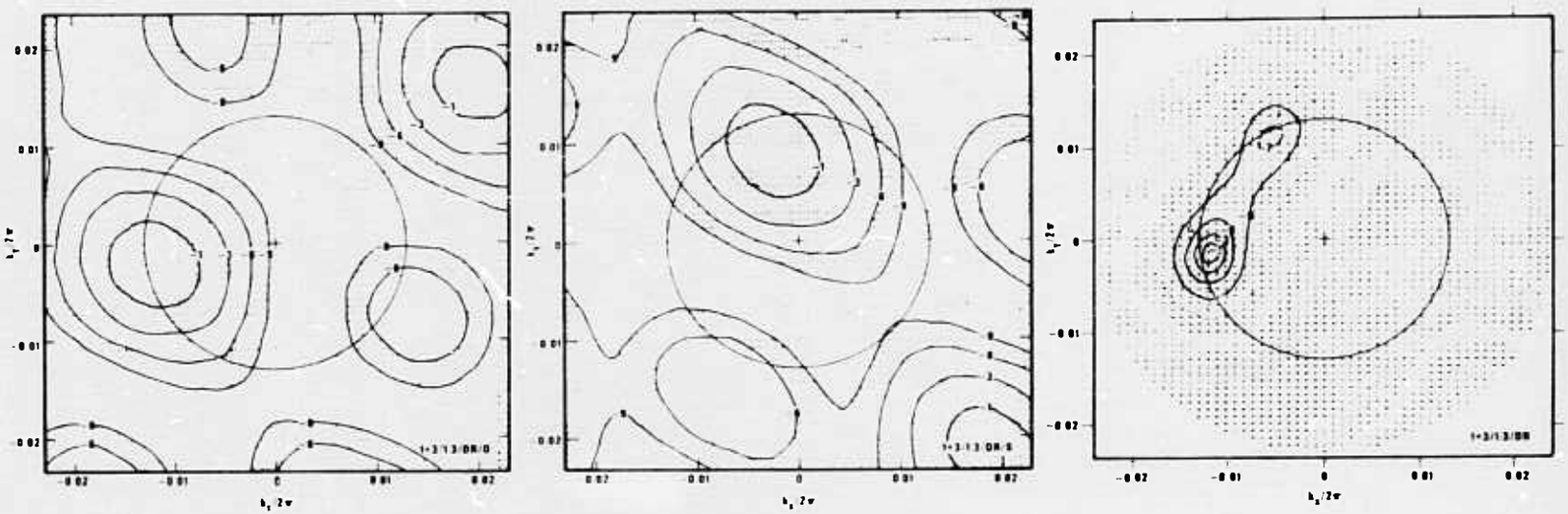

Original FKPLOT Stripped FKPLOT TSML

Figure 64. F-K spectra of A0 and the D rings for Events 3 and 1 combined in a 5 to 1 ratio.

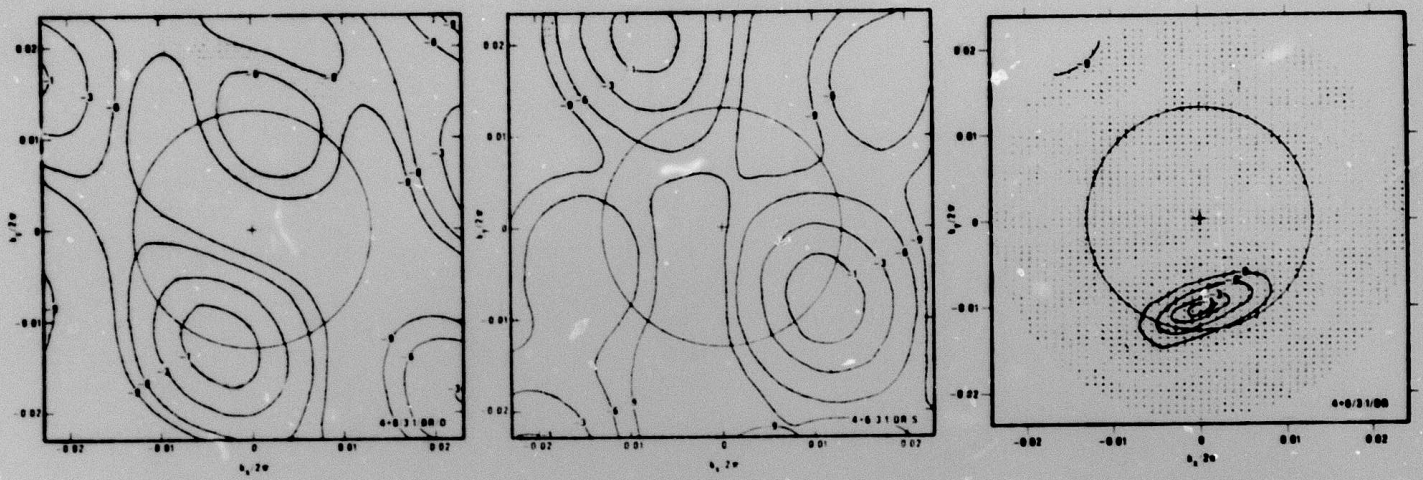

Original FKPLOT | Stripped FKPLOT | TSML

Figure 65. F-k spectra of A0 and the D rings for Events 4 and 6 combined in a 3 to 1 ratio.

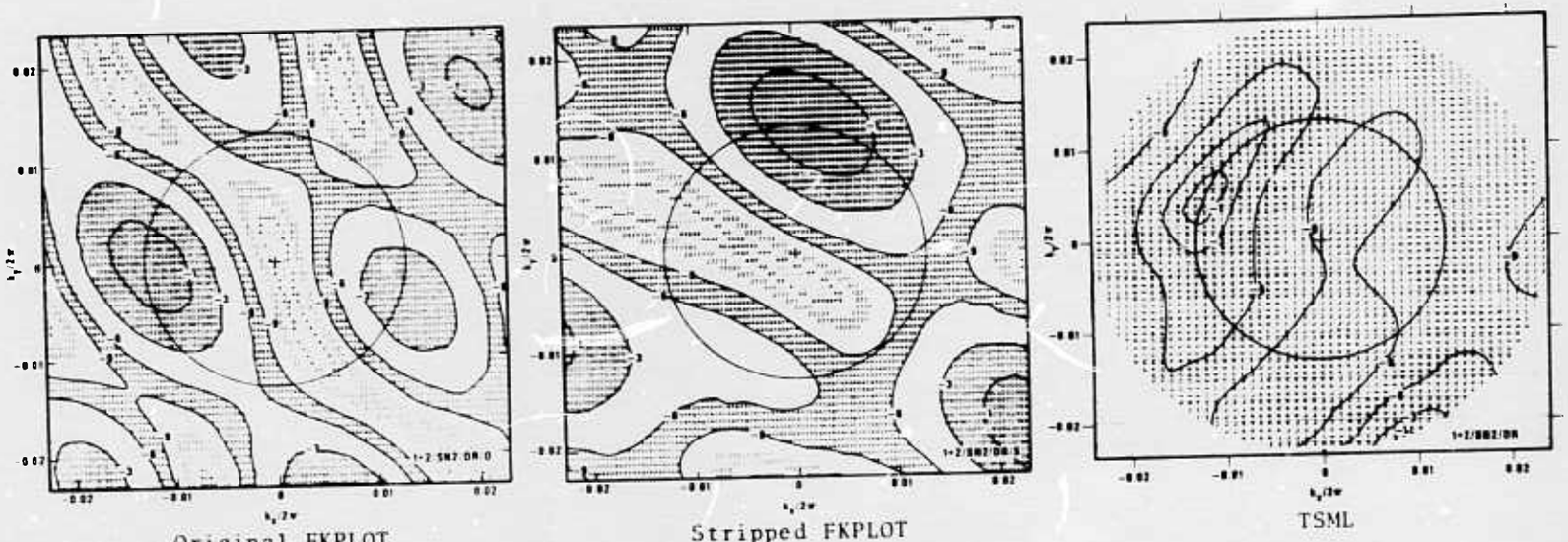

Figure 66. F-K spectra of A0 and the D ring for Events 1 and 2 combined with noise. S/N=2.

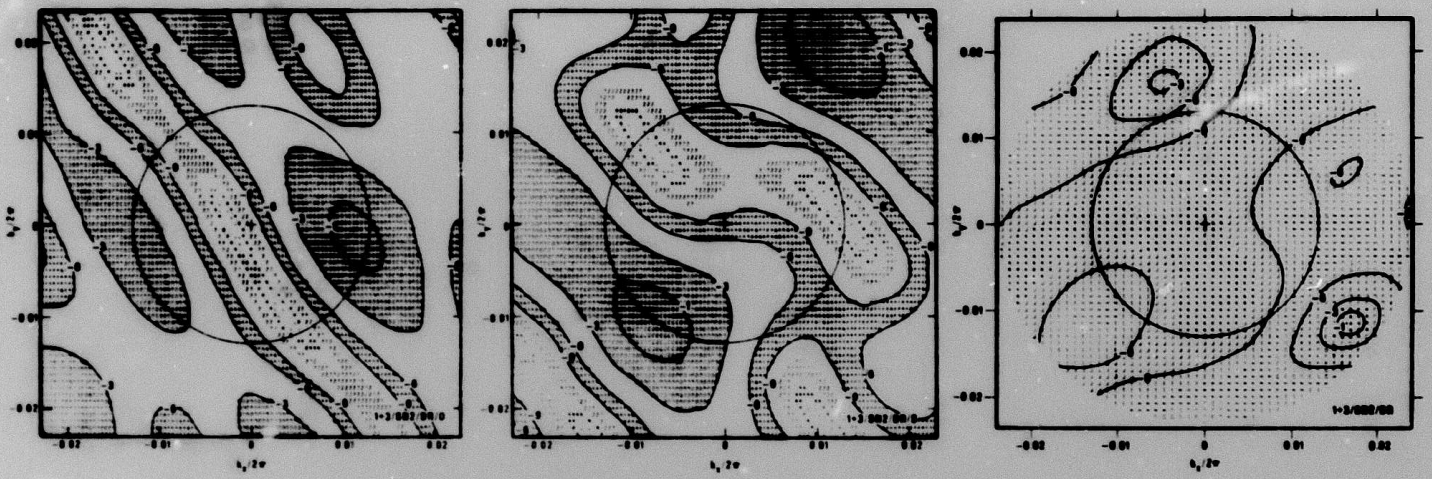

Original FKPLOT Stripped FKPLOT TSML

Figure 67. F-K spectra of A0 and the D ring for Events 1 and 3 combined with noise. S/N=2.

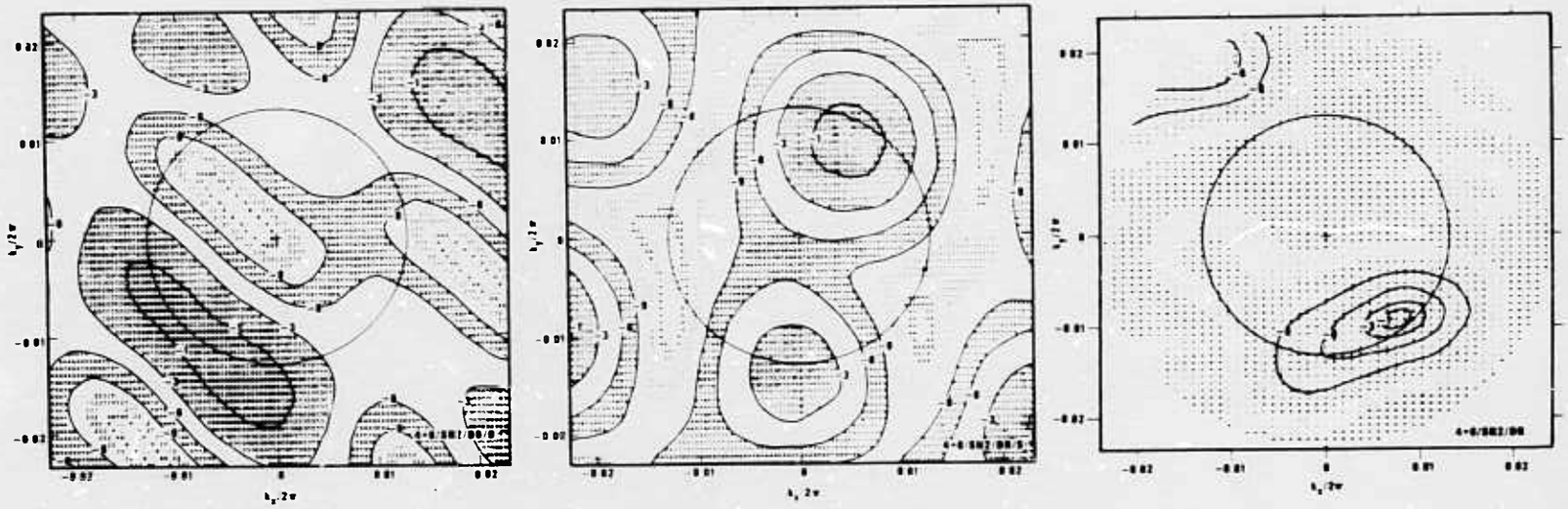

Original FKPLOT

Stripped FKPLOT

TSML

Figure 68. F-K spectra of A0 and the D ring for Events 4 and 6 combined with noise. S/N=2.

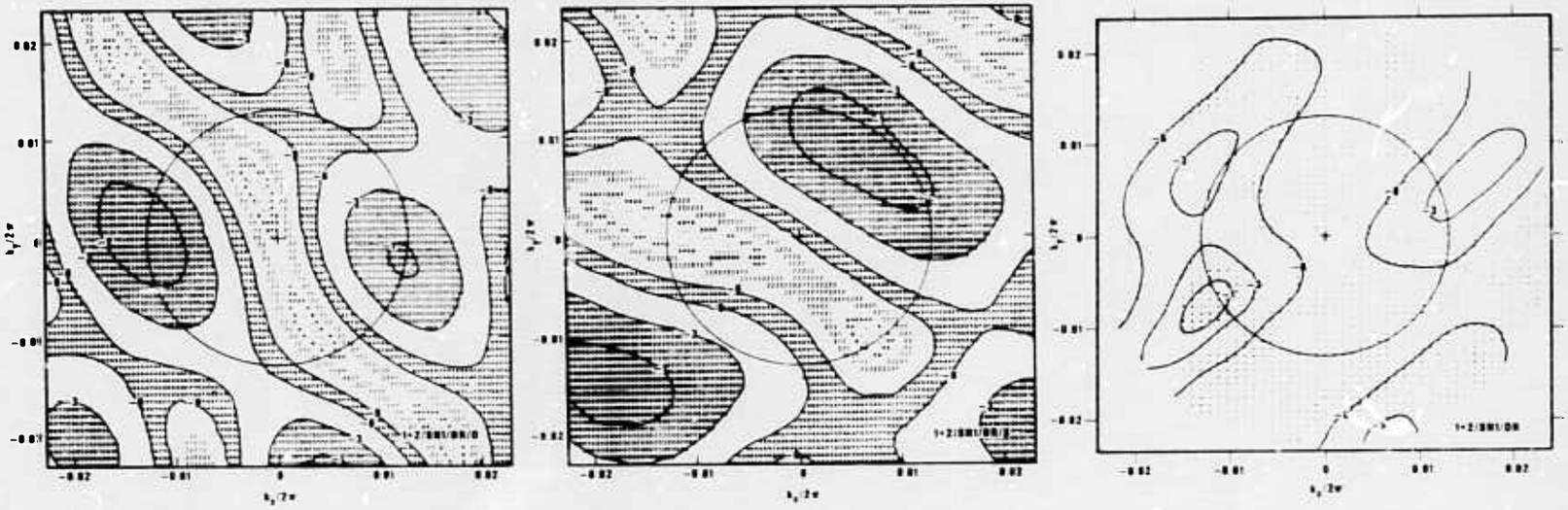

Original FKPLOT Stripped FKPLOT TSML

Figure 69. F-K spectra of A0 and the D ring for Events 1 and 2 combined with noise. S/N=1.

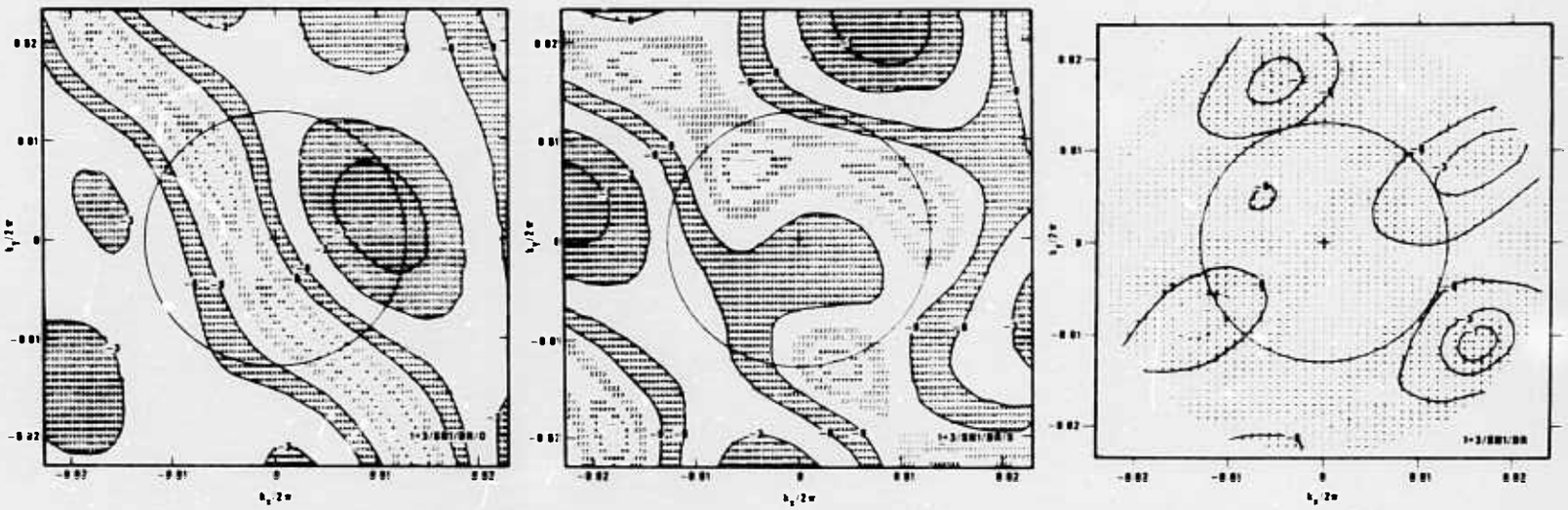

Original FKPLOT

Stripped FKPLOT

TSML

Figure 70. F-K spectra of A0 and the D ring for Events 1 and 3 combined with noise. S/N=1.

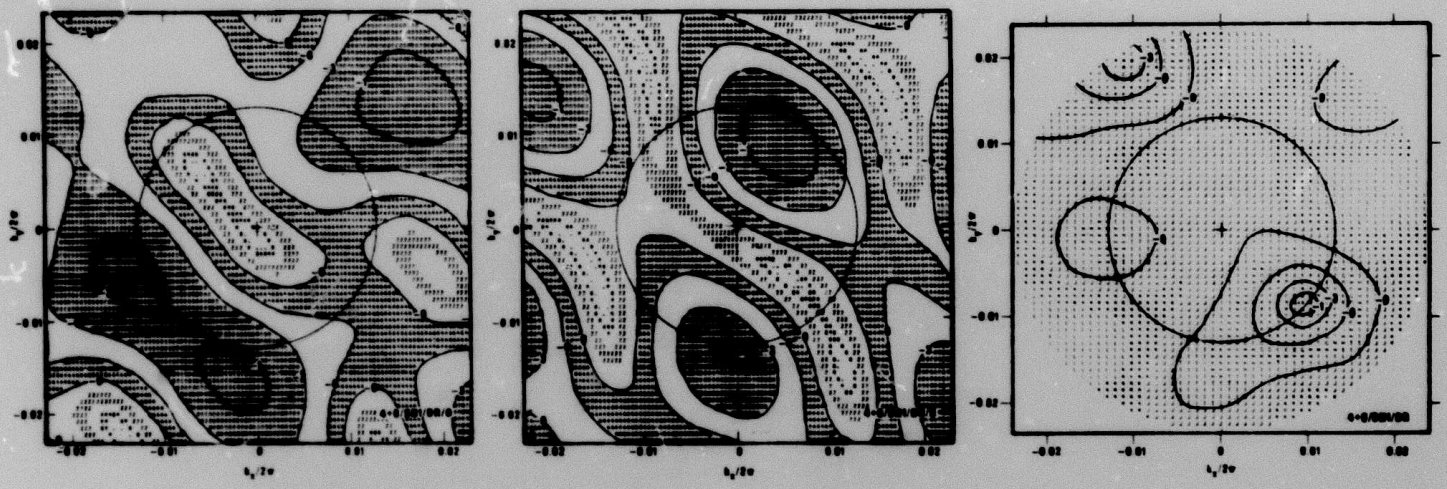

Original FKPLOT Stripped FKPLOT TSML

Figure 71. F-K spectra of A0 and the D ring for Events 4 and 6 combined with noise. S/N=1.

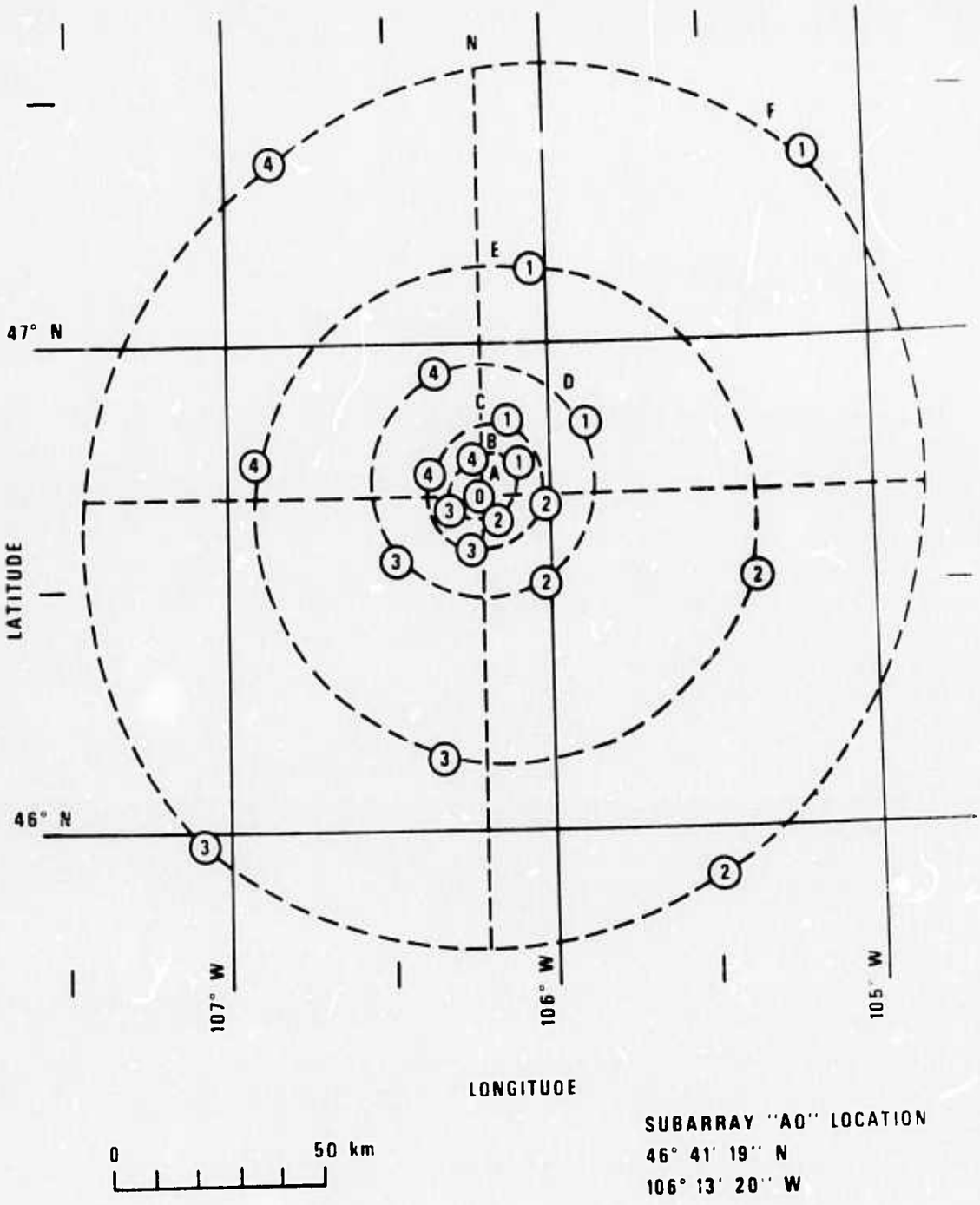

Figure 72. Configuration of the Large Aperture Seismic Array in Montana.

TABLE I

Epicentral Data

	Region	Date	Origin Time*	Location*		Depth km	From LASA Dist. km	From LASA Azimuth degrees	m_b	M_S
Event 1	Phillipine Islands Region	8 Jan 72	05:27:53	20.9N	120.2E	33	11155	316.5	6.2	6.3
Event 2	New Britain Region	28 Jul 71	01:10:24	5.1S	152.9E	33	11229	274.4	6.0	6.4
Event 3	New Hebrides Islands	24 Jan 72	03:55:42	13.0S	166.4E	28	10839	259.1	5.6	6.2
Event 4	Baja California	14 Apr 71	11:38:42	27.7N	112.4W	33	2176	196.5	5.4	5.2
Event 5	San Juan Province, Argentina	26 Sep 72	21:05:44	30.9S	68.1W	16	9421	147.9	5.9	5.8
Event 6	Guatemala	22 Jan 72	13:08:50	14.0N	91.0W	102	3895	153.7	5.5	-

* In some cases values for origin time are rounded to nearest second and locations' values are rounded to nearest tenth of a degree.

TABLE II

F-K Computed Data

Event	Description	Figure No.	ORIGINAL Velocity km/sec	ORIGINAL Azimuth degrees	ORIGINAL S/N	ORIGINAL F-Statistic	STRIPPED Velocity km/sec	STRIPPED Azimuth degrees	STRIPPED S/N *	STRIPPED F-Statistic
1		8	3.6	347	5.3	74.7	3.8	318	1.7	8.9
2		9	3.7	276	16.6	231.8	3.5	238	1.0	13.4
3		10	3.7	263	9.8	137.8	5.7	160	0.5	7.3
4		11	3.5	195	19.4	271.8	3.0	225	0.8	11.2
5		12	3.6	188	3.0	36.5	3.4	157	1.0	12.3
6		13	3.7	132	3.8	53.1	4.6	158	0.9	12.4
Noise		14	2.6	261	0.8	11.8	1.6	32	0.6	8.1
1 & 2		15	3.8	277	3.1	42.8	3.6	345	3.0	42.2
1 & 3		16	3.9	346	1.1	15.7	3.9	266	2.1	29.5
4 & 5		17	3.5	191	1.7	19.8	3.5	165	1.2	14.9
4 & 6		18	3.4	195	1.4	19.6	3.7	129	3.3	46.2
2 & 1	3/1 Ratio	19	3.7	276	8.8	123.7	3.6	344	1.1	15.4
3 & 1	3/1 Ratio	20	3.8	265	5.6	78.8	3.7	342	1.0	13.9
4 & 5	3/1 Ratio	21	3.4	196	8.3	99.9	3.5	166	1.9	22.6
4 & 6	3/1 Ratio	22	3.5	195	8.6	120.7	3.6	123	1.3	18.8
1 & 2	S/N = 2	23	3.7	277	3.6	50.8	3.8	347	1.7	23.3
1 & 3	S/N = 2	24	3.7	268	1.1	15.0	3.7	63	0.7	10.2
4 & 5	S/N = 2	25	3.7	176	1.3	15.6	3.4	202	1.0	11.8
4 & 6	S/N = 2	26	3.4	195	1.5	21.2	3.6	130	1.4	19.9
1 & 2	S/N = 1	27	3.6	276	3.1	44.0	3.6	56	0.7	10.1
1 & 3	S/N = 1	28	3.3	62	1.2	16.1	4.1	266	0.9	12.7
4 & 5	S/N = 1	29	3.7	173	0.9	11.3	2.7	73	0.8	10.2
4 & 6	S/N = 1	30	3.4	195	1.1	15.9	3.4	40	0.8	10.5
1	No F Ring	31	3.4	353	17.3	173.1	3.0	297	1.2	11.6
2	No F Ring	32	3.6	276	17.5	175.0	2.5	246	1.3	12.6
3	No F Ring	33	3.6	263	28.9	289.1	4.4	324	0.9	8.8
4	No F Ring	34	3.6	196	25.8	258.5	2.8	115	0.8	7.9
5	No F Ring	35	3.8	184	5.2	46.8	3.5	29	0.7	6.5
6	No F Ring	36	3.7	133	5.6	55.8	4.0	172	1.6	16.0
Noise	No F Ring	37	2.5	262	1.1	10.8	1.7	34	0.9	9.2
1 & 2	No F Ring	38	3.6	280	2.3	23.1	3.5	351	4.8	48.1
1 & 3	No F Ring	39	1.8	61	0.7	7.5	3.9	98	0.9	9.5

TABLE II (Continued)

F-K Computed Data

Event	Description	Figure No.	ORIGINAL Velocity km/sec	ORIGINAL Azimuth degrees	ORIGINAL S/N	ORIGINAL F-Statistic	STRIPPED Velocity km/sec	STRIPPED Azimuth degrees	STRIPPED S/N*	STRIPPED F-Statistic
4 & 5	No F Ring	40	3.7	178	2.8	24.9	3.1	95	0.6	5.3
4 & 6	No F Ring	41	3.4	188	1.2	11.6	3.6	128	4.2	42.4
2 & 1	3/1 Ratio No F Ring	42	3.6	277	7.6	75.6	3.6	350	1.7	17.0
3 & 1	3/1 Ratio No F Ring	43	3.6	264	9.9	9.5	3.7	345	2.1	21.0
4 & 5	3/1 Ratio No F Ring	44	3.4	199	9.5	85.4	4.1	161	1.8	16.5
4 & 6	3/1 Ratio No F Ring	45	3.5	192	7.5	75.0	3.1	121	3.9	38.8
1 & 2	S/N = 2 No F Ring	46	3.5	279	2.8	28.4	3.8	352	2.0	20.3
1 & 3	S/N = 2 No F Ring	47	3.7	71	1.1	11.3	3.3	254	1.0	10.3
4 & 5	S/N = 2 No F Ring	48	3.8	176	2.3	20.6	2.3	58	0.7	6.7
4 & 6	S/N = 2 No F Ring	49	3.3	187	1.3	13.5	3.4	128	1.2	12.5
1 & 2	S/N = 1 No F Ring	50	3.5	278	2.6	26.3	4.2	353	1.0	9.7
1 & 3	S/N = 1 No F Ring	51	3.6	64	1.5	14.9	3.5	260	1.7	17.1
4 & 5	S/N = 1 No F Ring	52	3.8	175	1.4	12.4	3.0	73	1.0	8.9
4 & 6	S/N = 1 No F Ring	53	3.2	187	1.0	10.1	3.1	246	1.0	9.6
1	D Ring + AO	54	3.6	357	18.6	74.5	1.6	34	5.9	23.5
2	D Ring + AO	55	3.8	275	24.3	97.3	1.1	44	2.0	8.2
3	D Ring + AO	56	3.8	264	48.4	193.7	2.0	97	1.8	7.2
4	D Ring + AO	57	3.6	193	146.1	584.5	1.6	353	2.7	10.7
6	D Ring + AO	58	3.5	133	9.1	36.3	1.6	78	2.1	8.5
Noise	D Ring + AO	59	2.1	46	3.8	15.2	1.9	136	1.5	6.0
1 & 2	D Ring + AO	60	1.6	165	2.8	11.4	3.0	353	2.9	11.7
1 & 3	D Ring + AO	61	1.9	60	1.6	6.5	1.1	49	2.4	9.4
4 & 6	D Ring + AO	62	1.8	70	1.2	4.8	1.9	334	2.3	9.2
2 & 1	3/1 Ratio D Ring + AO	63	1.6	164	7.5	30.1	1.8	252	1.7	6.7
3 & 1	3/1 Ratio D Ring + AO	64	3.9	263	12.7	50.9	4.7	344	4.5	17.8
4 & 6	3/1 Ratio D Ring + AO	65	3.6	197	7.2	28.6	3.6	125	3.1	12.4
1 & 2	S/N = 2 D Ring + AO	66	1.7	166	2.4	9.5	1.6	128	2.3	9.0
1 & 3	S/N = 2 D Ring + AO	67	1.1	134	1.4	5.8	2.1	30	1.6	6.5
4 & 6	S/N = 2 D Ring + AO	68	2.0	53	1.2	4.7	1.7	253	3.3	13.2
1 & 2	S/N = 1 D Ring + AO	69	3.5	274	1.8	7.1	1.1	130	1.7	6.9
1 & 3	S/N = 1 D Ring + AO	70	1.2	132	1.6	6.6	2.0	20	5.3	21.3
4 & 6	S/N = 1 D Ring + AO	71	2.2	49	1.3	5.3	4.5	25	2.7	10.9

* Statistical measures of S/N ratio computed during the FKPLOT runs are measures of the deviation of the input from a single plane wave rather than that of ratios of signal level to background noise.

TABLE III

Summary of runs testing the relative resolution of TSML and FKPLOT

Amplitude and S/N Ratio	Combination	Full Array		No F Ring		D Ring Plus Center Element	
		TSML	FKPLOT	TSML	FKPLOT	TSML	FKPLOT
1:1 S/N>>1	2 & 1	X	X	X	X	X	X
	3 & 1	X	X	X	?	?	?
	4 & 5	?	?	0	0	-	-
	4 & 6	X	X	X	X	0	X
3:1 S/N>>1	2 & 1	0	X	0	X	0	0
	3 & 1	X	X	X	X	X	X
	4 & 5	?	X	0	X	-	-
	4 & 6	X	X	X	X	0	X
1:1 S/N~2	2 & 1	?	X	?	X	0	X
	3 & 1	0	0	0	0	0	0
	4 & 5	0	0	0	0	-	-
	4 & 6	X	X	?	X	0	0
1:1 S/N~1	2 & 1	0	0	0	X	0	0
	3 & 1	0	0	0	0	0	0
	4 & 5	0	0	0	0	-	-
	4 & 6	0	0	0	0	0	0

X Separation

0 No Separation

? Questionable or Ambiguous Separation